Relay Selection in Massive MIMO Wireless Energy Harvesting Cognitive Networks

Prepared by

Tatenda Kuwarika Mashiri – Student number **488606**

<u>Research Supervisors</u>

Prof Fambirai Takawira,

Dr Jules Mouatcho Moualeu

A dissertation submitted to the Faculty of Engineering and the Built Environment, University of Witwatersrand, Johannesburg, in fulfilment of the requirements for the degree of Master of Science in Engineering.

August 2020

Declaration

I declare that this dissertation is my own unaided work. It is being submitted for the degree of Master of Science in Engineering to the University of the Witwatersrand, Johannesburg. It has not been submitted before for any degree or examination to any other University.

....

(Signature of Candidate)

……………. day of ………………………… year ………………….

Abstract

In recent years, there has been an explosive growth in bandwidth-hungry wireless devices and applications which has, in turn, caused a strain on the provisions of the present electromagnetic spectrum. Several technologies have been studied and implemented in the quest to try and alleviate this growing scarcity of the spectrum. This work, therefore, tries to address some of these challenges by looking at spectrum utilisation techniques and how optimal they can be implemented to improve the spectral efficiency and overall system performance.

This research seeks to investigate the sum-rate and outage performance of an energy harvesting cognitive massive multiple-input multiple-output (MIMO) multi-relay assisted network with underlay spectrum sharing. The secondary network is permitted to opportunistically access the licenced primary network frequency band provided that the intra-cell interference imposed on the primary base station due to concurrent secondary network transmissions does not exceed the pre-set interference temperature and hence maintain the quality-of-service (QoS) requirements of the primary network. The introduction of relays improves the system performance by increasing the network coverage and this research analyses the performance of the cognitive relay networks by looking at (i) the effect of primary user interference on the relay and subsequently relay selection, (ii) the outage probability of the secondary network being assisted by an amplify-and-forward (AF) relay and (iii) the impact of the number of relay antennas and the number of relays. The power-constrained secondary network nodes harvest energy from concurrent transmissions of the energy sufficient primary users. A time switching protocol is implemented in this work for energy harvesting and closed-form expressions for the harvested energy and achievable sum-rate are derived. To that end, this research seeks to quantify the trade-off between the achievable sum-rate of the network and the harvested energy. The primary base station and secondary destination employ zero-forcing detection and performance is investigated over Rayleigh fading.

Dedication

~To my late mum and dad~

....the memories remain fresh....

~Happiness & Tanatswa Mashiri~

.....this one is for you.....

Acknowledgements

Firstly, I would like to thank the Almighty for giving me the strength, peace of mind and wisdom to carry out this research. My most humble gratitude goes to Professor Fambirai Takawira who offered me a chance to pursue my MSc when I thought I could not further my studies anymore. I also would like to extend my gratitude towards Dr Jules M Moualeu, who together with Prof Takawira, provided guidance to me throughout my research and both afforded me the opportunity to go and present my work at a conference.

I would also like to take this opportunity and express my heartfelt gratitude to my wife, Happiness Mashiri, for the encouragement, unwavering support and prayers which saw me through to the completion of this research. I am highly indebted to my family, my sisters for being there when the chips were down and gave me a reason to fight on. Many thanks go to Centre for Telecommunications Access and Services (CeTAS) for funding my research through Prof Takawira and to my CeTAS colleagues for the brotherhood that prevailed through the years we were together. This made the work bearable.

Finally, I am grateful to my friend, Malvern Chamisa, who was also my research-mate. The journey was an enjoyable one with this guy and only wish we do more of this in the future.

Table of Contents

Declaration i

Abstract ii

Dedication iii

Acknowledgements iv

Table of Contents v

List of Figures ix

List of Tables xi

Glossary of Terms and Abbreviations xii

Chapter 1 – Introduction 14

1.1 Background - Wireless Communications 14

1.2 Background – Research Focus 16

1.3 Problem statement and Motivation 18

1.4 Research Question 20

1.4.1 Sub-questions 20

1.4.2 Main Contributions 20

1.4.3 Publications 21

1.5 Organisation of the Dissertation 22

1.6 Chapter Summary 23

Chapter 2 Literature Review - Cognitive Radio and Cooperative Communications 24

2.1 Introduction 24

2.2 Wireless Radio Spectrum 24

2.2.1 Spectrum Management 24

2.2.2 Dynamic Spectrum Access (DSA) 26

2.3 Cognitive Radio 26
2.3.1 Main functions of Cognitive Radio 27
2.3.2 Underlay Model 28
2.3.3 Overlay Model 28
2.3.4 Interweave Model 29
2.4 Cooperative Communications 30
2.4.1 Relaying Network Design 31
2.4.2 Modes of Operation 31
2.4.3 Relaying Strategies 32
2.5 Multi-Relay Scenario – Relay Selection 33
2.5.1 Relay Selection Schemes 33
2.5.2 Relay Selection Strategies 34
2.5.3 Relay Selection Criteria 35
2.6 Conclusion 37

Chapter 3 Literature Review – Wireless Energy Harvesting and Massive MIMO 38

3.1 Introduction 38
3.2 Wireless Energy Harvesting 38
3.2.1 Time Switching Protocol 40
3.2.2 Power Splitting Protocol 41
3.2.3 Energy Harvesting in Wireless Networks 42
3.3 Background on Massive MIMO 44
3.3.1 Point-to-Point MIMO 46
3.3.2 Multi-User MIMO 47
3.3.3 Massive MIMO 48
3.4 Conclusion 51

Chapter 4 – Sum-Rate of a Massive MIMO Spectrum Sharing Network 53

4.1 Introduction 53

4.2 System Model 53

4.2.1 Proposed Network Architecture 53

4.2.2 Signal Model of the Secondary Network 55

4.2.3 Energy Harvesting Model – Time Switching 57

4.2.4 End-to-End SINR *(Secondary Network)* 58

4.2.5 Signal Model of the Primary Network 59

4.2.6 End-to-End SINR *(Primary Network)* 60

4.3 Achievable Sum-Rate Definitions 60

4.4 Asymptotic Sum-Rate Analysis 61

4.4.1 $N_P \to \infty,\ N_S \to \infty\ and\ N_R \to \infty$ 61

4.5 Sum-rate against the harvested energy 62

4.5.1 Asymptotic harvested energy at the relays 62

4.5.2 Asymptotic harvested energy at the secondary users 63

4.5.3 Asymptotic harvested energy and average sum-rate trade-off 64

4.6 Numerical Results and Discussions 64

4.7 Innovative Aspect of our Proposed System 71

4.8 Conclusion 72

Chapter 5 – Outage Performance of a Massive MIMO Spectrum Sharing Network 73

5.1 Introduction 73

5.2 System Model 73

5.3 Outage Probability 74

5.3.1 Problem Formulation 74

5.4 Numerical Results and Discussions 75

5.5 Conclusion 79

Chapter 6 - Relay Selection for Massive MIMO Spectrum Sharing Networks 81

6.1 Introduction 81

6.2 Relay Selection Model..81

6.2.1 System and Signal Model...82

6.2.2 Selection Schemes..83

6.3 Numerical Results and Discussions....................................84

6.4 Conclusion..89

Chapter 7 – Conclusion 91

7.1 Concluding remarks...91

7.2 Future Directions 93

References 95

Appendix A – Achievable Sum-Rate 105

A.1 Received signal at the SBS...105

A.2 Derivation of the asymptotic SINR 106

List of Figures

Figure 2.1: System model of a Cognitive Radio Network……………………………………...27

Figure 2.2: Simple Cooperative Relay Network…………………………………………...31

Figure 2.3: Multi-relay cooperative communication system with best relay selection………33

Figure 4.1: System model of a cognitive MIMO multi-relay network with underlay spectrum sharing……………………………………………………………………………………..54

Figure 4.2: Achievable sum-rate versus the average first-hop SNR for a M-user secondary network……………………………………………………………………………………….65

Figure 4.3: Average sum-rate against the secondary network average first-hop SNR……….66

Figure 4.4: Average sum-rate vs average first-hop SNR at different secondary user transmit powers levels and different base station antenna configurations…………………………….67

Figure 4.5 Average sum-rate vs the average secondary base station SNR……………………68

Figure 4.6: Achievable Sum-Rate versus the number of secondary base station antennas…..69

Figure 4.7: Sum-rates versus α for a 6-user relay network……………………………………70

Figure 5.1: Outage probability of a 4-user network with varying numbers of the secondary base station antennas………………………………………………………………………………75

Figure 5.2: Outage probability against the interference temperature values at two different base station antenna configurations…………………………………………………………………76

Figure 5.3: Outage probability as a function of γ_{th}…………………………………………………78

Figure 5.4: Outage probability against the time switching factor, α………………………...79

Figure 6.1: System model only showing the multiple relay cluster……………………….....82

Figure 6.2: Average sum-rate against average first-hop SNR for 4-user 2-relay network……84

Figure 6.3: Average sum-rate against the average first-hop SNR for 2 different relay selection strategies that consider maximising the worst data-stream SINR…………………………....85

Figure 6.4: Average sum-rate against the average first-hop SNR for 2 different relay selection strategies that consider the best source-to-relay average SINR………………………………86

Figure 6.5: Sum-rate against the time switching factor for different number of relays………87

Figure 6.6: Outage probability of a multi-relay multi-user network…………………………88

List of Tables

Table 4.1: Summary of the channel matrices………………………………………………...….55

Table 4.2(a) Energy harvesting at the secondary user……………………….……………57

Table 4.2(b) Energy harvesting at the relay………………………………………………57

Glossary of Terms and Abbreviations

AF	amplify-and-forward
AWGN	additive white gaussian noise
BRS	best relay selection
CR	cognitive radio
CSI	channel state information
DF	decode-and-forward
FDD	frequency-division duplexing
HSU	harvest-store-use
HU	harvest-use
i.i.d	independent and identically distributed
ICASA	Independent Communications Authority of South Africa
IoT	internet of things
ITU	International Telecommunications Union
MIMO	multiple-in multiple-out
MMSE	minimum mean squared error
MU-MIMO	multi-user multiple-in multiple-out
ORS	opportunistic relay selection
PBS	primary base station
PRS	partial relay selection

PS	power splitting
QoS	quality of service
RF	radio frequency
RFCC	radio frequency combining circuit
SBS	secondary base station
SINR	signal-to-interference-plus-noise-ratio
SINR	signal-to-interference-and-noise ratio
SNR	signal-to-noise-ratio
SWIPT	simultaneous wireless information and power transfer
TDD	time-division duplexing
TS	time switching
TSR	time switching receiver
WEH	wireless energy harvesting
WIT	wireless information transfer
WPT	wireless power transfer
ZF	zero forcing

Chapter 1 – Introduction

With the astonishing increase in wireless applications, the present radio spectrum has been stretched to its capacity to handle this explosive expansion. The next generation of wireless technologies which is the fifth generation (5G) and beyond networks, look set to bring on board significantly faster connectivity rates than the present fourth generation (4G). The faster speeds provide an ideal communication infrastructure for a network of interconnected devices known as the internet-of-things (IoT). The IoT is envisioned to be a key driver in the growth of the succeeding generations of wireless technologies. However, this paradigm poses a threat of overcrowding the already congested wireless spectrum and this motivates our current research work to devise mechanisms that ensure efficient spectrum utilization.

This chapter provides a brief history and transformation of wireless communications and also introduces the background of the technologies that this research will implement. The research question and contributions of this research are also discussed in this chapter. The organisation of the remaining chapters is also outlined.

1.1 Background - Wireless Communications

Wireless communication technologies have greatly altered the way people communicate over the years and have added positively to the growth of economies and livelihoods of people. Unlike wired communication systems, wireless communications allowed for accessibility almost anywhere around the world thereby improving the passing of information between two or more people or services. The evolution from early applications like simple Morse code to the live-streaming of videos has been necessitated by the continuous developments and deployments of wireless technologies (from Global System for Mobile Communications (GSM) up to Long Term Evolution (LTE) standards and beyond). The development of wireless networks has been in phases known as generations starting from the 1st generation (1G) to the 4th generation (4G). Much research is now primarily focused on the release of the more advanced 5th generation.

1G was the first commercially automated wireless network, made up predominantly of analogue standards that relied on signal amplification to the ranges upward of 150MHz for communication purposes. Due to the obvious advantages of digital signalling over analogue signalling, the development and deployment of the second-generation (2G) were imminent. The second generation was first deployed in the 1990s and mainly made provisions for voice services. The 2nd generation was based on digital communications and this paved the way for the gradual support of data services in this generation. Basic data services such as email and short messaging were supported by the 2nd generation. The increased likelihood of cellular phones usage gave birth to newer second-generation standards like 2.5G standards.

The pressure kept mounting on the second-generation standards as higher transmission data rates were becoming inevitable and this led to the third generation (3G). 3G was meant to provide peak transmission rates of at least 200kbits/s which was relatively higher than the preceding 2G and 2.5G standards. Application services included wide-area voice services, mobile television and mobile internet access amongst others. This generation marked the advent of smartphones. As the influx of smartphones and bandwidth-hungry devices continued to grow, it only meant faster speed requirements needed to be met. Long Term Evolution (LTE), which is 3.9G, and LTE Advanced (4G) brought higher data speeds by making use of additional spectrum and multiplexing techniques. Transmissions speeds in the regions of 300Mbits/s are attainable in the fourth generation. Multiplexing technologies like multiple-input multiple-output (MIMO) enhanced the system capacity that helped in accommodating the higher data rates.

The aggregate world population continues to grow and so is the growth in smart devices usage. This exponential growth in information transfer continues to strain the available electromagnetic spectrum. The statistics provided by the international telecommunications union (ITU) show a 12.5% rise in active mobile data users between 2014 and 2016 only [1]. Critical operations that require ultra-low latency and super-fast response times are also on the rise and all this has pushed the need for ultra-fast connectivity networks. The next generation of wireless technologies has been studied to bring on board remarkably very fast connectivity speeds compared to the preceding wireless generations. More and more research has been channelled towards optimising the gains of 5G. Techniques that look into improving the spectrum usage, which is still very much under-utilised, have been proposed. This research subsequently feeds into this pool by studying several technologies and combining them to analyse the aggregate improvement they yield on the network throughput. This research will focus on the gains that are obtainable from implementing massive MIMO (also known as *large-scale antenna system*), cooperative relaying, cognitive radio and wireless energy harvesting.

These are studied to try to address issues around large user-network connections, improved system throughput, reduced interference, and improved energy efficiency.

1.2 Background – Research Focus

Cognitive radio (CR) technology has emerged as a capable means of decongesting the spectrum by allowing the unlicensed cognitive users (secondary users) to share the licenced band of the primary users [2]. The cognitive radio networks can be further explained in three main paradigms namely underlay, overlay and interweave [3]. The overlay approach allows simultaneous primary and secondary transmissions by letting the secondary users to use some of its power to assist primary transmissions. The interweave approach bases its operation on the existence of temporary space-time-frequency voids known as spectrum holes. The holes are not in constant use in both the primary and secondary network bands. The underlay model of operation also known as the spectrum sharing network, which is going to be the focus of this research, allows both the secondary and the primary users to simultaneously utilise the licensed primary network bandwidth provided that the primary network performance is not affected beyond a certain level. In this underlay paradigm, it implies that the uplink transmission of the secondary network is governed by secondary-to-primary interference constraint and this constraint may result in increased secondary network outage occurrences and reduced secondary network coverage.

Most of the devices in this paradigm are not connected to the conventional power grids and will rely on battery power. In most cases, the devices will be placed in areas that are not easily accessible or in dangerous environments and the problem arises when the batteries need replacement or recharging. Radio frequency energy harvesting from ambient interference, an eco-friendly and self-sustainable technique, has risen as a promising technology in increasing the sustainability of wireless networks and ultimately improve the energy efficiency of a network. Based on either the time switching (TS) or power splitting (PS) energy harvesting methods, information decoding, and energy harvesting can take place at a node [4].

As highlighted earlier, most current research is driven towards improving spectrum utilization and cooperative communications (see [5] - [7]) has emerged as a key enabling technology in overcoming many limitations in wireless systems by increasing reliability and coverage. This concept of relaying communication in CR networks with cooperative spectrum sharing has attracted a lot of attention in recent years. This is because, in underlay cognitive radio networks, the secondary user has strict power constraints so that the interference power is less than a threshold value and due to such a constraint (interference constraint), the transmit power of the secondary user is usually low. Therefore, the implementation of relays has proven to increase the reliability between secondary transmitter and secondary destination by increasing the network coverage area and subsequently the spectral efficiency. Other than just the spectral efficiency, cooperative relaying also improves the energy efficiency of a system by minimizing the transmit powers of nodes through different paths between the source and the destination.

In this continued quest to improve wireless communications, the implementation of massive multiple-in-multiple-out (MIMO) in a wireless communication network has also been studied to potentially increase the spectral and energy efficiency gains in 5G due to spatial multiplexing and through beamforming [8]. With 5G technology being regarded as the future of wireless communications due to its fast data transmission rates, massive MIMO can support these transmission rates by simplifying the required signal processing with the implementation of robust and simple linear precoding approaches such as the minimum mean squared error (MMSE) and zero-forcing schemes. By exploiting a large number of antennas, the beamforming can be exploited to prevent fading and subsequently mitigate interference to the licenced primary users. Massive MIMO, therefore, provides a better system performance by providing high data transmission rates, improved link reliability and improve energy efficiency through the reduction of power consumption and increase the number of degrees of freedom in space.

The above-discussed components of wireless communications clearly show that ongoing research interests are focused on trying to make component designs that accommodate 5G, tackle the future capacity constraints, improve energy efficiency, link reliability and increase the network coverage area. This research is therefore focused on the co-existence of secondary and primary networks where the secondary users opportunistically access the licenced primary network spectrum. It also looks at how introducing relays in a spectrum sharing network can improve the spectral efficiency of a cellular network. It is worth noting that in a spectrum sharing multi-relay network, relay selection significantly improves the diversity order.

The issues of energy efficiency are very critical when it comes to wireless devices and wireless communications. Therefore, energy harvesting is proposed in this research to analyse how the aggregate energy efficiency of the system can be improved by implementing radio frequency energy harvesting. Massive MIMO offers improved degrees of freedom which attenuates small-scale fading and interference as the number of antennas goes to infinity hence this research will analyse the performance of massive MIMO in a cooperative spectrum sharing wireless energy harvesting network and subsequently examine how these technologies improve the next generation of wireless technologies, 5G.

1.3 Problem statement and Motivation

The coexistence of primary and secondary networks with cooperative relaying has been studied in works [9], [10], [11] – [13]. The authors in [10] study the outage probability of an amplify-and-forward (AF) cognitive single-antenna relaying network where the best relay is activated for transmission of information to the destination. The end-to-end performance and effects of partial and opportunistic relaying strategies under Nakagami-*m* fading parameters of a cooperative AF relaying spectrum sharing system are studied in [5]. The closed-form expressions for the system capacity of a cooperative decode-and-forward (DF) spectrum sharing scheme are derived in [11] and the outage probability of the same system under interference constraints is analysed in [12]. The achievable sum-rate of a two-way single-antenna relay network is studied in [13] without either relay selection or energy harvesting. Wireless energy harvesting is not considered in this work since the secondary network nodes are assumed to have fixed power supplies. Quite significant research work has also looked at cognitive cooperative MIMO systems [14] - [16]. Sum-rate expressions of a cognitive radio massive MIMO two-way relay network with relay selection are derived in [14]. The achievable sum-rate of a non-cooperative wireless powered multi-cell underlay spectrum-sharing cognitive system is investigated in [15] where there is a direct communication link between the source and destination. Introducing relays to the work in [15] allows this research to study how cooperative communications change the system performance of a network. The effect of primary interference on the relays is investigated in an underlay spectrum-sharing network. The work in [16] implements the time-switching protocol and AF relaying scheme to investigate the trade-off between sum-rate and the harvested energy in a single relay massive MIMO network. The elementary trade-off between the energy and information transfer rates over a single noisy channel is investigated in [17] and the authors in [18] study the different trade-offs between harvested energy and information rate by considering both the separated receiver and collocated receiver structures.

These observations in the aforementioned literature motivate this work to introduce the concept of massive MIMO to a cooperative cognitive network. Massive MIMO is capable of providing huge spectral and energy efficiency gains compared to the conventional MIMO systems [19]. This forms the basis of this research considering that not much work has been done on a multiuser multi-relay massive MIMO-enabled cooperative cognitive system. Much aforementioned research on spectrum sharing massive MIMO systems has either considered single-hop systems (see [20] - [22]) or downlink transmission of single-cell secondary systems (see [23] - [24]), and this motivates the current work to consider an uplink transmission of a multi-user multi-relay system. Wireless energy harvesting is also implemented in the proposed system to improve the energy efficiency of the proposed system by powering the energy-constrained secondary network nodes for their transmissions. These secondary users and cognitive relays can harvest energy from the energy-sufficient primary users when they simultaneously transmit. Considering this proposed model, the quality of the secondary user transmissions and the standard of relaying the signals to the secondary destination will be affected by the power received at the secondary user and the cognitive relays from the primary user signals. This implies that the secondary source and the relay(s) have to accurately determine their receiver parameters (time switching ratios) to optimize the overall system performance while satisfying their energy needs. This regard further motivates this research to investigate the impact of primary user interference on relay selection which remains unexplored to the best of the candidate's knowledge. This research collectively aims to analyse the performance of the proposed system in terms of the signal-to-noise-and-interference ratio, the achievable sum-rate and the secondary network outage probability.

This research brings forth the integration of massive MIMO and wireless energy harvesting into a cooperative cognitive network to meet the research's objective of maximising the system capacity and minimising the system outage probability under the maximum PU interference constraint. In summary, this research's contribution will be guided by the following interests:

- A multi-user multi-relay massive MIMO wireless energy harvesting cooperative cognitive radio system. In this model, both the secondary source and the relays will harvest energy from the energy sufficient primary user signals based on the time-switching receiver (TSR) structure. The Harvest-Use mode of energy harvesting is implemented as the research assumes that there are no batteries to store any energy. The best relay will be selected to assist the transmission of data from the secondary source to the secondary destination. Single relay selection will be implemented because multiple relay selection will significantly increase the interference on the primary network.

- The effects of co-channel interferences (CCI) from concurrent primary transmissions on the secondary network in terms of the harvested energy and system outage probability are investigated. Moreover, derivation of the exact expression of the outage probability (OP) for the secondary network is obtained.
- Expressions for the achievable sum-rate and harvested energy are derived and subsequently the trade-off between the two are discussed. The trade-off between the benefits of energy harvesting and the negative effects of primary interference is also discussed.
- The Zero-Forcing (ZF) pre-coder scheme is implemented in this work as this research tries to preserve the performance vs computational complexity trade-off.

1.4 Research Question

To what extent does the relay selection and massive-MIMO affect the system performance of a multiuser multi-relay energy harvesting cooperative cognitive radio network in terms of sum-rate and outage probability?

1.4.1 Sub-questions

- How do the interference constraint and the transmit power constraint affect the best relay selection in selecting a single relay out of the N available relays?
- How does the number of antennas and number of relays impact the end-to-end outage probability and sum-rate of the system?
- How can the energy efficiency of secondary network nodes be improved in a cognitive radio network?

1.4.2 Main Contributions

This research aims to formulate and address the issues pertaining to increased system throughput and improved energy efficiency through relay selection of a multiuser energy harvesting cognitive massive-MIMO relay network with underlay spectrum sharing.

Motivated by the above discussions, this research strives to contribute the following:

- Propose an underlay cognitive massive MIMO with an energy harvesting multi-relay network. In this model, both the energy-constrained secondary source and relays harvest energy from the primary user transmissions and use the harvested energy for their subsequent transmissions.
- Derive mathematical expressions of the end-to-end signal-to-interference-plus-noise ratio and the asymptotic analysis for system achievable sum-rate over Rayleigh fading channels. Relay selection is also performed in the proposed scheme to select the best relay node(s) to help in the secondary network transmissions. While relaying provides improved spectral efficiency, multiple relays and relay selection yield better gains. To provide evidence of the accuracy of the proposed scheme, Monte Carlo simulations are run to assess the accuracy of the proposed analytical expressions and hence provide practical conclusions.

The following objectives feed into the main contributions of this research:

- maximise the sum-rate of the underlay spectrum sharing model with massive MIMO and multiple relays through relay selection under the primary base station peak interference constraint.
- improve the energy efficiency of the spectrum sharing system by integrating energy harvesting.
- minimise the outage probability of the secondary network by deducing the optimal number of primary transmitters and subsequently observe the effect of primary interference on the performance of the secondary network.

1.4.3 Publications

The following conference and journal papers have resulted from this research,

- Tatenda Mashiri, Fambirai Takawira and Jules. M. Moualeu, "Relay Selection in Massive MIMO Wireless Energy Harvesting Cognitive Network", - *IEEE AFRICON 2019* Conference, Accra, Ghana, September 2019.
- Tatenda Mashiri, Fambirai Takawira and Jules. M. Moualeu, "Massive MIMO Wireless Energy Harvesting Multi-Relay Network with Underlay Spectrum-Sharing", - Journal paper under preparation

1.5 Organisation of the Dissertation

The rest of the dissertation is organised as follows:

Chapter 2: This chapter gives an extensive background on the literature of cooperative communications in a cognitive network. It provides the essential framework for such a system including the spectrum sharing modes, relaying strategies and the relay selection schemes.

Chapter 3: This chapter talks about the past and present work on massive MIMO systems. It also introduces detection schemes in massive MIMO looking at the advantages and disadvantages of each scheme. This chapter also discusses the background information on conventional single-hop massive MIMO networks and subsequently extends to massive MIMO spectrum sharing networks with cooperative relaying. Aspects of energy harvesting in a network are also introduced in this chapter. Different energy harvesting modes and the past work on how they are implemented in a massive MIMO cooperative communications network are discussed in this chapter

Chapter 4: This chapter presents the proposed scheme. The system model is introduced in this chapter and the performance of the system is analysed in terms of the system sum-rate. Analytical expressions for the sum-rate are derived and are compared against the Monte-Carlo simulations to show the correctness of our mathematical expressions.

Chapter 5: In this section of the dissertation, the system performance of the proposed scheme in terms of outage probability is analysed. Monte Carlo Simulations are plotted for the exact outage probability curves and system performance is quantified from these curves.

Chapter 6: This chapter of the dissertation introduces relay selection into the proposed system model. Two different relay selection schemes are compared in this chapter and the results for each scheme subsequently presented. Relay selection is performed for different schemes where each user selects its own relay for transmissions, or all the users transmit through a single relay. Performance of the system with relay selection is also compared against the system performance of single relay models.

Chapter 7: This chapter concludes the dissertation and presents the overall contribution of this research. It provides an aggregate summary of all the obtained results and interprets how they feed into the ongoing 5G research. Future work recommendations are also laid out in this chapter.

1.6 Chapter Summary

This chapter formed the skeleton structure for this research by looking at the brief introduction to wireless communications, a framework of the proposed solutions, defined the problem statement and motivation, formulated the research question and finally outlined the contributions of this research.

Chapter 2 Literature Review - Cognitive Radio and Cooperative Communications

2.1 Introduction

This chapter provides a brief introduction to the wireless radio spectrum and how wireless communication challenges from early days led to the birth of current technologies such as cognitive radio. This, therefore, extends this chapter to provide a detailed background on the emergence of cognitive radio, its different implementation schemes and work that has been done on implementation of cognitive networks in this continued quest to decongest the overcrowded spectrum. It also includes a thorough presentation of the literature review on cooperative communications and how the two are integrated into a wireless network to improve spectral efficiency.

2.2 Wireless Radio Spectrum

The radio frequency spectrum is part of the electromagnetic spectrum, a medium on which wireless communications take place. Usable regions of this electromagnetic spectrum for communication purposes range from 3 kHz to 300 GHz. This usable region of the spectrum is segmented into bands of different widths and different uses. Each band comprises of many channels that can be used for communications in the case of the radio frequency band. To avert the destructive interference effects, different service frequencies are not designed to overlap. The demand for wireless services continued to soar but the electromagnetic spectrum is a fixed resource, better ways of managing the spectrum were needed and hence this gave birth to regulations that would govern the radio frequencies.

2.2.1 Spectrum Management

Regulations to the usage of radio frequencies ensured efficient use and distribution of the available spectrum. Due to the limitations in technology in the early days of wireless communications, signal interference was the biggest issue and needed to be dealt with. To address this setback, licences were issued exclusively. Frequency allocations for similar services were assigned to respective bands. This spectrum management policy is known as the

Fixed Spectrum Access (FSA). The 300 kHz to 535 kHz frequency band is reserved for aeronautical communications in the US while analogue TV communications are limited to between the 400 MHz to 700 MHz frequency band, just to mention a few examples. This made regulation easier and thereby minimised the challenges of interference. Within these bands, the problems of inter-band interference still needed to be addressed and this led to user-per-channel allocations within bands.

Each country can regulate independently but the International Telecommunications Union (ITU) controls the international standards for allocation. Examples of these international standards are the 800 MHz, 900MHz, 1600MHz, 2300MHz and the 2600MHz spectrum bands set aside for GSM and this implies that globally, those bands are used specifically for GSM only [25]. Wireless devices are, therefore, by law, designed and manufactured with capabilities to connect to such internationally allocated spectrum bands allowing the device to utilise that band regardless of its geographical location.

The Independent Communications Authority of South Africa (ICASA) is the regulatory body in South Africa and it oversees all spectrum allocations within the country. ICASA regulates the electromagnetic spectrum into the radio frequency bands at the national level in South Africa, a process known as an allotment. An allotment makes it easy to identify and manage available or vacant spectrum for further assignments. ICASA also conducts auctions where companies bid for the bands. This regulatory body also dictates the criteria with which how to access the spectrum, for example in the case of the 790MHz – 862MHz band which has been freed for International Mobile Telecommunications (IMT) implementation. Two or more license holders can be licensed to the same frequency band and this implies that spectrum sharing is permitted and attainable. This aspect of spectrum sharing has gone a long way in improving spectral efficiency by decongesting the spectrum. In the same regard, the Federal Communications Commission (FCC) has also studied and reviewed that, although many operators or users are still unlicensed, the spectrum is still very much under-utilised as they are many unused licensed channels at any given time. Some operators are only licensed a limited amount of spectrum and this creates a bottleneck in the operations and transmissions of that operator and causes congestion. These two scenarios show the uneven distribution and allocation of spectrum. Powerful companies also bid for huge amounts of spectrum and can afford to operate with these licences even in an area with less number of users and this, in turn, leads to under-utilisation [26]. In South Africa, urban data traffic is significantly higher than data traffic in rural areas. Equal allocation of spectrum bands to the urban and rural areas would result in spectrum under-utilisation in the rural areas and congestion in the urban spectrum. These kinds of scenarios need a proper spectrum management.

Wireless usage on the other hand, continues to grow and these challenges in spectrum management continue to put more pressure on the spectrum. ICASA published that revenues collected from mobile services increased by slightly above 4% between 2015 and 2016 [27]. This showed the continued growth in demand for wireless services. Several techniques to improve spectral management have been devised and these included frequency division duplexing (FDD), time division duplexing (TDD), amongst others. Communication evolved from being half-duplex to full duplex. These still could not completely ease the pressure on the available spectrum. This has led to more focus being put on Software Defined Radios (SDRs), a concept originally brought up in the 1980s, to come in as a Dynamic Spectrum Access (DSA) technology which was superior than the FSA policy.

2.2.2 Dynamic Spectrum Access (DSA)

DSA involves two approaches namely the spectrum property rights and the dynamic spectrum allocation. License holders are free to trade spectrum amongst themselves thereby limiting on the issues of underutilisation or overutilization. DSA also provisions for spectrum to be allocated in a given time and particular area to certain services. The DSA has two main models which are the open sharing model and the hierarchical access model. The open sharing model is of the idea of unmanaged and unlicensed spectrum allocation. This is the same approach used in Bluetooth and Wi-Fi technologies. This model can only be implemented on a small scale in concentrated areas with common spectrum usage needs. The second model of DSA, as mentioned above, is the hierarchical access model which outlines the co-existence of primary users (PUs) and secondary users (SUs). This co-existence is interpreted in 3 common ways which are interweave, underlay and overlay. These spectrum sharing approaches constitute what is described as Cognitive Radio (CR), software-defined radio that can learn and change to fit its present environment but self-reconfiguring its network parameters.

2.3 Cognitive Radio

Cognitive radio has emerged as an efficient way to help decongest the now overcrowded spectrum. The following describes the main functions of a cognitive radio network.

2.3.1 Main functions of Cognitive Radio

The following are the main functions of a cognitive radio network (CRN)

- Spectrum sharing: This refers to the fair distribution of spectrum among SUs in the network and may also entail sharing a particular channel between two or more SUs based on their user requirement. This function is necessary to minimise interference among users [28].
- Spectrum sensing: Refers to the ability of the network to detect unused spectrum without interfering with the PUs or other SUs. Sensing also detects the arrival of the licensed user in the spectrum [28].
- Spectrum management/decision: This refers to the identification of the best possible spectrum to meet user requirements which may be data rate, delay sensitivity and packet error rate [29].
- Spectrum mobility: Refers to the ability of the network to maintain user communication requirements seamlessly during the transition to better spectrum.

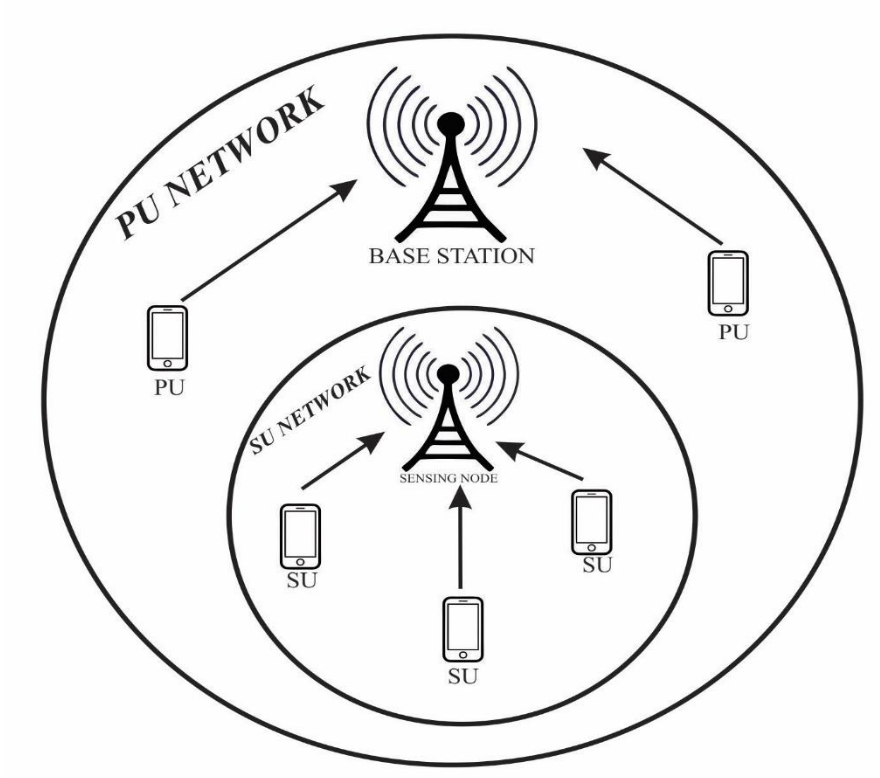

Figure 2.1: System model of a cognitive radio network

Several cognitive radio techniques can be employed in this continued quest to solve the congested spectrum problems. These techniques can be implemented by allowing the primary users' signals underlying, overlaying or interweaving the secondary users' transmission signals [30]. These schemes will need to maintain the condition that the unlicensed secondary users do not affect the licensed users' performance. The underlay technique allows the secondary users to share the licensed primary users' spectrum band as long as the quality of service constraint is observed. The overlay approach, just like the underlying approach, allows the concurrent transmissions of the licenced and unlicensed users by allowing the secondary users to assist in relaying primary user transmissions. The overlay scheme is dependent on the transmission power metric. The secondary users split their power between transmitting their signals and the remainder in assisting primary user transmissions. The interweave approach utilises the presence of spectrum holes that are left unused by the licensed users. The secondary users can, therefore, initiate their communications by using these frequency 'voids'.

2.3.2 Underlay Model

The underlay model is based on the assumption that the cognitive users know all the interferences they cause on the non-cognitive users. The cognitive users are the unlicensed secondary and the non-cognitive users are the licensed primary users with the quality-of-service (QoS) requirements that need to be maintained. The underlay paradigm allows for concurrent primary and secondary network transmissions provided the interference from the cognitive users is controlled and kept below a tolerated limit ensuring that the secondary users' transmissions do not affect the performance of the primary users. Multiple techniques can be used to help minimise the interference that the secondary users impose on non-cognitive users. These include implementing the use of many antennas for transmission and this will allow secondary user transmissions to be directed away from the licensed users' receivers. The reduction of secondary users transmit power is also another method of managing the interference suffered at the primary user receivers. The above-mentioned measures are quite constraining, and this limits the transmissions in this paradigm to short-range communications. Techniques like introducing relays, which will be discussed later, work well with the underlay spectrum sharing scheme to increase coverage.

2.3.3 Overlay Model

The overlay model also permits the concurrent transmissions of primary and secondary users. The overlay model bases its operation in 2 different approaches: the selfish and the selfless approach. In the selfish approach, the secondary user uses all its transmit power to "do" its transmissions. This approach implements the dirty paper coding technique to cancel interference. This approach deviates from the cognitive radio principle of protecting primary users. The selfless approach depends on power splitting between secondary user own transmissions and secondary users assisting in primary user transmissions. The secondary user allocates some of its power to help in relaying the primary user transmissions to the primary receiver and the remainder of its power to carry out its transmissions. This is made possible with the assumption that the primary user message code is known by the secondary users. This in turn, improves the primary user signal-to-noise ratio as its transmissions will be assisted. The secondary users' transmissions have a certain degree of interference that they impose on the licensed primary users. The trade-off between the increase in primary user SNR and secondary users' interference warrants that the transmission rates of the primary users remain unchanged.

2.3.4 Interweave Model

The interweave model is based on the existence of spectrum holes in the licenced spectrum. The existence of these 'frequency voids' varies with geographical location and time and can be utilised for secondary user communications. This technique speaks into frequency reuse of these spectrum holes thereby improving spectrum utilisation. The interweave model has the least interference amongst the main CR paradigms.

In summary, the above spectrum sharing models can be differentiated in the following ways: overlay and underlay paradigms allow for simultaneous transmissions of the primary and secondary users while the interweave model does not permit concurrent communications of the cognitive and non-cognitive users. The underlay model requires knowledge of the interference that the secondary users impact on the primary users' network while the overlay paradigm entails that the secondary users require knowledge of the primary users' code-word and message for them to be able to properly assist in relaying this information. The secondary users assist in the primary users' transmissions by splitting their transmit power. This, however, has an amount of interference that is felt on the primary users' receivers. The interweave model requires knowledge about the user activity and this is what paves way for the location of frequency voids. Some work has been done to combine the advantages of these paradigms with the best example being work that has been looked at in [31] which combined the advantages of the overlay and the interweave spectrum sharing paradigms. The cognitive users transmit power in the underlay model is determined by the interference constraint and the cognitive users in the overlay model can transmit at basically any power since this power is split between its transmissions and relaying the non-cognitive users' transmissions. The interweave paradigm has the secondary users transmit power limited by the range of its spectral hole sensing.

The cognitive radio main drawback, especially in the underlay and interweave models, is the limitation in the transmit power of the secondary users. This negatively impacts cognitive transmissions in terms of reliability and network coverage. To improve on these limitations, technologies like cooperative relaying can be implemented. This technology will help in reducing transmissions distances thereby reducing on the path-loss suffered between transmitters and receivers.

2.4 Cooperative Communications

This technique allows intermediate nodes that assist with transmissions between transmitters and receivers. These nodes are referred to as relays and have the main objective of forwarding the source information to the destination, thereby improving the network coverage and system reliability [30]. The operation of cooperative communications is dependent on knowledge of the transmitted signal by the 'assister' which is the relay. This technique improves the transmission reliability, improves robustness to channel impairments, extends the network coverage area and increases the system throughput – without the requirement of additional transmit power. Detrimental effects of path loss are also reduced as the distances of transmissions would have reduced which will improve the end-to-end signal attenuation rates. Line-of-Sight (LOS) propagation has been studied to perform better than scattered propagation in terms of end-to-end signal-to-interference ratio. High transmission rates can be implemented to counter this drawback on multipath fading. Multipath fading causes outages and many diversity techniques have been studied to help counter these outages. These are frequency diversity, space diversity, time diversity and cooperative diversity. Of all the above-stated diversity techniques, cooperative diversity has the best wireless link rate-costs trade-off [32].

As illustrated in Figure 2.2, cooperative relaying introduces more than one paths of transmitting signals from the source to the destination. If one of the routes is in an outage, messages can still be transmitted using the other route and this reduces the chances of an outage.

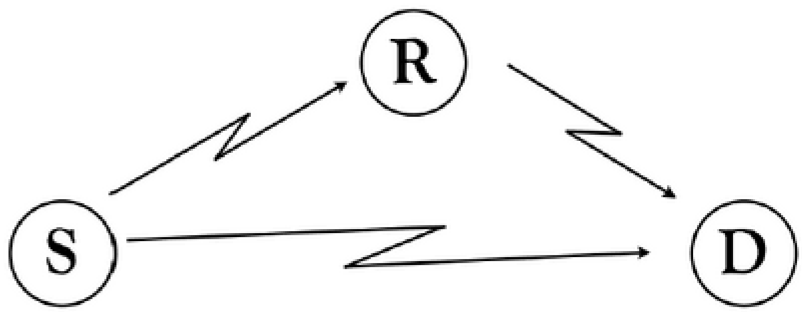

Figure 2.2: Simple cooperative relay network

2.4.1 Relaying Network Design

The relay transmissions model can be set up in two common topologies namely the serial relay transmission topology and the parallel relay transmission topology. For long distances, where power gain is of importance, the serial relay transmission topology suits better. In this model, signals are passed from one relay to the next in hops. Channels are kept orthogonal as much as possible to minimise on interference. In scenarios where multi-path fading is heavy and negatively impacting the serial relay transmission topology, the parallel relay transmission topology is more economical and more efficient to deploy. The parallel topology provides many transmission channels thereby increasing the chances of successful transmission from source to destination. With the signals having followed several routes from the source to the destination, there is need, at the destination, to combine these separate channels into the original message from the sender and many combining schemes can be implemented. These include the common maximal ratio combining (MRC), equal gain combining (EGC) and selection combining (SC) diversity schemes. Some schemes like the RAKE combining receiver, widely used in a code division multiple access (CDMA), the zero-forcing (ZF) receiver and the minimum mean square error (MMSE) equaliser are also present. All these have been studied to achieve SNR gains.

2.4.2 Modes of Operation

The operation modes of relays can be full-duplex or half-duplex. The full-duplex (FD) mode allows the relay to receive messages from the sender while transmitting messages to the receiver at the same time. The major drawback of the FD mode is the losses suffered from self-interference. The half-duplex (HD) mode has been considered in much literature ([31] - [36]), because of the reduced complexity in dealing with self-interference. The HD, however, also comes with several disadvantages that include a reduction in multiplexing gain by employing two orthogonal time slots. Carefully timing two HD relays, can mimic the operation of a full-duplex relay although it brings on board the issue of inter-relay interference. A combination of both modes is feasible although it comes at a complexity cost. Separating the receive and transmit antennas on the relay will go a long way in suppressing the self-interference and thereby maximising on spectral efficiency. To both the FD and HD operation modes, the following duplex principles can be applied: Time Division and Frequency Division Relaying. As the names correctly direct, the relaying operation is based on different time slots and alternate frequency bands respectively.

2.4.3 Relaying Strategies

Cooperative relaying is distinguished into three main relaying strategies namely amplify-and-forward (AF), decode-and-forward (DF) and compress-and-forward (CF).

- Amplify-and-Forward: the relay receives and amplifies the signal, translates the frequency, and retransmits the amplified signal [36].
- Decode-and-Forward: In this strategy, the relay overhears source transmissions, decodes them, and passes the signals to the destination [37].
- Compress-and-Forward: This strategy works almost similar to the DF. This strategy permits the relay to compress the received signal from the source and pass it to the destination without decoding the signal [38].

Much work has been done on cooperative relaying centred on the AF and DF relaying strategies. This process of decoding by the relay is known as making a hard decision. The relay does this without the end-to-end link knowledge thereby making a hard decision. In the amplify-and-forward protocol, the relay receives and amplifies the signal before it retransmits the amplified signal to the destination. The relay amplification factor is multiplied with the signal source-to-relay SNR and this will be the amplified signal. There is not much hard decoding that takes place in amplify-and-forward and efficiency is dependent on a well-received signal-to-noise ratio otherwise it would just forward mostly noise. Some recent works have started on combining the two protocols (see [39] – [41]).

2.5 Multi-Relay Scenario – Relay Selection

The performance of a cooperative communication system can be enhanced by using multiple relays, rather than a single relay, which forwards the same information to the destination. Specifically, the introduction of multiple relays is designed to maximise the end-to-end SNR of a system thereby reducing the outage probability and increasing the sum-rate of a system. However, using all the relays available in the system all the time for the secondary users in a cognitive radio system may not be a practical idea because the interference caused by the relays to the primary base station may exceed the threshold. The other major drawback of using many relays for transmission is that it is resource intensive. The system throughput also suffers when relays transmit in orthogonal channels. All this has promoted the need to perform relay selection and several single and multiple relay selection schemes have been developed [42].

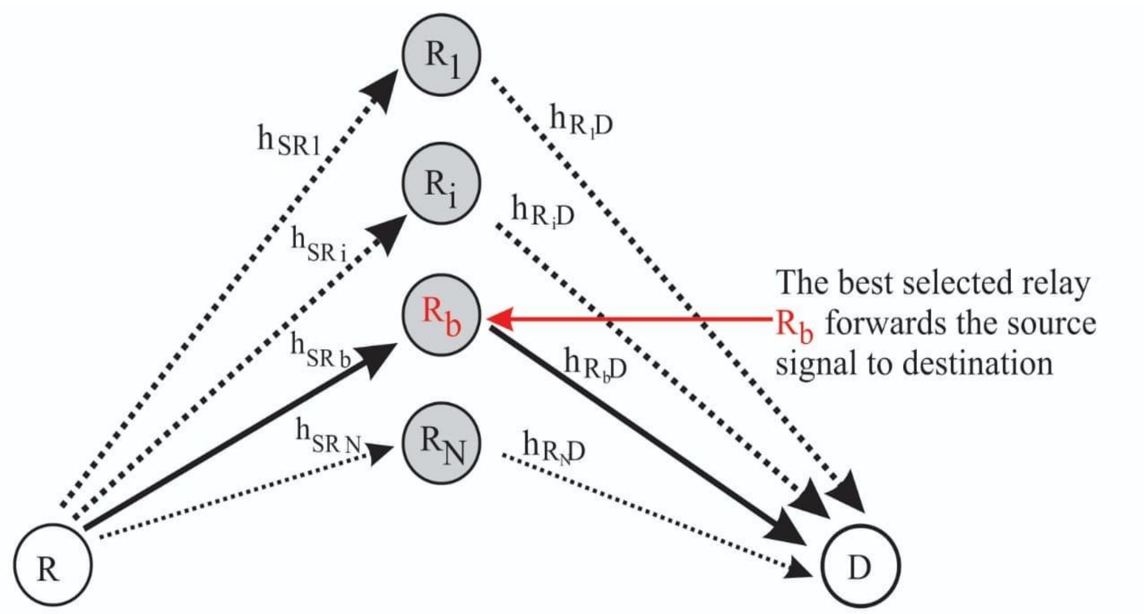

Figure 2.3: Multi-relay cooperative communication system with best relay selection

2.5.1 Relay Selection Schemes

Relay selection is the process of selecting the best relay(s) from a pool of available relay to assist with the transmissions from the source to the destination. The process can be executed by either selecting a single relay to do the transmissions, which is known as the single relay selection scheme or by selecting many relay nodes to assist in transmissions, known as the multiple relay selection scheme. The single relay selection schemes select just one node to act as the relay and these schemes include:

- Best Relay Selection: selects the relay which provides the path with maximum SNR. This is the most favourable selection scheme
- Nearest Neighbour Selection: selects the nearest relay to the destination. This selection scheme is not limited to distance but entails selecting a relay with the best channel to the receiver or transmitter.
- Best Worse Channel Selection: selects the relay which has the best channel conditions in its worse channel. In half-duplex relays, each relay has two channels, the source-to-relay and the relay-to-destination channels. By carefully analysing the worse of the two channels for every relay present, the relay with the best 'worse' channel cooperates.
- Best Harmonic Mean Selection: selects the relay with the highest harmonic mean. The relay function metric in this scheme is the harmonic mean of the source-to-relay and relay-to-destination channels' magnitudes.

The general assumption in single relay selection schemes is that each relay only knows its channel conditions and the receiver knows all the channels for all the available relays. The single relay selection scheme focuses on maximising the worst SNR of the nodes.

The second relay selection scheme is the multiple relay selection scheme which permits the selection of more than one node to cooperate. In the presence of say N relays and with each relay having two choices, then there is a $2^N - 1$ chance of a relay being selected for transmission [43]. The general assumption, like in a single relay selection scheme, is the receiver knows all the channels and hence it can always search for the most favourable path(s). Multiple relay selection uses the concept of relay order to trigger the selection of a set of relays [44]. This selected set of relays will still maximise the worst SNR of the nodes. Other multiple relaying selection schemes include linear complexity and quadratic complexity.

2.5.2 Relay Selection Strategies

There are two well-known strategies for relay selection namely the opportunistic relay selection (ORS) and the partial relay selection (PRS). Opportunistic relay selection, also known as the best relay selection (BRS), considers the channel state information (CSI) of the source-to-relay phase and the relay-to-destination phase. This strategy involves selecting a relay, from a pool of available relays, with the highest end-to-end SNR. Relay selection in this protocol is based on instantaneous channel conditions and this implies that the effects of shadowing and fading are well-considered at each selection point. Previous knowledge of the channel by the relay cannot be used to select the relay. Issues like distance contribute to this selection process to a lesser extent. Due to strict orthogonal rules, communication amongst the relays is almost non-existent and this is one of the advantages of this protocol, minimum overhead incurred in selecting the relay. A single relay in best relay selection can attain the same diversity as N relays transmitting at the same time.

Partial relaying, unlike ORS, only requires the CSI of the first hop, source to relay, or only the second hop from the relay to destination thereby improving the feedback-overhead efficiency of the system. Partial relay selection is based on the average SNR. Although this strategy of selection is not best suited for time-sensitive networks and operations, it does bring some positives with it that also improve network efficiency and lower cost of operation. Partial relay selection has several schemes that include reactive relay selection and proactive relay selection. In reactive relay selection, the selection process is done after the user has transmitted already. This implies that the relays will only react to the transmitted SNR and thereby trigger selection. The relay-to-destination transmissions are then carried out using the selected relay. On the other hand, proactive relay selection is done before the source transmissions. Be it single relay selection or multiple relay selection, it is only the selected relay(s) that will take part in relaying the data to the destination.

2.5.3 Relay Selection Criteria

2.5.3.1 Max-Min Relay Selection Criteria

A variety of criteria for relay selection have been proposed as a way of maximizing capacity or minimizing outage probability in conventional relay networks [45] - [47]. The max-min criterion, which maximizes the minimum of signal-to-noise ratios (SNRs) of the source-to-relay link and relay-to-destination link, has proven optimal for this purpose [46]. The two most common schemes are bottleneck based and the maximum harmonic mean based best relay selection (BRS) [47].

$$l^{*} = \arg \underbrace{max}_{k} \; min\left\{ \left| h_{S_k} \right|^2, \left| h_{k_D} \right|^2 \right\}, \quad (2.1)$$

where l^{*} is the selected relay index in conventional relay networks. This implies that the relay is chosen based on the channel gains, $\left| h_{S_k} \right|$ and $\left| h_{k_D} \right|$, of the relaying links.

2.5.3.2 Max-Max Relay Selection

This selection protocol maximizes the maximum of the signal-to-noise ratios (SNRs) of the source-to-relay link and relay-to-destination link to reduce the outage probability of the system.

$$b^* = \arg\underbrace{max}_{k}\ max\left\{\left|h_{S_k}\right|^2, \left|h_{k_D}\right|^2\right\}, \tag{2.2}$$

where b^* is the selected relay index in conventional relay networks. This implies that the relay is chosen based on the channel gains, $\left|h_{S_k}\right|$ and $\left|h_{k_D}\right|$, of the relaying links. This selection criterion achieves optimal gains when used in conjunction with buffer aided relays. Buffer aided relays allow for the flexibility in selecting a relay for either reception or transmission or both. The selection in conventional relays considers the same relay for both reception and transmission although the best relay on the source-to-relay link might not be the best for the relay-to-destination link. This research will, however, only consider the conventional relays.

Reference [10] studies an amplify-and-forward relaying underlay spectrum sharing system. The system model in this paper implements the best relay selection scheme and we subsequently analyse the outage probability of the system. Pamela *et al* in [49] looks at partial relay selection in an underlay cognitive network with primary-user interference constraints. A node, based on the partial relaying scheme, is selected from a cluster of relays to transmit the information. The partial selection of the participating relay is based on the channel conditions of source-to-relay links $S \rightarrow R$, $n = 1, \ldots, N$. Exact and asymptotic closed-form expressions for the outage probability of the CRN are derived considering the effects of the primary source and the primary interference temperature on the performance of the secondary network. Unlike in [49], [50] analyses partial relay selection by choosing the best relay that maximises the instantaneous channel strength of the relay-to-destination link. Both the works in [49] and [50] conclude that this selection criterion is optimal in terms of outage performance.

The work in [51] analyses a cognitive radio network with best relay network selection. Closed-form expressions for the outage probability for the secondary network are derived, with the constraint of observing a target outage probability for the primary transmissions (primary outage probability). This paper proposes a system model with relay assisted transmission and relay selection. The relay selection methods include best relay selection method, the nearest relay selection method, two best relays selection method and the two nearest relays selection method. The performance analysis investigates the outage probability and Monte-Carlo simulations are provided to assess the correctness of the mathematical derivations. The selection of two relays shows a diversity gain as compared to the selection of just one relay. In conclusion, the outage performance of the proposed schemes shows that the best relay selection method outperforms the other schemes. The selection of two relays has a significant performance improvement.

The aforementioned research investigates interference-limited relays with zero interference at the destination. The authors in [52] study relay selection on an interference-limited destination and with zero interference at the relays. As will be shown later in this dissertation, this current work will incorporate the effect of the PU interference on both the secondary network relay nodes and at the secondary destination. Literature in [53] uses blind techniques such as independent component analysis (ICA) for non-Gaussian random variables [54], blind source separation (BSS) techniques for Gaussian signals [55], [56] or other methods [57] to mitigate the interference from the primary users at the secondary destination and this disarms the authors in analysing the effect of PU interference at the destination. They also model the noise at all secondary terminals as unit variance, $n \sim \aleph(0,1)$ where $\aleph$ defines the normal distribution. This motivates this research to consider the primary user interference and noise at the secondary destination.

2.6 Conclusion

This chapter introduced the concept of cognitive radio and how much ground this technology has covered in trying to decongest the overcrowded spectrum and improve spectral efficiency. Different models are explained and the respective advantages that come with each model. One of the disadvantages of spectrum sharing which is the constraint on transmit power remains a problem that needs to be addressed. As explained in this chapter, cooperative communications have been studied to counter the transmit power constraints and thereby increasing link reliability and extending network coverage. Relay selection concepts have also been introduced and have shown how they improve the overall performance of a wireless system. The following Chapter 3 introduced other technologies that can be used together with the spectrum sharing and cooperative relaying techniques to obtain a collectively improved system.

Chapter 3 Literature Review – Wireless Energy Harvesting and Massive MIMO

3.1 Introduction

This chapter introduces the concept of wireless energy harvesting to a wireless communication system. As mentioned before in the introduction of this dissertation, issues surrounding energy efficiency are critical to the next generation of wireless communications. Power sensitive applications are on the rise and hence the quality-of-service (QoS) becomes an aspect that cannot be tampered with. Coupled with energy efficiency, another aspect that forms the core of 5G wireless communications is transmission speeds. Speeds in the orders of gigabits are set to come with 5G and research has been focused on techniques to attain such speeds. One of the promising methods towards attaining such speeds has been the implementation of a technology known as massive multiple-in multiple-out (MIMO). This chapter provides a brief description of massive MIMO, its different schemes and how it can be merged with other studied techniques to improve the overall system performance.

3.2 Wireless Energy Harvesting

Energy harvesting, an eco-friendly and self-sustainable technique, has risen as a promising technology in increasing the sustainability of wireless networks. It is a process of harnessing heat or sound energy from radio frequency signals and converting the energy into electricity. Providing the energy harvesting capability to wireless devices enables the network nodes to repeatedly obtain energy from radio frequency (RF) signals and this, in turn, provides a promising future for wireless networks in terms of self-sufficiency and long-lasting performance. Due to the need to support some critical applications with quality-of-service (QoS) requirements, energy efficiency in wireless networks has always been an area of major concern and significant work has been done in this field but more issues still remain to be addressed. With the proliferation of wireless applications and services, rapid growth in traffic demands and the number of subscribers is inevitable, hence the transmit energy consumption becomes critical.

The concept of wireless power transfer (WPT) was originally developed by Nikola Tesla in the nineteenth (19^{th}) century, where energy is transmitted from a power source to a destination over the wireless medium. In 1891, Tesla managed to light electric lamps by wirelessly transferring power. The idea looked to have been shelved because of the fairly low energy transfer efficiency since only a small fraction of the transmitted energy would be harvested and earlier electronic gadgets were bulky and experienced high-power consumptions. With the continuous improvements in the design of electronic devices, communication systems became low-power consuming networks and this motivated the revival of this concept of wireless power transfer.

Wireless power transfer (WPT) was pursued to maximise the efficiency of energy transmission and on the other hand the aim of wireless information transfer (WIT) is to maximise the rate and capacity of information transmission. This paved the way for the integration of the two techniques into simultaneous wireless information and power transfer (SWIPT) [58] which many wireless communications applications have implemented. This was made possible by the fact that the design objectives of the two systems can be merged without too much complexity. SWIPT, also known as in-band energy harvesting, brings on-board the advantage of conveying controllable, constant and efficient on-demand wireless information and energy simultaneously, which offers a low-cost option for sustainable operations of wireless communication systems without hardware adjustments on the transmitter side. However, research in (see [59] – [60]) has recognised the trade-off that exists between transmitted information and transferred energy and pointed out the need to redesign existing wireless networks. Smart antenna technologies and new receiver designs can be properly exhausted to practically implement the SWIPT concept in actual wireless networks [60]. This concept drives the idea of energy self-sufficiency to low power communication networks based on the fact that transmitted RF signals carry both information and energy.

In [60], it is also concluded that both information decoding (ID) and energy harvesting (EH) cannot be performed on the same signal generally due to practical limitations as the RF energy harvesting process would distort the information content. This limitation is tackled in the design of the two main receiver architectures namely the separated receiver architecture and the co-located receiver architecture. The separated receiver architecture, also known as antenna-switching, provides an energy harvester and information receiver with independent antenna(s) so that they detect different channels. Energy harvesting and information transfer are performed independently and concurrently that is, if a system has two receivers for instance, when one receiver is decoding information in one-time slot, the other receiver can switch into energy harvesting mode and take advantage of the same signal in that very same time slot to harvest energy. The co-located receiver architecture allows an energy harvester and an information receiver to share the same antenna(s) so that they detect the same channel(s). Since a single antenna can be adopted in this architecture, SWIPT allows for the scavenging of information and energy simultaneously by implementing the time switching and power splitting energy harvesting methods. These methods enable information decoding and energy harvesting to take place at a node.

3.2.1 Time Switching Protocol

The time switching protocol is based on a simple switcher which allows the node to periodically receive and decode information or harvest energy, hence the term switching. The power of the harvested energy at a time-switching receiver b, from the source a is calculated as follows:

$$P_{a,b} = \eta P_a \left|h_{a,b}\right|^2, \qquad 3.1$$

where $P_{a,b}$ is the power of the harvested energy as the signal is transmitted from the source a to receiver b and P_a is the source transmit power. η is the conversion efficiency and $h_{a,b}$ is the channel gain from source a to receiver b. Receiver nodes can exploit time switching by taking turns to either decode information or harvest energy simultaneously. In the case of a single receiver, the antennas have to switch between information decoding and energy harvesting and this is a typical case of the co-located information decoder and energy harvesting receivers. Using the same antenna for both information decoding and energy harvesting makes this protocol less complex. The time switching sequence and the signal can also be jointly optimised to yield the most favourable system performance. Studies in [61] have established the motivations that would promote the implementation of time switching. Firstly, time switching can be implemented on pre-existing off-the-shelf separately designed antennas for information decoding and energy harvesting and this reduces the receiver's complexities. Secondly, time switching can effectively utilize both the energy/information receiver power sensitivity differences and the channel or interference power dynamics to optimise its switching operation. This implies a receiver can be in energy harvesting mode when the channel interference is high and be in the information decoding mode when the channel interference is at its lowest. Interference is an undesirable condition in a wireless communication channel and mitigation approaches have been studied extensively. These include decoding strong interferences or merely regarding it as noise when the interference is weak [62]. The work in [63] has looked at the "interference alignment" approach as another way to control interference but recent research works have established that interference can be utilised as a source of wireless energy harvesting. The receiver can operate in either of the three sub-optimal receiver mode-switching rules which are the periodic switching, interference-based switching and the signal-to-interference and noise ratio (SINR) based switching [61]. In [61], these switching rules are being studied on single-user setup and more research can be directed to a multi-user setup and deal with how many transmit-receive links in an interference channel can work together to utilise interference by balancing between information decoding and energy harvesting. Another SWIPT receiver architecture implements the energy harvester circuit and the information decoder as two different receivers with separate antennas both served by the common transmit antenna.

3.2.2 Power Splitting Protocol

A power splitting protocol, based on a power splitter, splits the received RF signal into two streams for the information receiver and RF energy harvester with different power levels according to the set power splitting ratio. The power of the harvested energy at a power-splitting receiver b, from the source a is calculated as follows:

$$P_{a,b} = \eta P_a \left|h_{a,b}\right|^2 \theta_b, \qquad 3.2$$

where η is the energy harvesting efficiency factor, P_a denotes the source transmit power and $\left|h_{a,b}\right|^2$ is the channel gain between source a and receiver b, and $\theta_b \in [0,1]$ represents the power-splitting co-efficient for receiver b and it is the fraction of the radio frequency signals reserved for energy harvesting. The power splitting ratio can be jointly optimised together with the signal for improved antenna performance. For each receiving antenna, there is at least one power splitting device. The technique of power splitting allows for both information transfer and wireless energy harvesting to occur simultaneously without the need to switch receivers like what happens in the time switching protocol. The antennas are designed to be able to autonomously adjust the power splitting ratios between information decoding and energy harvesting.

3.2.3 Energy Harvesting in Wireless Networks

The trade-off between the information decoding rate and the amount of harvested energy can be optimised. The authors in [59] characterise the differences between power splitting and time switching protocols and examine their achievable rate-energy regions. More studies on power splitting and its impact on the trade-off between the achievable information transfer and the average harvested energy are investigated in [64]. As stated earlier, the amount of transmitted information and transferred energy cannot be generally maximised at the same time and this gives rise to the need for more work in redesigning existing wireless networks. The time-switching and power splitting energy harvesting methods come in with some complexities too. Strict time synchronisation has to be taken into consideration when dealing with time switching while hardware nonidealities may degrade system performance in power splitting. Another major disadvantage that comes with time switching is the fact that information transmission is not continuous since some time slots will be dedicated to energy harvesting only and this becomes critical in instances where the Quality of Service (QoS) is of paramount importance. Antenna switching receivers have been proposed in [58] as these are easy to implement in practical SWIPT designs. This can be regarded as a special case of power splitting. Suppose a receiver has a total of N antennas and the L strongest paths are allocated for information decoding and the remainder, $N - L$, are used for energy harvesting and/or vice versa. The allocation sequence is investigated numerically and theoretically then subsequently applied. This mechanism does not require any extra hardware and it is based on pre-existing schemes like the channel estimation Generalised Selection Combiner (GSC) techniques [59] hence reduced complexity. Other schemes that can be used for antenna assignment are the power splitting based optimal scheme and the binary knapsack optimal scheme and these are high complexity schemes in that they respect the limitation that each antenna can be used for both decoding and rectification. The outage probability for these schemes is analysed in [65] for a multiple-in multiple-out (MIMO) relay channel. Focus in this study is on the multiple antenna decode and forward relay. Each antenna is either used for information decoding or rectification and the output of each antenna is connected to one of the radio frequency combining circuits (RFCC) namely RFCC1 and RFCC2. RFCC 1 is used for combining all information decoding antennas and RFCC 2 combines all rectifying antennas.

Conventionally the performance of a wireless communication system is based on the efficiency of information transfer and reception but with radio frequency energy harvesting in consideration, the trade-off between transmitted information and transferred energy has to be taken into account [59]. Incoming energy-flow into a radio frequency energy harvester can be categorised into two different modes of use namely harvest-use (HU) and harvest-store-use (HSU) [63]. In HU, the harvested energy is used for information transmission immediately whereas in HSU the harvested energy can be stored for later use. The HSU mode suffers from the existence of storage loss and subsequently reduced battery efficiency in practical batteries. Harvest-use-store uses the harvested energy for data transmission and stores the remaining energy for the next transmission phase.

Efficiency of energy harvesting depends on the efficiency of the antenna [65] and work in [66] has shown that the implementation of massive MIMO networks provides unprecedented gains in spectral efficiency and can yield more harvested energy. Many transmit antennas can allow for some of the antennas to be used for beamforming and this could significantly improve the efficiency of information and energy transfer [67]. The authors in [59] study two scenarios where the first scenario looks at separate information decoder and energy harvester. This implies different MIMO channels from the transmitter. The second scenario considers co-located information receiver and energy receiver hence the same MIMO channels from the transmitter. The different trade-offs for the different scenarios are studied. The transmission power per user and per antenna is also reduced and the outage probability performance is significantly improved [68]. Multiple antennas allow for out-of-band radio frequency energy harvesting to take place as the node can be able to harvest energy from the frequency band different from that used for data communication. This also paves the way for the concept of energy cooperation. Different network topologies with MIMO configuration have been reviewed to establish a favourable trade-off between system performance and complexity [60]. Multiple antennas come short in that they require multiple rectifying circuits and this, in turn, increases the complexity of the system. Co-channel interference (CCI) has to be taken into account and various strategies that counter interference has to be implemented in SWIPT systems. Information can be transmitted along interference-free channels and energy is transferred on the remaining channels. User scheduling can also be employed to allow receiver antennas to switch their roles between energy harvesting and information decoding based on channel conditions and this increases the trade-off region between the information transfer rate and the harvested energy [65]. Various authors [69] and [70] have also studied the contribution of EH relay assisted SWIPT systems and their edge over the conventional systems with self-powered nodes. Power allocation strategies have been analysed and implemented to ensure that the outage probability deteriorates more quickly at a rate of 1/SNR (signal-to-noise ratio) [70].

Relay selection is a technique that has shown that the quality of the source-to-relay path is crucial for the determination of transmission consistency (reliability) from the source to the relays and also the amount of the harvested energy at the relay. Some studies show that there has been recent vast consideration of applying energy harvesting techniques to relay networks [20], [71] and [72]. The work in [69] has examined the amplify and forward relaying systems where an energy-constrained relay harvests energy from the source signal for information transmission. The decode and forward relay system is analysed in [71]. Energy harvesting AF relaying network with the channel suffering from interferences and the Nakagami-m fading has also been studied by [73] and has proven that the time switching relaying protocol is more sensitive to energy harvesting than the power splitting protocol under the same channel parameters and state.

3.3 Background on Massive MIMO

Massive *multiple-input multiple-output* (MIMO), the technology of equipping a communication system with a very large number of service antennas, has become an interesting area of study due to its potential to greatly improve the spectral and energy efficiency of a system. The number of antenna elements at the transmitter and/or receiver can be in the order of hundreds or thousands which promotes the simultaneous transmission of data to several users at any given time. With the continued increase in the expansion of mobile networks, massive MIMO is a promising solution in meeting the demand for higher data capacity and increased throughput. Adding more antennas is always favourable for higher throughput, reduced transmission power, consistent uniform substantial service everywhere in cellular cells, and reduced complexity in signal processing. The exponential growth in wireless data traffic has been mainly due to the emergence of smartphones, tablets, personal computers with high-intensity data transfer functionalities like video streaming and other smart communication devices.

As the amount of the available electromagnetic spectrum remains constant [27], this has created a problem in wireless systems in trying to meet and service the ever-increasing demand. Massive MIMO systems, also known as *Large-scale antenna systems,* have emerged as a feasible and the most useful solution in addressing this problem. Massive MIMO systems simplify the required signal processing with the implementation of robust and simple approaches such as MMSE and zero-forcing precoding schemes. Authors in [25] have shown that massive MIMO systems could achieve data rates over 17Mb/s for each of the 40 users in a 20MHz channel in both the uplink and downlink directions and an overall spectral efficiency of 26.5 bps/Hz under realistic propagation assumptions. Since the number of service antennas is notably more than the number of users, this allows for the transmitted signals to be shaped or directed in such a way that counters interference. Massive MIMO is scalable and an increased number of antennas at the transmitter/receiver would also mean a large number of degrees of freedom provided by the propagation channel and hence improved reliability. The authors in [26] have shown that a single antenna user in a massive MIMO system can reduce its transmit power in proportion to the number of antennas at the base station (BS) with perfect channel state information (CSI) or the square root of the number of BS antennas with imperfect channel state information, to achieve the same results as in a single input single output (SISO) system. This improves the overall energy efficiency of the system. Also, compared to a SISO system, a massive MIMO system with sufficient transmit power, has a wider operational range and this improves the aggregate efficiency of the system.

Massive MIMO uses spatial multiplexing (SM) to send several data streams. Unlike time-division multiplexing which transmits various data streams at different times and frequency division multiplexing which transmits data over different frequencies, spatial multiplexing allows an antenna array to transmit various data streams, all occupying the same time resources and over the same frequency resources. Spatial multiplexing requires channel state information to facilitate mapping of the data streams onto the respective signals that drive each of the antennas and each user receives only the data stream that is intended for it. Increasing the number of antennas relative to the number of users paves way for improved beamforming which multiplies the data rates of transmission to users, effective power control and hence uniformity of service throughout the cell. The uplink operation of a massive MIMO system is essentially the same as the downlink operation though in a reverse direction. Spatial multiplexing is also exploited in the uplink in that the users transmit their data streams at the same time and over the same frequencies towards the antenna array. Multiplexing and de-multiplexing operations are done at the end of a propagation channel and this implies that the two operations use measured channel characteristics other than estimates or assumed channel properties. This allows proper utilisation of the measured channel characteristics. The following subsections explain, in detail, point-to-point MIMO, multi-user MIMO and massive MIMO.

3.3.1 Point-to-Point MIMO

Point-to-point MIMO link encompasses the transmission of data from a transmitter with a concentrated array of many antennas to a user with a concentrated array of several antennas as well. Point-to-point MIMO uses time division and frequency division multiplexing techniques. The author in [27] formulated that the spectral efficiency of the link in a point to point MIMO is given by

$$C \propto \min(M, K)\log_2(\rho_d),\ \ \rho_d \gg 1, \tag{3.3}$$

where ρ_d is the expected signal-to-noise ratio (SNR) at any of the receivers provided one or more of the transmit antennas is operating at full power, M is the number of transmit antennas and K is the number of receive antennas. The above equation clearly shows that by simply increasing the number of antennas, the throughput of the system can be increased as well. The general perception of transmission in point to point MIMO systems is that the transmit antennas send a vector-valued signal component which contains defined pieces of data. As the vector-valued signal travels along the channel, it is multiplied with the channel matrix to produce a vector of the signal which is retrieved at the receiver. For well-known channel properties, the receiver can perfectly extract the transmitted component from the received vector signals. The MIMO received signal can be written as

$$\mathbf{y} = \mathbf{Hx} + \mathbf{n}, \tag{3.4}$$

where **y** is the K x 1 received signal vector, **x** is the M x 1 transmit vector and **n** is N_r x 1 noise vector and also includes interference. **H** is the channel matrix given as $\mathbf{H} \in \mathbb{C}^{K\text{x}M}$. Each ($n$,$k$) element of the matrix **H**, $h_{n,k}$ represents the channel coefficient between the kth transmitter and the nth receiver antenna for $1 \leq k \leq M$ and $1 \leq n \leq K$. Transmission of a signal vector produces better performance as compared to single symbol transmission [25]. To gather information about the characteristics of a channel before transmitting signals, a pilot signal with known properties is transmitted through the channel first and is detected. The received signal is compared against the transmitted pilot signal and hence figure out the elements of the channel matrix. Point-to-point MIMO is restricted to a maximum of 8 transmit antennas and 8 receive antennas under the current 802.11ac wireless standard. This limits the scalability of point-to-point MIMO to nothing beyond the 8 x 8 MIMO system. This is one of the drawbacks of point-to-point MIMO. In [27], a formulation of the sample duration of the pilot signal in the uplink and downlink operations is presented and is shown to be, at the barest minimum, equal to the sum of the number of transmit and receive antennas or better still greater than the sum.

$$\tau_d + \tau_u \geq M + K, \tag{3.5}$$

where τ_d and τ_u are the sample durations of the pilot/reference signal in the downlink and uplink respectively. Equation (3.5) implies that increasing the number of antennas would require a proportional increase in the amount of pilot sampling which is undesirable. Another drawback of point-to-point MIMO is that more signal processing is required at both the transmit side and receiver to experience system performances close to Shannon capacity. The above drawbacks are mitigated by implementing Multi-User MIMO.

3.3.2 Multi-User MIMO

A multi-user MIMO (MU-MIMO) system is typically a transmitter with multiple antennas that serve a set of several independent single antenna users concurrently. One of the strategies used in MU-MIMO is dirty paper coding (DPC) which can achieve a linear capacity increase in the transmit antennas regardless of the number of receive antennas [74]. DPC is a technique for efficient transmission of information through channels exposed to interference that is known by the transmitter. The overall Shannon sum capacity of the uplink in MU-MIMO systems is given by [28]

$$C_{sum\ up} = log_2 \det \left(I_k + \frac{\rho_u}{K} . G_u^H G_u\right), \tag{3.6}$$

where G_u is the M x K frequency response of the channel matrix between the user and the base station, I_k is the K x K identity matrix, G_u^H refers to the conjugate transpose, ρ_u is the expected signal-to-noise ratio (SNR) at any of the transmitters and det(.) is the determinant of the matrix. The users are not capable of communicating with each other and this entails that processing equipment is only needed at the transmitter end. This makes MU-MIMO relatively cheaper.

MU-MIMO is less susceptible to the propagation environment as compared to the point-to-point MIMO due to the multi-user diversity nature of MU-MIMO [28]. MU-MIMO results in improved energy efficiency because, from the transmitter, the emitted energy can specifically be directed only towards the terminals. This principle is known as beamforming and MU-MIMO uses the same principle to reduce interference because the transmitter can correctly avoid transmitting into interference zones. Knowledge of the channel matrix is required by the receiver in both the uplink and downlink operations and the separate users need to acquire the channel matrices for the respective downlink channels. The time it takes to gather this channel state information grows with an increase in the number of antennas and users as illustrated in equation (3.6) and this is one of the drawbacks of MU-MIMO. The complex encoding/decoding techniques in MU-MIMO prevent it from being scalable. The complexity of these techniques increases with an increase in the number of antennas and the performance of the encoding/decoding technique depends on the near-perfect acquisition of CSI which is practically difficult to achieve.

3.3.3 Massive MIMO

Massive MIMO systems differ from previously discussed systems in several ways. In uplink transmission. the number of base station antennas is increased to be way greater than the number of transmit terminals, *K>>M>>1.* The channel model of massive MIMO is as follows

$$\mathbf{G} = \mathbf{H}\mathbf{D}^{\frac{1}{2}}, \tag{3.7}$$

where $\mathbf{H} \in \mathbb{C}^{K\text{x}M}$ accounts for small scale fading with $|\mathbf{H}|_{km} = h_{km}$, and $\mathbf{D}^{\frac{1}{2}}$ is a K x K diagonal matrix whose diagonal elements constitute a K x 1 vector of path loss and shadow fading. It is shown that the performance of massive MIMO is based upon the law of large numbers [7]

$$\left(\frac{\mathbf{G}^H\mathbf{G}}{K}\right)_{K\gg M} = \mathbf{D}^{\frac{1}{2}}\left(\frac{\mathbf{H}^H\mathbf{H}}{K}\right)_{K\gg M}\mathbf{D}^{\frac{1}{2}} \approx \mathbf{D}. \tag{3.8}$$

The number of base station antennas greatly surpasses the number of transmitters. Massive MIMO systems have more degrees of freedom in terms of transmission of signals. MIMO diversity and MIMO multiplexing are the most studied transmission models. In spatial diversity, multiple transmit antennas allow for multiple copies to be transmitted and this improves the overall efficiency of data transmission and reception. In spatial multiplexing, a high-rate signal is broken down into multiple lower rate streams and each stream is transmitted from a different transmit antenna in the same frequency channel. This entails a linear increase in the transmission rate with the number of receive or transmit antennas for the same bandwidth. Therefore, spatial multiplexing maximises the capacity of the system. Of the two, spatial multiplexing allows for the maximum transmission rate because multiple orthogonal data streams are transmitted simultaneously. Because many streams reach the base station, there is a need to detect these streams. Classic massive MIMO detection algorithms include maximum likelihood detection (MLD) and sphere decoding (SD) [30]. MLD achieves a full diversity gain but is more computationally complex than the sphere decoding. These systems also make use of simpler linear precoding multiplexing techniques at both the uplink and downlink whose performance improves with an increase in the number of antennas. The most popular ones are zero-forcing (ZF), minimum mean square error (MMSE) and matched filter. With linear detection schemes at the *K*-antenna destination, the received signal is separated into *M* streams by multiplying it with a *K* x *M* linear detection matrix, ***A.***

(a) Linear Precoding

Linear precoding algorithms are more feasible because of their reduced complexity compared to maximum likelihood. The major advantage of matched filtering is that the signal processing can be performed at each independent antenna and the fault on another antenna will not affect the next antenna. This also allows for selective usage of the antennas, like intentionally turning some antennas off and leaving the others on. Another linear precoding and decoding method that can be used is zero-forcing (ZF) which [31] has established to operate better than matched filtering and conjugate beamforming under high SINR conditions.

(i) Zero-Forcing

The zero-forcing detector is a classic scheme used to decouple a MIMO channel into multiple sub-streams and is designed to completely do away with interference provided that the channel matrix is reversible a phenomenon known as pseudo-inverse of the channel matrix. This scheme requires that $K \geq M$ to ensure that the matrix $\mathbf{H}^H\mathbf{H}$ is invertible. The ZF matrix is given as follows

$$\mathbf{A}_{ZF} = (\mathbf{H}^H\mathbf{H})^{-1}\mathbf{H}^H. \tag{3.9}$$

The main disadvantage of zero-forcing is noise enhancement. The noise power is multiplied by $\mathbf{A}_{ZF}$ and this significantly reduces the performance of the ZF detector.

(ii) MMSE Precoding

MMSE takes into account the noise term and, unlike ZF, this reduces the effects of noise amplification. $\mathbf{A}_{MMSE}$ can be expressed as

$$\mathbf{A}_{MMSE} = (\mathbf{H}^H\mathbf{H} + \sigma^2\boldsymbol{I}_K)^{-1}\mathbf{H}^H, \tag{3.10}$$

where $\sigma^{\mathbf{2}} = \frac{\mathbf{1}}{\boldsymbol{SNR}}$ and $\boldsymbol{SNR}$ is the signal-to-noise ratio. This implies that at high SNR, MMSE performs just like the ZF detector. Research in [30] has established that imperfect channel state information does not affect the performance of linear coding schemes. As the number of antennas increases, the effective gain generally grows although with a decreasing proportionality factor due to increasing estimation error. In contrast to MU-MIMO, where time to gather CSI grows with the increase in the number of antennas, collection of channel state information in a time division duplex (TDD) massive MIMO systems is not affected by the number of antennas. As explained earlier, Massive MIMO uses spatial multiplexing which requires very good channel state information in both directions of data flow. This is achieved by sending out pilot signals first to determine the channel matrices. In the uplink, the user terminals send the pilot signals which the base station uses to estimate the channel response for each user terminal. In the downlink, the base station transmits the pilot signal which the user terminals use to estimate the channel response of the base station. This, however, poses a problem in massive MIMO systems in that the pilot signals should be orthogonal and with the huge number of transmit antennas at the base station, the number of time-frequency resources for downlink pilots needed would be very high as well. This makes massive MIMO expensive than the conventional MIMO systems discussed earlier on. This also implies that the number of uplink resources required to send the estimated channel responses from the user terminals back to the base station would be in the order of hundreds since the number of channel responses that each terminal approximates is directly proportional to the number of base station antennas. This makes other multiplexing techniques like TDD favourable.

(b) Channel Estimation

This is a technique that massive MIMO systems use to gather the frequency responses of the actual propagation channels. As discussed earlier, this can be achieved by sending out pilot signals with known parameters and detect the signal at the receiver. The receiver then estimates the frequency response. As discussed earlier too, the amount of time-frequency resources needed for pilot training is proportional to the number of antennas at the transmitter. Channel estimation schemes are different depending on the system duplexing mode namely frequency-division duplexing (FDD) and time-division duplexing (TDD)

(i) Channel estimation in FDD systems

In frequency-division duplexing (FDD) systems, the uplink and downlink use different frequency bands. And this implies that the channel state information for the uplink and downlink will be different. Uplink in massive MIMO systems is pretty less complex in that the antennas at the terminals send out the orthogonal pilot signals to the base station and channel estimation is done at the base station. The time required for this training is not dependent on the number of antennas at the base station. For the downlink, the base station sends out pilot signals to the terminals and the terminals will send back the estimated channel state information for each of the downlink channels to the base station. In the downlink operation, the time taken for this training is dependent on the number of transmit antennas at the base station. This, in turn, means that the implementation of FDD channel estimation becomes unfavourable as the number of base station antennas increases.

(ii) Channel estimation in TDD systems

Time-division duplexing (TDD) systems rely on the channel reciprocity assumption and this way, only the uplink channel estimation will be sufficient to estimate the channel properties. The channel state information (CSI) is estimated at the base station (BS) and the BS will use this CSI to detect the uplink data and subsequently produce beamforming vectors for the downlink flow of data. This process requires a minimum of M channel uses. TDD allows scalability in massive MIMO systems while FDD is optimal in smaller systems. With the aforementioned background of massive MIMO, the future of wireless telecommunications with massive MIMO looks set.

3.4 Conclusion

This chapter introduced the concept of harvesting energy from the ambient radio frequency signals to power the energy-constrained network nodes. This has proved to be very beneficial and cost-effective in cases where the batteries of these nodes are not easily accessible or in dangerous places. As purported by the aforementioned literature review, this technology brings with it several advantages that include efficient utilisation of ambient energy, the clean harnessing of energy, extended lifetime of batteries and the readily available radio frequency signals to harvest from just to mention a few. To a lesser extent, the intermittent nature of renewable energy sources like solar makes energy harvesting undesirable. Some of the advantages include the fluctuating supply of energy and complex designs of the practical energy harvesting circuits and modules. With much research being carried out on how to improve this technology, energy harvesting is poised to yield tangible improvements in the energy efficiency of a network thereby enhancing the performance of a network.

One of the biggest enablers of the next generation of wireless communications has been the development of massive MIMO. This chapter also clearly presented the background of deploying a large number of antennas at a node and looks at the work that has been done in this respect. As channels become orthogonal, spectral efficiency increases. The work in [71] – [73] forms a foundation for further studies to look at the gains in efficiency as the number of antennas grows. This chapter also introduced the concept of combining these technologies with other technologies to improve system performance. With all the aforementioned techniques, this work sets out to combine cognitive radio, cooperative relaying, wireless energy harvesting and massive MIMO. Analysis of how much improvements can be attained in a wireless network is also performed. The trade-offs are studied and put into consideration.

Chapter 4 – Sum-Rate of a Massive MIMO Spectrum Sharing Network

4.1 Introduction

This chapter presents and analyses the system capacity performance of a wireless network with cognitive radio, cooperative communications, massive MIMO and wireless energy harvesting technologies all combined into one functional system model. Most studies in the literature ([14] and references therein) have considered energy sufficient secondary users and energy-constrained relay. This current work extends that work by considering both the secondary user and relay as energy-constrained and are both dependent on harvesting from the concurrent primary user transmissions. Some of the performance metrics have been studied and these include the average error rate, outage probability, latency and throughput. This chapter only considers the throughput as a performance measure of the proposed system.

4.2 System Model

4.2.1 Proposed Network Architecture

An uplink transmission of a single cell, multi-user amplify-and-forward (AF) half-duplex relays in an underlay spectrum sharing cognitive system is considered as shown in Figure. 4.1.

The primary network in the cell consists of K single-antenna primary transmitters and an N_P-antenna primary base station (PBS). The number of antennas at PBS can grow unbounded with respect to the number of the primary users, i.e., $N_P >> K$. All the primary user (PU) transmitters are assumed to be located closely in one central point. The secondary network in each cell consists of M single-antenna secondary user (SU) transmitters, N amplify-and-forward relays - denoted by R_n with $n \in \{1, . . , N\}$- each with N_R antennas, and an N_S-antenna secondary base station (SBS). The secondary users transmit to the secondary base station through the cognitive

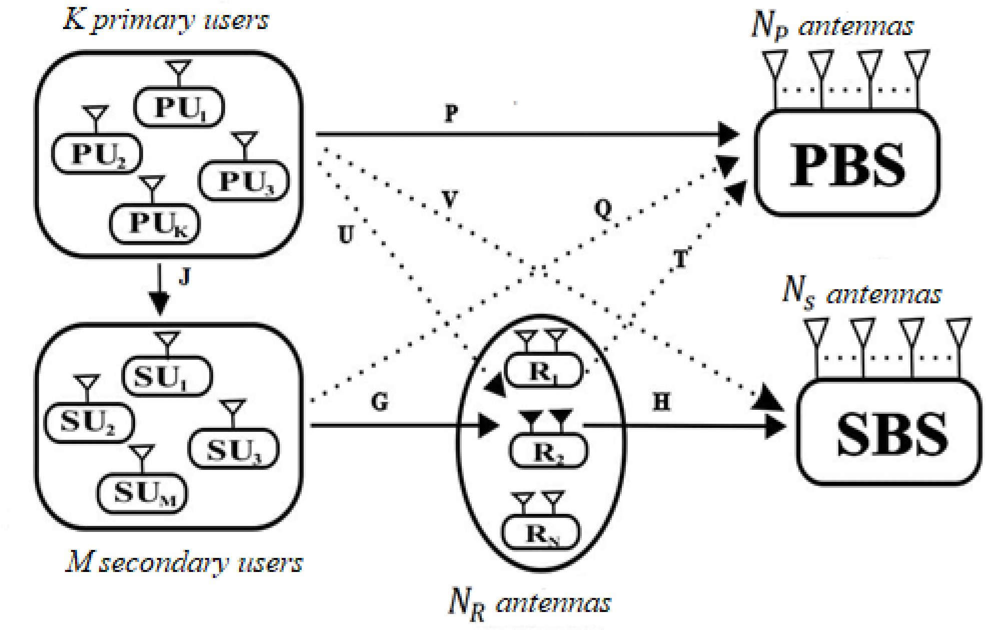

Figure 4.1: A cognitive MIMO multi-relay network with underlay spectrum sharing.

relays by accessing the licensed primary user spectrum as long as the interference at the primary base station does not exceed the peak interference threshold [5]. This implies that the secondary users can perform concurrent transmissions as long as the interference at the PBS does not exceed the peak interference threshold, interference temperature [54]. The primary network nodes will be powered by a fixed energy source.

There is no direct path between the secondary transmitter and SBS due to poor channel conditions or heavy shadowing. Moreover, all channel amplitudes are assumed to be independently distributed, frequency Flat-Rayleigh fading, i.e., the channel coefficients are constant for each transmission block but vary independently between different blocks. The intra-cell S-R, S-PBS, PU-PBS, PU-R, PU-SBS and PU-SU channel coefficient matrices are modelled as

$$\mathbf{B} = \tilde{\mathbf{B}}\mathbf{D}_B^{1/2}, \tag{4.1}$$

where $\mathbf{B} \in \{\mathbf{G}, \mathbf{Q}, \mathbf{F}, \mathbf{U}, \mathbf{V}, \mathbf{J}\}$ and $\tilde{\mathbf{B}} \sim \mathcal{CN}_{P\,X\,Z}(\mathbf{0}_{P\,X\,Z}, \mathbf{I}_P \otimes \mathbf{I}_Z)$[11] capture the independent, quasi-static block-Rayleigh fading. The ZxZ diagonal matrix, $\mathbf{D}_B = \mathrm{diag}(\zeta_{B_1} \ldots \zeta_{B_z} \ldots . \zeta_{B_Z})$, accounts for the path loss, where ζ_{B_Z} denotes the path-loss between the z[th] user and any antenna at the relay or the base station. The intra-cell R-SBS and R-PBS channel coefficient matrices are modelled as

$$\mathbf{R} = \tilde{\mathbf{R}}\mathbf{D}_R^{1/2}, \tag{4.2}$$

where $\mathbf{R} \in \{\mathbf{H}, \mathbf{T}\}$ and $\tilde{\mathbf{R}} \sim \mathcal{CN}_{P\,X\,Z}(\mathbf{0}_{P\,X\,Z}, \mathbf{I}_P \otimes \mathbf{I}_Z)$ captures the independent, quasi-static block-Rayleigh fading of the respective channels. The diagonal matrix, $\mathbf{D}_R = \zeta_R \mathbf{I}_{N_R}$, accounts for the path loss, where ζ_R denotes the path-loss between any antenna at the relay and any antenna at the base station.

Table 4.1: Summary of the channel matrices

F	PU to SBS
G	SU to R
H	R to SBS
U	PU to R
V	PU to PBS
Q	SU to PBS
T	R to PBS
J	PU to SU

4.2.2 Signal Model of the Secondary Network

As aforementioned, both the secondary and primary networks are allowed to coexist provided the interference caused on the latter by the former is below a given threshold to maintain a certain quality of service (QoS). In this regard, the transmit powers at the SU transmitter and relay are given respectively by

$$P_S = \min\left(P_{S_{max}}, \frac{I_P}{\mathcal{E}\{\mathrm{Tr}(\mathbf{W}_P\mathbf{Q}\mathbf{Q}^H\mathbf{W}_P^H)\}}\right), \tag{4.3}$$

$$P_R = \min\left(P_{R_{max}}, \frac{I_P}{\mathcal{E}\{\mathrm{Tr}(\mathbf{W}_P\mathbf{T}\mathbf{T}^H\mathbf{W}_P^H)\}}\right), \tag{4.4}$$

where $P_{S_{max}}$ and $P_{R_{max}}$ are the maximum transmit power levels at the secondary users and relay, respectively, I_P denotes the interference temperature, $\mathcal{E}\{x\}$ is the expectation of x, and

$\mathrm{Tr}(x)$ denotes the trace operator. Additionally, $\mathbf{W}_P$ represents the received zero-forcing (ZF) detector at PBS to suppress multiuser interference and is given by

$$\mathbf{W}_P = (\mathbf{F}^{\mathbf{H}}\mathbf{F})^{-1}\mathbf{F}^{\mathbf{H}}. \tag{4.5}$$

To employ the received ZF, the antenna configurations should satisfy the following condition: $\min(N_P, N_S) \geq \max_{n\in\{1,\dots,N\}} N_{R_n}$. The uplink transmission of information in the secondary network is divided into two orthogonal time slots. During the first time slot, the received signal at the relay can be expressed as

$$\mathbf{y}_R = \sqrt{P_S}\mathbf{G}\mathbf{x}_S + \sqrt{P_P}\mathbf{U}\mathbf{x}_P + \mathbf{n}_R, \tag{4.6}$$

where P_P represents the transmit power at the primary users, $\mathbf{x}_S$ and $\mathbf{x}_P$ are the transmit symbol vectors of the SUs and PUs, respectively, with both satisfying $\mathcal{E}[\mathbf{x}_S\mathbf{x}_S^H] = \mathbf{I}_M$ and $\mathcal{E}[\mathbf{x}_P\mathbf{x}_P^H] = \mathbf{I}_K$, and $\mathbf{n}_R$ is the additive white Gaussian noise (AWGN) vector at the relay with zero mean and variance $\mathcal{E}[\mathbf{n}_R\mathbf{n}_R^H] = \sigma_R^2\mathbf{I}_{N_R}$. The first term of (4.6) accounts for the desired signal from the SUs, while the second term corresponds to the intra-cell interference caused by the concurrent primary user transmissions in the same cell. In addition, P_S is the harvested power at the secondary user obtained from the harvested energy as we will discuss in the next sections.

The energy-constrained relay also harvests energy from the primary user transmissions and uses this energy to amplify and forward the amplified signal to the secondary base station. An amplification factor is used at the relay to constrain its average transmit power to satisfy the interference constraints at the PBS given by

$$\Phi_R = \sqrt{\frac{P_R}{P_S Tr(\mathbf{G}^{\mathbf{H}}\mathbf{G}) + P_P Tr(\mathbf{U}^{\mathbf{H}}\mathbf{U}) + \sigma_R^2 N_R}}. \tag{4.7}$$

In the second timeslot $(1-\alpha)T/2$, the relay transmits an amplified version of its received signal in (4.6) to SBS. To this end, the R-to-SBS transmitted signal can be written as

$$\mathbf{x}_R = \Phi_R\mathbf{y}_R. \tag{4.8}$$

Similar to (4.5), the SBS also performs the ZF detection to suppress multiuser interference given by

$$\mathbf{W}_s = \left((\mathbf{HG})^H(\mathbf{HG})\right)^{-1}(\mathbf{HG})^H. \tag{4.9}$$

After performing mathematical manipulations, the received signal at the secondary base station can be written as

$$\mathbf{y}_S = \sqrt{P_S}\Phi_R\mathbf{x}_S + \sqrt{P_P}\Phi_R\mathbf{W}_S\mathbf{H}\mathbf{U}\mathbf{x}_P + \Phi_R\mathbf{W}_S\mathbf{H}\mathbf{n}_R + \sqrt{P_P}\mathbf{W}_S\mathbf{V}\mathbf{x}_P + \mathbf{W}_S\mathbf{n}_S, \quad (4.10)$$

where $\mathbf{x}_S$ is the desired signal transmitted from the source. The first term of equation (4.10) accounts for the desired signal at the SBS whilst the second term accounts for the intra-cell interference from the primary user transmissions experienced by the relay. The third term in (4.10) is the amplified signal that is transmitted from the relay towards the SBS and the fourth term is the intra-cell interference from the primary user transmissions experienced by the secondary base station. Further in (4.10), $\mathbf{n}_S$ is the additive white Gaussian noise (AWGN) at the secondary base station with zero mean and $\mathcal{E}[\mathbf{n}_S\mathbf{n}_S^H] = \sigma_S^2\mathbf{I}_{N_S}$.

4.2.3 Energy Harvesting Model – Time Switching

The coherence interval, *T* is divided into two orthogonal time frames, one for energy harvesting and the other for information transfer. The fraction of the block time in which the secondary source and the relay harvest energy from the primary user transmissions is denoted by αT, where $0 \leq \alpha \leq 1$. The remaining block time (1-α)*T*, used for information transfer, is further divided into two equal orthogonal slots of length (1-α)*T/2* for the user-to-relay and relay-to-SBS information transmissions. All the energy harvested during the energy harvesting phase is assumed to be used for information transmission. The relay simply forwards what it receives, and the transmission rate is chosen so that the data is transmitted perfectly, accurately, and completely [48].

Table 4.2(a) Energy harvesting at the secondary user

Secondary user harvests energy: $\boldsymbol{\alpha T}$	SU information transmission to R: **(1-$\boldsymbol{\alpha}$)*T/2***	Secondary user harvests energy: **(1-$\boldsymbol{\alpha}$)*T/2***

Table 4.2(b) Energy harvesting at the relay

Relay harvests energy: $\boldsymbol{\alpha T}$	Relay receives information from secondary users: **(1-$\boldsymbol{\alpha}$)*T/2***	Relay transmits information to the secondary base station **(1-$\boldsymbol{\alpha}$)*T/2***

The secondary users and relays harvest energy from the signals of the PU transmitters as illustrated in Table 4.2(a) and Table 4.2(b).

The secondary users harvest from the concurrent primary user transmissions according to the following:

$$E_{H_s} = \frac{\eta(\alpha+1)T}{2} P_P \mathrm{Tr}(\mathbf{J}^{\mathbf{H}}\mathbf{J}), \tag{4.11}$$

where $0 < \eta < 1$ is the energy conversion efficiency. It is worthwhile noting that, it is assumed that all the harvested energy at the secondary user is used in the user-to-relay information transmission phase.

The energy-constrained relays also harvest energy from the intra-cell CCI due to concurrent primary user transmissions during the energy harvesting time αT. The harvested energy at the relay is given by

$$E_{H_R} = \eta\alpha T P_P \mathrm{Tr}(\mathbf{U}^{\mathbf{H}}\mathbf{U}). \tag{4.12}$$

The relays use all the energy harvested during this energy harvesting slot for information transmission in the second timeslot. From (4.11) and (4.12), the transmit power of the secondary users and the relays can be deduced and can be expressed as (4.13) and (4.14) respectively.

$$P_{S_{max}} = \frac{E_{H_S}}{(1-\alpha)T/2},$$

$$P_{S_{max}} = \frac{\eta(\alpha+1)P_P \mathrm{Tr}(\mathbf{J}^{\mathbf{H}}\mathbf{J})}{1-\alpha}. \tag{4.13}$$

Relay transmit power is given by

$$P_{R_{max}} = \frac{E_{H_R}}{(1-\alpha)T/2},$$

$$P_{R_{max}} = \frac{2\eta\alpha P_P \mathrm{Tr}(\mathbf{U}^{\mathbf{H}}\mathbf{U})}{1-\alpha}. \tag{4.14}$$

4.2.4 End-to-End SINR *(Secondary Network)*

Using (4.9) and (4.10), and after performing mathematical manipulations, the SINR γ_m of the mth data sub-stream at the SBS can be expressed as follows

$$\gamma_m = \frac{\Phi_R^2 P_S}{\sum_{n=1}^{3} P_{I_n} + P_{I_4}}, \tag{4.15}$$

where P_{I_n} for $n \in \{1, 2, 3\}$ represents the interference powers and P_{I_4} accounts for the AWGN received at SBS, and are given respectively by

$$P_{I_1} = P_P \Phi_R^2 [\mathbf{W}_S \mathbf{H} \mathbf{U} \mathbf{U}^{\mathbf{H}} \mathbf{H}^{\mathbf{H}} \mathbf{W}_S^H]_{m,m}, \tag{4.16}$$

$$P_{I_2} = \Phi_R^2 \sigma_R^2 [\mathbf{W}_S \mathbf{H} \mathbf{H}^{\mathbf{H}} \mathbf{W}_S^H]_{m,m}, \tag{4.17}$$

$$P_{I_3} = P_P [\mathbf{W}_S \mathbf{V} \mathbf{V}^{\mathbf{H}} \mathbf{W}_S^H]_{m,m}, \tag{4.18}$$

$$P_{I_4} = \sigma_S^2 [\mathbf{W}_S \mathbf{W}_S^H]_{m,m}, \tag{4.19}$$

where P_{I_4} accounts for the AWGN received at the SBS.

4.2.5 Signal Model of the Primary Network

This research assumes that the uplink transmission from the primary user nodes to the primary base station occurs during the complete uplink transmission phase of the secondary relay network which is from the secondary user-to-relay and the relay-to-SBS phases. In the first $(1-\alpha)T/2$ time slot, the received signal at the PBS can be written as

$$\mathbf{y}_{P,1} = \mathbf{W}_P\left(\sqrt{P_{\mathrm{P}}}\mathbf{F}\mathbf{x}_{\mathrm{P}} + \sqrt{P_S}\mathbf{Q}\mathbf{x}_S + \mathbf{n}_P\right), \tag{4.20}$$

where $\mathbf{W}_P$ has already been defined in (4.5). The first term of (4.20) accounts for the desired signal at the PBS from the same cell primary user nodes. The second and third terms represent the intra-cell interference due to concurrent secondary user transmissions in the same cell and the AWGN at the cell PBS with zero mean satisfying $\mathcal{E}[\mathbf{n}_P \mathbf{n}_P^H] = \sigma_P^2 \mathbf{I}_{N_P}$ respectively.

In the second time slot of its uplink transmission, the received signal at the PBS can be written as

$$\mathbf{y}_{P,2} = \mathbf{W}_P\left(\sqrt{P_{\mathrm{P}}}\mathbf{F}\mathbf{x}_{\mathrm{P}} + \mathbf{T}\mathbf{x}_{\mathrm{R}} + \mathbf{n}_P\right), \tag{4.21}$$

where the first term of (4.21), $\sqrt{P_{\mathrm{P}}}\mathbf{F}\mathbf{x}_{\mathrm{P}}$, accounts for the desired signal at the PBS, whilst the second term represents the intra-cell interference from concurrent relay transmissions in the same cell. The term $\mathbf{x}_{\mathrm{R}}$ has been explained in (4.8) and $\mathbf{n}_P$ is the AWGN at the PBS with zero mean and $\mathcal{E}[\mathbf{n}_P\mathbf{n}_P^H] = \sigma_P^2\mathbf{I}_{N_P}$.

4.2.6 End-to-End SINR *(Primary Network)*

To derive the end-to-end SINR of the PBS in the second half of uplink transmission, equation (4.21) is used to obtain the closed-form expression for the SINR γ_k, of the *k*th data sub-stream at the PBS

$$\gamma_{k,2} = \frac{P_P}{\sum_{n=1}^{3} P_{I_n} + P_{I_4}}, \tag{4.22}$$

where P_P is the desired signal power and P_{I_n} for $n \in \{1, . . , 3\}$ represents the interference powers.

$$P_{I_1} = P_S\Phi_R^2[\mathbf{W}_P\mathbf{T}\mathbf{G}\mathbf{G}^{\mathbf{H}}\mathbf{T}^{\mathbf{H}}\mathbf{W}_P^H]_{k,k}, \tag{4.23}$$

$$P_{I_2} = P_P\Phi_R^2[\mathbf{W}_P\mathbf{T}\mathbf{U}\mathbf{U}^{\mathbf{H}}\mathbf{T}^{\mathbf{H}}\mathbf{W}_P^H]_{k,k}, \tag{4.24}$$

$$P_{I_3} = \Phi_R^2\sigma_R^2[\mathbf{W}_P\mathbf{T}\mathbf{T}^{\mathbf{H}}\mathbf{W}_P^H]_{k,k}, \tag{4.25}$$

$$P_{I_4} = \sigma_P^2[\mathbf{W}_P\mathbf{W}_P^H]_{k,k}, \tag{4.26}$$

where P_{I_4} accounts for the AWGN received at the PBS in the second transmission slot.

Using equation (4.20) helps to derive the end-to-end SINR of the PBS, in the first half of the uplink transmission, and get the closed-form expression for the SINR $\gamma_{k,1}$, of the *k*th data sub-stream at the PBS

$$\gamma_{k,1} = \frac{P_P}{P_{I_1} + P_{I_2}}, \tag{4.27}$$

$$P_{I_1} = P_S[\mathbf{W}_P\mathbf{Q}\mathbf{Q}^{\mathbf{H}}\mathbf{W}_P^H]_{k,k}, \tag{4.28}$$

$$P_{I_2} = \sigma_P^2[\mathbf{W}_P\mathbf{W}_P^H]_{k,k}. \tag{4.29}$$

4.3 Achievable Sum-Rate Definitions

The average achievable sum-rate at the SBS can be defined as follows

$$\mathcal{R}_S = \frac{(1-\alpha)}{2} \sum_{m=1}^{M} \log_2(1+\gamma_m), \tag{4.30}$$

where γ_m is the end-to-end SINR of the mth data sub-stream (4.15) received at the SBS. Substituting (4.15) into (4.30) will give us

$$\mathcal{R}_S = \frac{(1-\alpha)}{2} \sum_{m=1}^{M} \log_2\left(1 + \frac{\boldsymbol{\Phi}_R^2 \boldsymbol{P}_S}{\sum_{n=1}^{3} P_{I_n} + P_{I_4}}\right). \tag{4.31}$$

Similarly, the average sum-rate at the PBS can be defined as

$$\mathcal{R}_P = \frac{1}{2} \sum_{i=1}^{2} \sum_{k=1}^{K} \log_2\left(1 + \frac{P_P}{\sum_{n=1}^{3} P_{I_n} + P_{I_4}}\right), \tag{4.32}$$

where $\gamma_{k,2}$ and $\gamma_{k,1}$ are defined in (4.22) and (4.27), respectively. The pre-log factors of $(1-\alpha)/2$ and $1/2$ in equations (4.31) and (4.32) respectively are because of the two time-slots, users-to-relay and relay-to-destination time-slots.

4.4 Asymptotic Sum-Rate Analysis

The asymptotic sum-rate analysis for this model is derived for many antenna configurations at both the primary and secondary networks. The analytical expressions provide practical design insights into the impact of various parameters on the performance of the network. This work considers the case when the number of antennas at the relays, secondary base station and primary base station all grow very large, ie. $N_R \to \infty, N_S \to \infty,$ and $N_P \to \infty,$ respectively.

4.4.1 $N_P \to \infty,\ N_S \to \infty$ and $N_R \to \infty$

The number of antennas at the relay and secondary destination can grow without bound while maintaining the ratio $\lambda = N_S/N_R$. The same applies to the number of PBS antennas which can grow without bound while keeping the ratio $\beta = N_P/N_S$ fixed. The number of primary and secondary user nodes (K and M respectively) are kept at arbitrary finite values with respect to N_P and N_S. As per massive MIMO concepts [75], the transmit powers of primary and secondary user nodes are scaled inversely proportional to the number of PBS antennas and relay antennas respectively, $P_P = E_P/N_P$ and $P_S = E_S/N_R$, where E_P and E_S are constants. Therefore, by letting $N_P, N_S, N_R \to \infty$, the asymptotic SINR of the mth data sub-stream at the SBS can be derived as shown below (complete derivation is shown in Appendix A.2):

$$\gamma_m^{\infty} = \lim_{N_S, N_{R\to\infty}} \left(\frac{P_S N_R^2}{\sum_{n=1}^{4} P_{I_n} N_R^2}\right) = \frac{E_S P_R}{\sigma_R^2\left(P_R \zeta_{G_m}^{-1} + \sigma_S^2 \zeta_H^{-1} \zeta_{G_m}^{-1}/\lambda\right)}. \quad (4.33)$$

By substituting equation (4.33) into equation (4.31), the asymptotic achievable sum-rate at the secondary base station can be derived as follows

$$\mathcal{R}_S^{\infty} = \frac{(1-\alpha)}{2} \sum_{m=1}^{M} \log_2 \left(1 + \frac{E_S P_R}{\sigma_R^2\left(P_R \zeta_{G_m}^{-1} + \sigma_S^2 \zeta_H^{-1} \zeta_{G_m}^{-1}/\lambda\right)}\right). \quad (4.34)$$

4.5 Sum-rate against the harvested energy

This sub-section looks into how the performance of the system varies with the amount of harvested energy. As explained in the literature review on how energy harvesting improves the energy efficiency of a system, this section intends to quantify these gains and also deduce the optimal operating points for a system to properly maintain a balance between energy harvesting and information transfer. This sub-section begins by deriving the asymptotic equations and then see how these compare to the simulations.

4.5.1 Asymptotic harvested energy at the relays

The harvested energy at the relay is shown in (4.14). According to [75], the transmit power at each primary and secondary user node is scaled inversely proportional to the number of PBS antennas and relay antennas, respectively, $P_P = E_P/N_P$ and $P_S = E_S/N_R$ where E_P and E_S are kept fixed. The number of antennas at the secondary base station and relay can grow without bound while maintaining the ratio $\lambda = N_S/N_R$ fixed. The same applies to the number of PBS antennas which can grow without bound while keeping the ratio $\beta = N_P/N_S$ fixed. The number of primary and secondary user nodes (*K* and *M* respectively) are kept at arbitrary finite values with respect to N_P and N_S.

The asymptotic harvested energy at the relay is derived as

$$E_{H_R} = \eta \alpha T P_P \mathrm{Tr}(\mathbf{U}^{\mathbf{H}}\mathbf{U}).$$

$$\lim_{N_R\to\infty} E_{H_R} = \frac{\eta\alpha T}{\beta\lambda} E_P Tr\left(\frac{\mathbf{U}^{\mathbf{H}}\mathbf{U}}{N_R}\right), \quad (4.35)$$

$$E_{H_R}^{\infty} = \frac{\eta\alpha T}{\beta\lambda} E_P Tr\left(\frac{\mathbf{U}^{\mathbf{H}}\mathbf{U}}{N_R}\right) = \frac{\eta\alpha T E_P}{\beta\lambda} Tr\mathbf{D}_U. \quad (4.36)$$

By assuming a simplified independent and identically distributed (i.i.d) fading model, one can obtain more understanding of the harvested energy by letting $\mathbf{D}_U = \zeta \mathbf{I}_K$ in (4.34). The asymptotic harvested energy at the relay for a i.i.d fading model becomes

$$E_{H_R}^{\infty} = \frac{\eta \alpha T E_P}{\beta \lambda} [Tr(\zeta \mathbf{I}_K)],$$

$$= \frac{\eta \alpha T E_P}{\beta \lambda} [\zeta K],$$

$$= \frac{\eta \alpha T E_P \zeta K}{\beta \lambda}. \quad (4.37)$$

From (4.37) it is clear that the harvested energy at the relay increases with K and hence intra-cell interference can be beneficial for improving the harvested energy. The same steps above can be followed to derive the asymptotic harvested energy at the secondary users.

4.5.2 Asymptotic harvested energy at the secondary users

The harvested energy at the SUs is shown in (4.13). According to [75], the transmit power at the secondary user node is scaled inversely proportional to the number of relay antennas, $P_S = E_S/N_R$ where E_S is kept fixed. The number of antennas at the secondary base station and relay can grow without bound while maintaining the ratio $\lambda = N_S/N_R$ fixed. The number of secondary user nodes, M , is kept at arbitrary finite values with respect to N_S.

The asymptotic harvested energy at the secondary user is derived as

$$\lim_{N_S \to \infty} E_{H_S} = \frac{\eta(\alpha+1)T}{2\beta} E_P Tr\left(\frac{\mathbf{J}^{\mathbf{H}}\mathbf{J}}{N_S}\right),$$

$$= \frac{\eta(\alpha+1)T E_P}{2\beta} Tr \mathbf{D}_J. \quad (4.38)$$

By letting $\mathbf{D}_J = \zeta \mathbf{I}_K$ in (4.38), a more insightful expression of the asymptotic can be derived. The asymptotic harvested energy at the secondary users becomes

$$E_{H_S}^{\infty} = \frac{\eta(\alpha+1)T E_P}{2\beta} Tr(\zeta \mathbf{I}_K),$$

$$= \frac{\eta(\alpha+1)T E_P}{2\beta} [\zeta K],$$

$$= \frac{\eta(\alpha+1)T \zeta K E_P}{2\beta}. \quad (4.39)$$

It becomes clear from (4.39) that the number of primary user transmitters has an effect on the amount of energy being harvested by the secondary users.

4.5.3 Asymptotic harvested energy and average sum-rate trade-off

The trade-off between the asymptotic harvested energy and average achievable sum-rate can now be derived by solving for the time switching factor, α, in equations (4.37) and (4.39). Substitute the results into (4.34) to obtain the trade-off between asymptotic harvested energy and the achievable sum-rate.

$$\mathcal{R}_S^{\infty} = \frac{(1-\alpha)}{2} \sum_{m=1}^{M} \log_2 \left(1 + \frac{P_S^{\infty} \Phi_R^{\infty}}{\Phi_R^{\infty} \sigma_R^2 \zeta_{G_m}^{-1} + \zeta_{G_m}^{-1} \zeta_H \sigma_S^2 / \beta}\right). \tag{4.40}$$

It is very important to be able to determine the optimal time-switching factor so that the trade-off between information transfer and energy harvesting is beneficial. Figure. 4.6, average achievable sum-rate vs the time-switching factor, allows the characterisation of the trade-off between the asymptotic harvested energy and the achievable sum-rate.

4.6 Numerical Results and Discussions

In this section numerical results are presented to examine the sum-rate performance of the proposed massive MIMO underlay spectrum sharing relay network with wireless energy harvesting. The sum-rate performance is shown as a function of the average first-hop SNR, average secondary base station SNR, number of SBS antennas and the time-switching factor. To gain more useful insights, this work analyses the asymptotic behaviour of the sum-rate as the number of antennas grows unbounded. Without loss of generality, the distances between the nodes are set as follows: secondary users-to-relay is set at 100m, relay-to-SBS is 100m, primary user-to-SBS is 1000m, secondary users-to-PBS, primary users-to-relay and the relay-to-PBS are all 500m. To maintain the maximum transmit power constraints on the PBS, the interference temperature is set at 30dBm and a path-loss exponent of 2.0 for all the figures. Other parameters specific to the different graphs are defined respectively.

In order to validate the simulation results in this chapter, the system model has been reduced by removing the primary network component to match the system model described in [76].

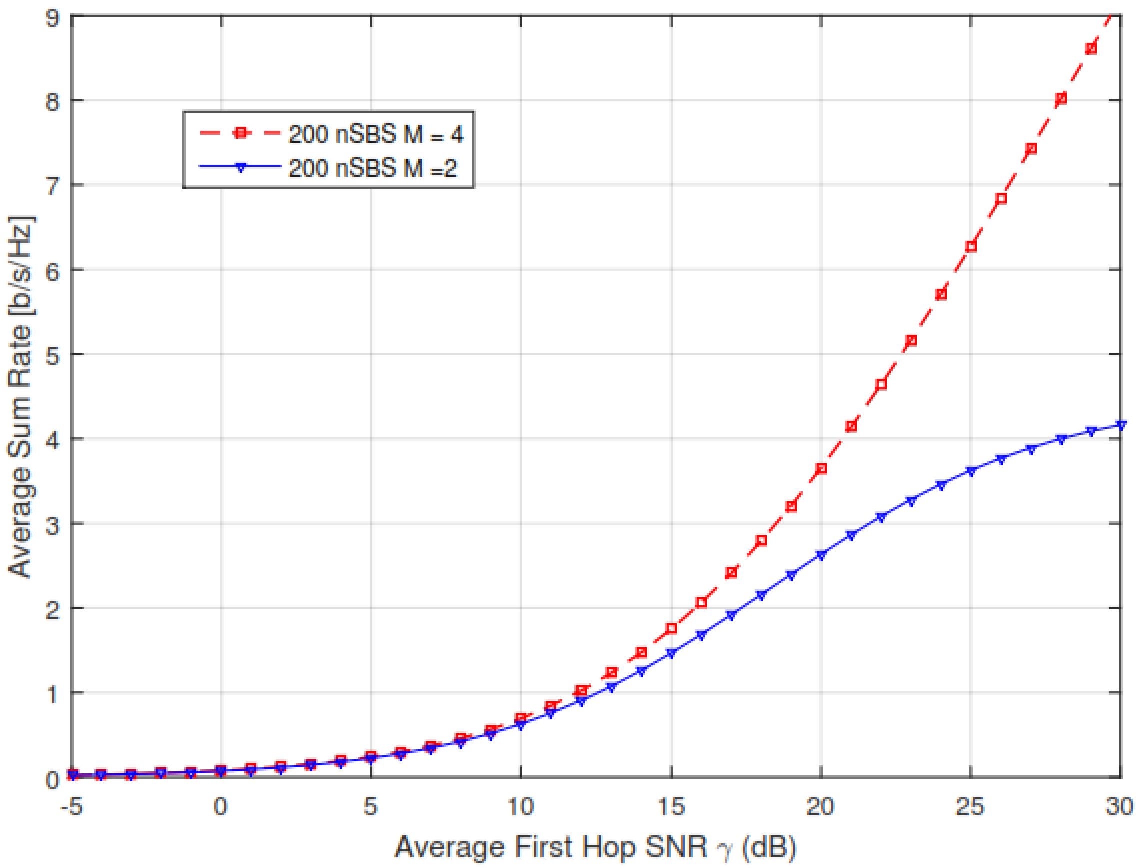

Figure 4.2. Achievable sum-rate versus the average first-hop SNR ($\bar{\gamma} = P_S/\sigma_R^2$) for a M-user secondary network

The system model in [76] considered a multi-user model and applied linear zero-forcing detectors at both the relay and the destination. The effects of both imperfect and perfect channel state information acquisition are also considered. This model in [76] differ slightly from this research's reduced single cell model that implemented zero-forcing at the destination only and considered perfect CSI. However, the results in Figure 4.2, for the different number of secondary users match the results presented in Fig. 1 Section IV of [76]. This proves the correctness of the simulation model and results in this chapter and will guide all the simulation model results in this chapter unless an analytical curve is plotted alongside to verify the accuracy of the corresponding simulation curve.

In Figure 4.3, a 6-user network is considered and wish to study how the network performance varies as the average SNR changes at different antenna configurations.

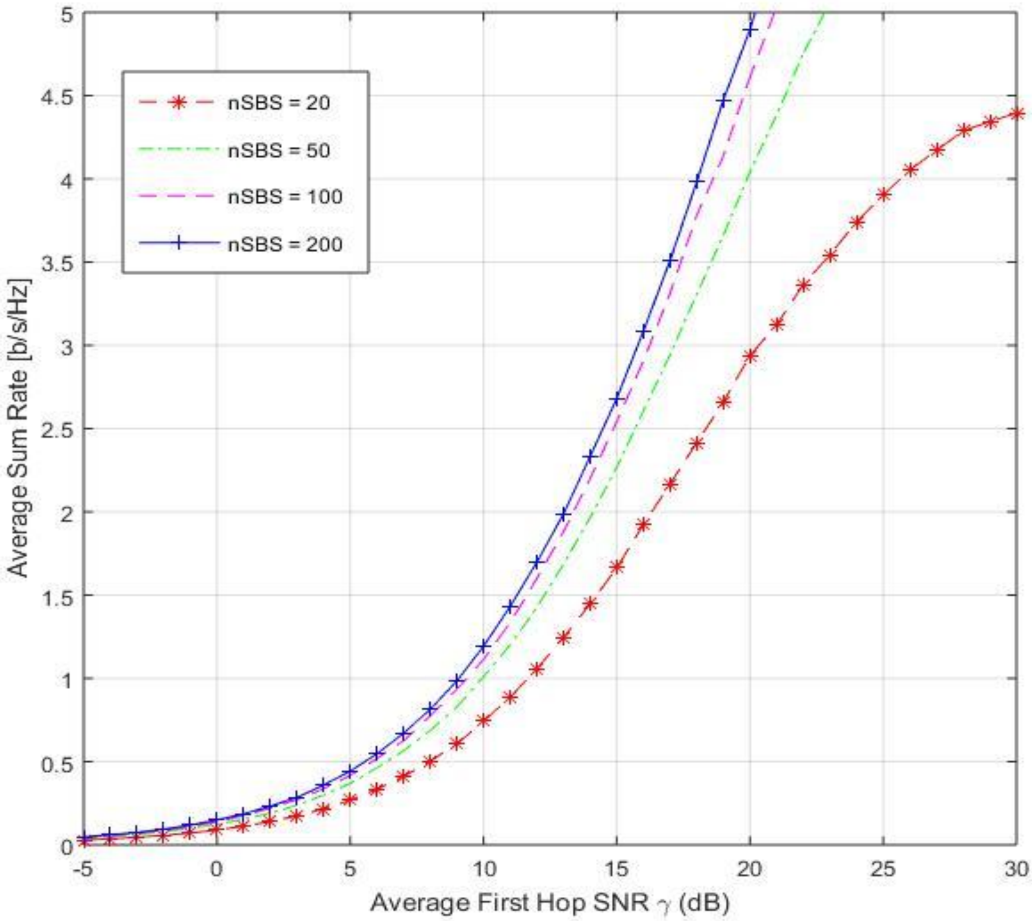

Figure 4.3: Average sum-rate against the secondary network average first-hop SNR ($\bar{\gamma} = P_S/\sigma_R^2$). $\sigma_R^2 = \sigma_S^2 = 5$dBm and $M = K = 6$.

The average sum-rate of a 6-user secondary network is plotted against the average first-hop SNR of the secondary network. The number of relay antennas is maintained at 10 and the number of SBS antennas varies from 20 to 200. The system performance improves as the numbers of SBS antennas increases from 20 to 200 although with decreasing gains. A gain of 1.0 b/s/Hz is obtained the number of antennas is increased from 20 to 50 but half of that gain, that is 0.5 b/s/Hz, is attained as the antenna configuration is doubled from 50 to 100 at the SBS. This shows that under set conditions the performance of a massive MIMO system increases only up to a certain point before the performance is constant. As the number of antennas increase, channels become orthogonal and this improves the performance of a network since interference would have been reduced. The major challenge that comes with the indefinite growth of the number of antennas is the increased complexity in detecting and combining the signals at the receiver. If not done properly, this will have a negative impact on the overall performance of the system.

As shown in [75], the transmit powers of the user nodes can be set inversely proportional to the number of base station antennas and still maintain the performance of the system healthy.

Figure 4.4 illustrates the system performance comparison between two different transmit powers at two different antenna configurations. Figure 4.4 parameters are the same as the system parameters used for Figure 4.3. The network with a bigger antenna configuration is set to a lower transmit power setting while the fewer antennas network has a higher transmit power setting. As shown in Figure 4.4, the two profiles are the same and follow the same trajectory. This supports the notion that by employing massive MIMO, the transmit powers of the users can reduce without affecting the performance of the system. Massive MIMO clearly improves the energy efficiency of a system.

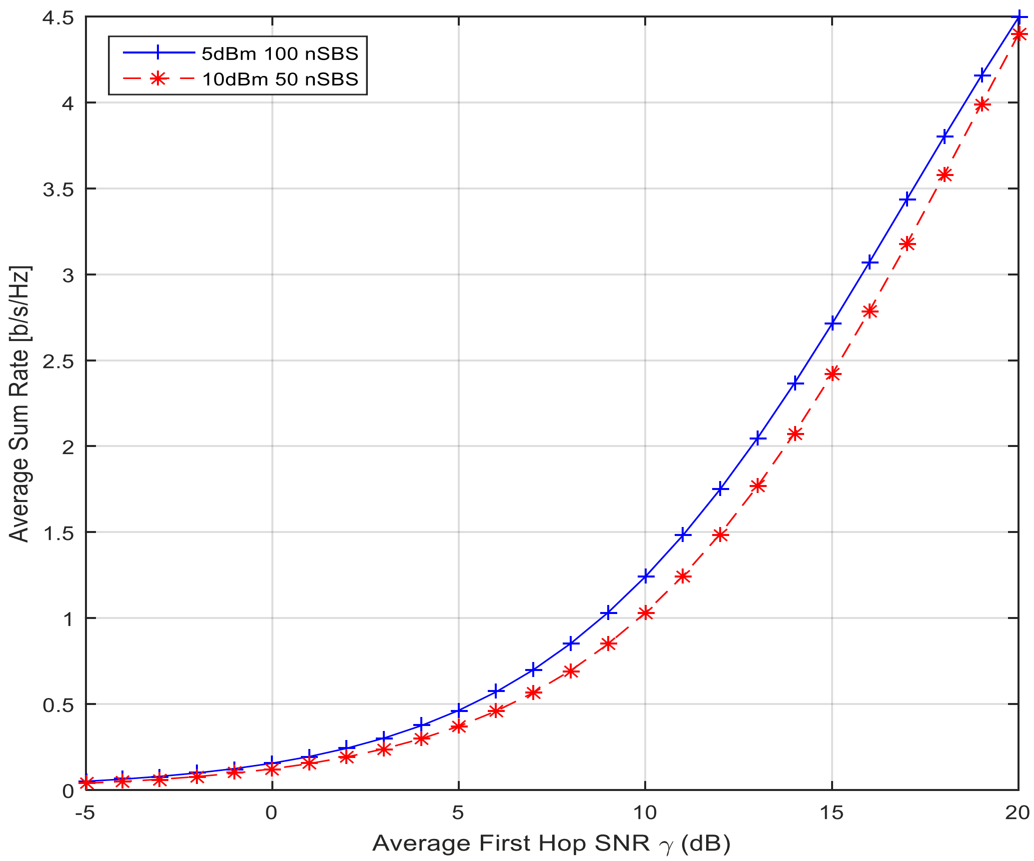

Figure 4.4: Average sum-rate vs average first-hop SNR ($\bar{\gamma} = P_S/\sigma_R^2$). at different secondary user transmit powers levels and different base station antenna configurations.

The first rule of thumb for a spectrum sharing network is that the secondary network transmissions should not affect the performance of the licensed primary users. This primary network enforces this by applying an interference temperature on the primary base station which limits the transmission powers of the secondary users to a set threshold. This protects the primary network but at the same time negatively impacts the secondary users if the set interference temperature is too low. With the advent of massive MIMO, this technology can be utilised to curb the transmit power constraint on the performance of the secondary network. The first way has just been explained and proved above in Figure 4.4 that the transmit power of the secondary users can be inversely proportional to the number of base station antennas but still maintain almost the same performance levels. The second method is to increase the number of base station antennas towards infinite and observe how this impacts the transmit power constraint defined on the primary base station.

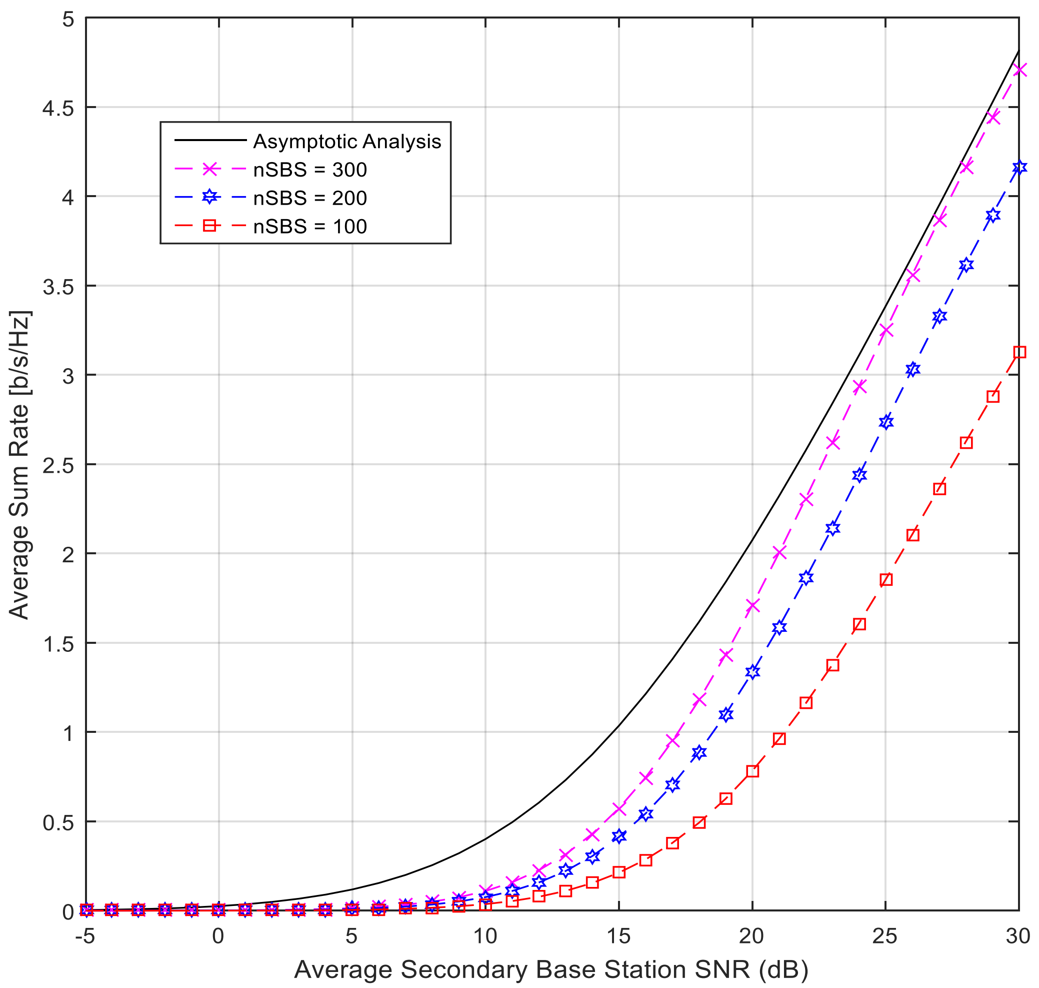

Figure 4.5 Average sum-rate vs the average secondary base station SNR with $M = K = 6$.

Figure 4.5 shows the variation between the average sum-rate against the average first-hop SNR. The asymptotic analysis curve depicts the performance of the system when the number of base station antennas is infinitely large. By employing the law of large numbers as in [75], the derivation for the asymptotic equations do away with the secondary network nodes transmit power limit and allow these nodes to operate at their peak average transmit powers (supported in appendix A.2). Figure 4.5 indicates that as the number of base station antennas continues to increase, the performance of the system approaches the asymptotic performance which allows the secondary network to operate at its peak average transmit power. Hence, it can be inferred from these results that massive MIMO improves system performance by disabling the transmit power constraints set on the primary base station.

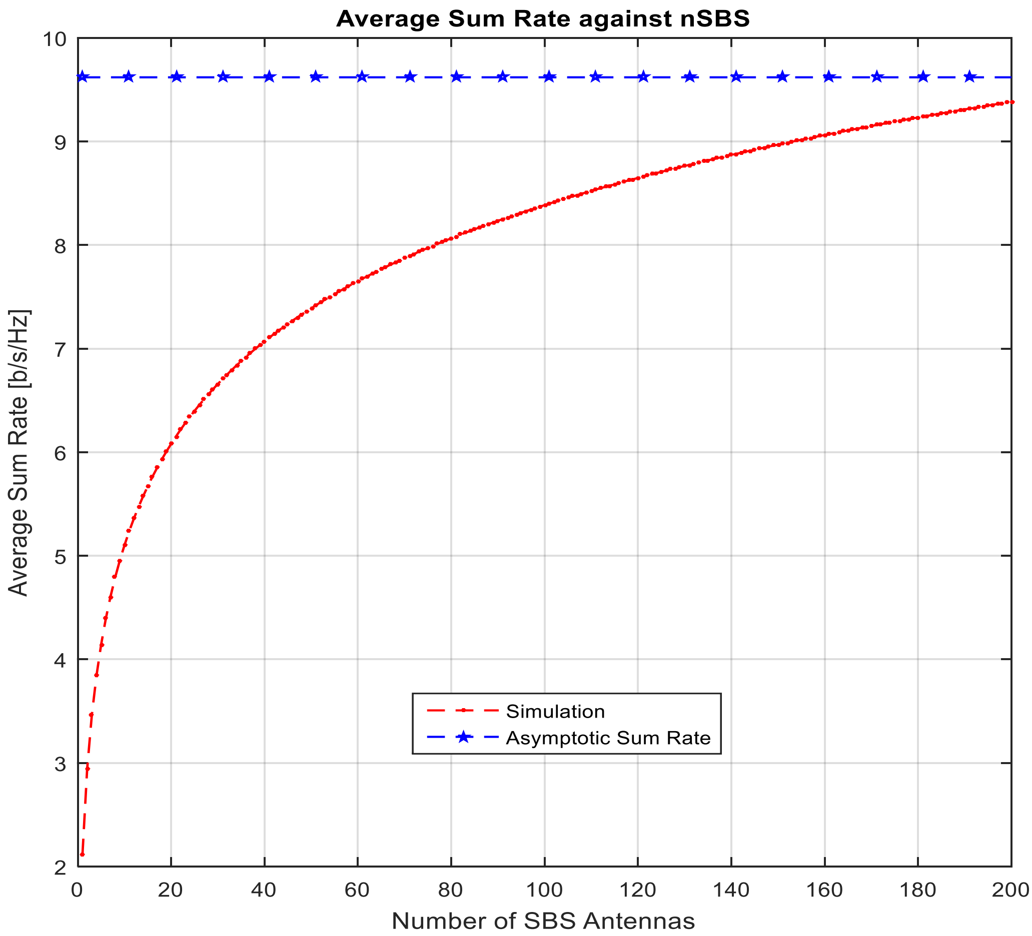

Figure 4.6: Achievable sum-rate versus the number of secondary base station antennas. $K = M = 6$.

Figure 4.6 shows the average sum-rate as a function of the number of base station antennas. A path-loss exponent of 2.0 is considered and the distances between the nodes are set as follows:

secondary users-to-relay is set at 100m, relay-to-SBS is 100m, primary user-to-SBS is 1000m, secondary users-to-PBS, primary users-to-relay and the relay-to-PBS are all 500m. The simulation graph approaches the analytical analysis as the number of base station antennas increases. The asymptotic curve is plotted by using equation (4.32). This approach by the simulation curve towards the asymptotic curve is a clear indication of how intra-cell interference can be asymptotically mitigated as the number of antennas grow towards infinite. By increasing the number of base station antennas from $nSBS = 1$ to $nSBS = 20$, we can notice an improvement in the sum-rate from roughly 0.6 $bits/s/Hz$ to about 6 $bits/s/Hz$. This is evidence of how sum-rate strictly increases as $nSBS$ increases. The transmit powers of the primary and secondary users are scaled inversely proportional to $nPBS$ and $nRel$ respectively.

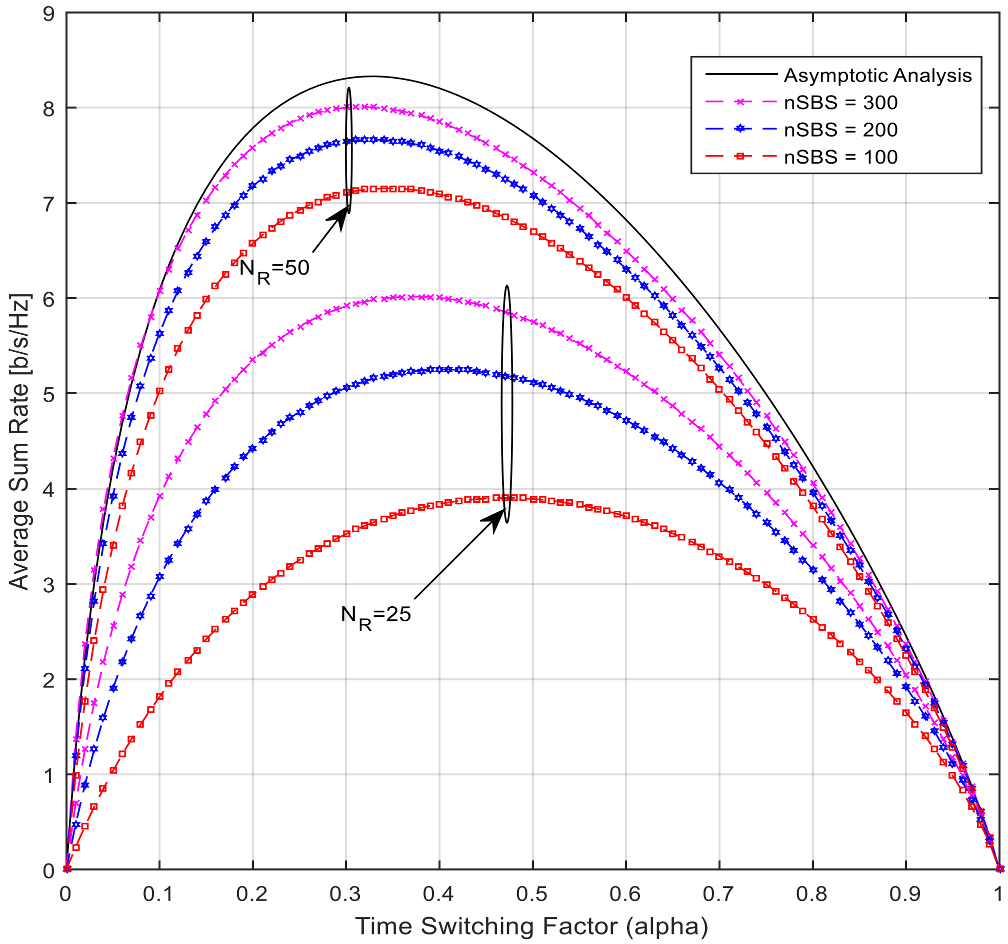

Figure 4.7: Sum-rates versus α for a 6-user relay network with $E_P = 34dBm$, $\sigma_R^2 = \sigma_S^2 = -10dBm$, $\eta = 0.7$, and $I_P = 30dBm$.

The achievable sum-rate of the secondary system is plotted against the time switching factor by varying the number of antennas at the secondary base station for two different relay antenna configurations. The analytical sum-rate curve is plotted by using (4.38) and the remaining exact sum-rate curves are plotted by using Monte Carlo simulations.

It is observed from Figure. 4.7 that the simulated curves approach the analytical curve as the number of SBS antennas increases. This is mainly because as the number of SBS antennas continues to increase unbounded, the channels become orthogonal thereby improving the overall performance of the system. It is noted that the maximum sum-rate is achieved for $\alpha \cong 0.3$. This is the point where the system is performing at its most optimal in terms of energy harvesting and information transfer. It is also observed that, as the time-switching factor α grows, the average sum-rate decreases. This is because as α increases, there is more harvested energy but less remaining time for information transfer which in turn lowers the sum-rate. An increase in the sum-rate as the number of antennas at the secondary base station increase towards infinity can be attributed to the fact that massive MIMO enabled nodes together with the ZF detector at the SBS can be used to lower the detrimental effects of CCI.

4.7 Innovative Aspect of our Proposed System

The proposed system is innovative and differs from the work presented in the literature (see [14] – [15], [77]) in many ways. Work in [14] investigated the sum-rate performance of an energy harvesting system but did not consider spectrum sharing. The results presented in Figure 4.7 show superior performance as compared to the results presented in [14]. A cognitive radio wireless energy harvesting model is considered in [15] but does not include cooperative communications. The system performance in [15] is also outperformed by the system performance results presented in this chapter. This can be attributed to the spectral efficiency benefits that come with cooperative communications. Figure 4.6 shows the superior performance the proposed system as compared to the performance of the system investigated in [77]. Authors in [78] consider a multi-hop model without the primary network.

4.8 Conclusion

In this chapter, an analysis on cooperative cognitive massive MIMO in an underlay spectrum-sharing network in terms of the achievable sum-rate is carried out. Also, the end-to-end SINR and the asymptotic achievable sum-rate are derived for an unbounded number of antennas at the relay nodes and base station. An EH-based operation is also analysed which considers energy-constrained secondary users and relays harvesting from the concurrent primary network transmissions. The trade-off between the achievable sum-rate and the time switching factor is discussed. It is noted that massive MIMO-enabled nodes can help mitigate the detrimental effects of CCI on the secondary system from the primary user transmissions. Furthermore, several other figures were plotted to deduce how massive MIMO assists in transmit power constraints that govern spectrum sharing networks. The numerical results proved that massive MIMO allows users to transmit at the maximum transmit powers without 'worrying' about the interference power constraint.

Chapter 5 – Outage Performance of a Massive MIMO Spectrum Sharing Network

5.1 Introduction

This chapter presents and investigates the outage performance of the proposed massive MIMO cognitive radio relay network with wireless energy harvesting. A thorough discussion of the system performance under different scenarios is also presented to quantify how massive MIMO, wireless energy harvesting and relaying impact the outage performance of a cognitive radio network.

When a network is in outage, its operation ceases and all communication during that event will be non-existent. It is therefore on the back of this background that during the planning stage of building a wireless network or better still deploying the next generation of wireless communications, it is imperative to conduct studies on how to keep the network live without outages. This topic analyses the chances on a scale of 0 to 100% how likely it is for the network to fall into outage.

5.2 System Model

The same model as the one discussed in Section 4.2.1 is analysed in this section and the outage performances of this model is quantified. The channel characteristics remains unchanged and all assumptions stand.

An uplink transmission of a single cell, multi-user amplify-and-forward (AF) half-duplex relays in an underlay spectrum sharing cognitive system is considered. In the relay-assisted network, there is no direct path between the secondary transmitter and SBS due to poor channel conditions or heavy shadowing. Moreover, all channel amplitudes are assumed to be independently distributed, frequency Flat-Rayleigh fading, i.e., the channel coefficients are constant for each transmission block but vary independently between different blocks.

5.3 Outage Probability

The outage probability is defined as the probability that the instantaneous end-to-end SINR , $\grave{\gamma}_k$, falls below a pre-defined threshold value, γ_{th} implying that the network is in outage when the equivalent SINR at each hop is below the threshold value, γ_{th} as

$$P_{out} = P_r\{\grave{\gamma}_k < \gamma_{th}\}, \tag{5.1}$$

where γ_{th} is related to the rate threshold. In this system model, the amplify-and-forward relay-assisted network is in outage when at least one of the two hops is in outage.

5.3.1 Problem Formulation

The end-to-end SINR of the underlying network is calculated in order to derive the numerical expression of the outage probability. As shown in equation (4.15), the SINR, γ_m, of the mth data sub-stream at the SBS is obtained as

$$\gamma_m = \frac{\boldsymbol{\Phi}_R^2 \boldsymbol{P_S}}{\sum_{n=1}^{3} P_{I_n} + P_{I_4}}, \tag{5.2}$$

where P_{I_n} for $n \in \{1, 2, 3\}$ represents the interference powers and P_{I_4} accounts for the AWGN received at SBS. γ_{th} is deduced from performing mathematical manipulations on the target rate equation. The target rate is given by

$$\mathcal{R}_{th} = \frac{1-\alpha}{2} \log_2(1 + \gamma_{th}). \tag{5.3}$$

Therefore, by making γ_{th} the subject of the formula is

$$\gamma_{th} = 2^{\frac{2\mathcal{R}_{th}}{1-\alpha}} - 1. \tag{5.4}$$

The outage probability can now be derived by substituting (5.2) and (5.4) into (5.1) to get

$$P_{out} = P_r\left\{\frac{\boldsymbol{\Phi}_R^2 \boldsymbol{P_S}}{\sum_{n=1}^{3} P_{I_n} + P_{I_4}} < 2^{\frac{2\mathcal{R}_{th}}{1-\alpha}} - 1\right\}. \tag{5.5}$$

Obtaining the closed-form expression for the proposed system model is complicated because of too many variables involved. Work in [10] and [18] derived closed form expressions because they only considered single antenna nodes. With massive MIMO enabled nodes investigated in this research, the number of variables is huge, and derivation becomes too complex.

5.4 Numerical Results and Discussions

In this section the simulation results for the underlying system are provided to evaluate the performance of the proposed system and analyse the impact of some key parameters on the system performance. The outage probability with respect to average first hop SNR, I_P, γ_{th} and α is studied here. Unless otherwise specified, the general system parameter values used for the figures are: secondary users-to-relay distance is 100m, relay-to-SBS is 100m, primary users-to-SBS is 1000m, secondary users-to-PBS, primary users-to-relay and the relay-to-PBS is 500m. To maintain the transmit power constraints on the PBS, the interference temperature is set at 30dBm and a path-loss exponent of 2.0. The target rate $\mathcal{R}_{th}$ is 1 bit/s/Hz.

Figure 5.1 shows the outage probability of the system when the average first hop SNR increases from -5 to 20dB. The outage probability is performed for three antenna configurations which are 90 antennas, 150 antennas and 300 antennas, at the SBS by implementing both the threshold rate as well as the threshold SINR. This verifies the correctness of our simulations. From Figure 5.1, it is clear that the outage probability decreases as the average first hop SNR increases. Also, it can be observed that the outage probability decreases when the number of antennas at

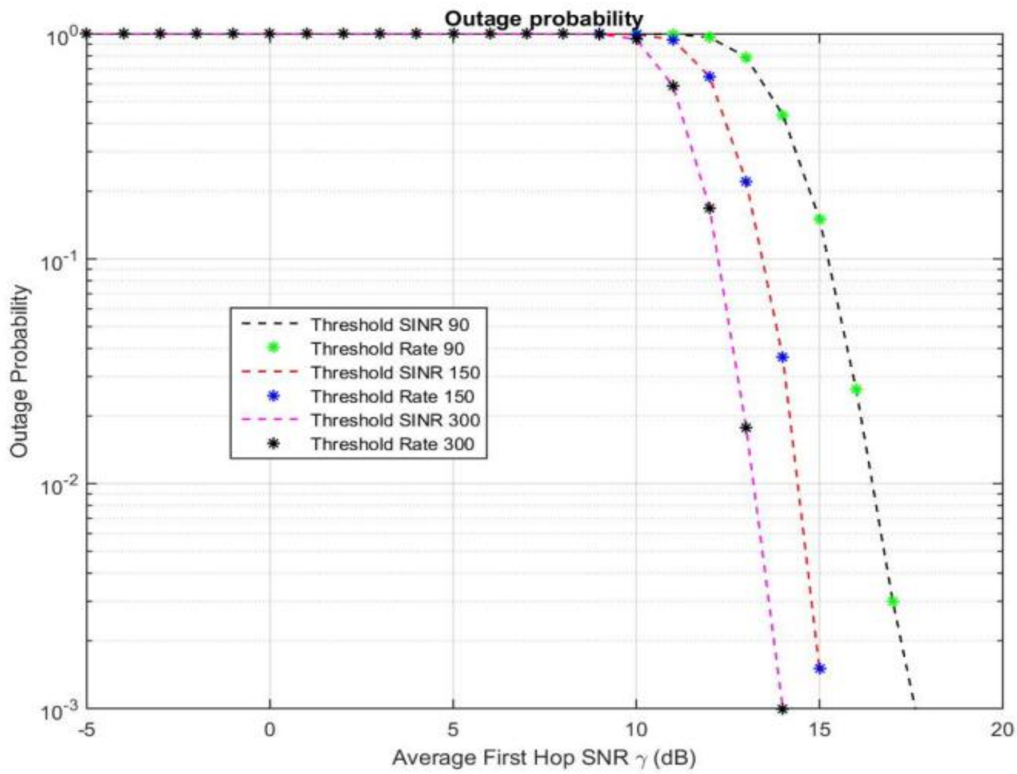

Figure 5.1: Outage probability of a 4-user network with varying numbers of the secondary base station antennas. $\bar{\gamma} = P_S/\sigma_R^2, \sigma_R^2 = \sigma_S^2 = 5$dBm and $M = K = 6$.

the SBS increases. At an average SNR of 15dB, the outage probability for a 90-antenna base station is around a tenth which is out-performed by the 150-antenna base station sitting at around a thousandth. This supports the notion that was earlier presented in Chapter 4, how massive MIMO improves the performance of a system. The performance, in terms of outage probability, gets better by allowing the number of antennas to grow.

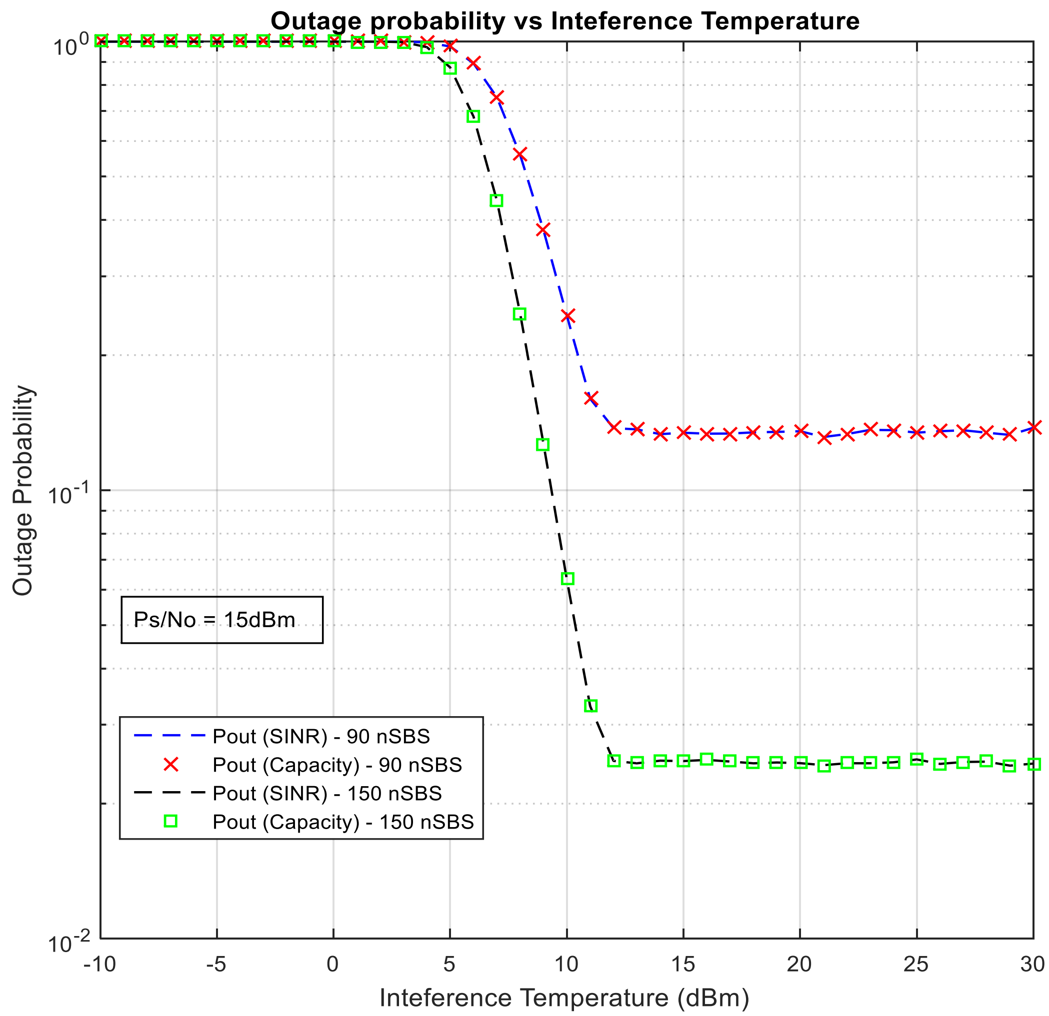

Figure 5.2: Outage probability against the interference temperature values at two different base station antenna configurations

In Figure 5.2 the outage probability of the system is presented as a function of the interference temperature, I_P. This performance metric allows for investigation on the impact of the interference constraint on the outage performance of the proposed system. A PU transmit power (P_{Ptx}) of 27dBm and γ_{th} = 5dB is used. From the obtained results it becomes easy to come up with conclusions on how technologies like massive MIMO feed into the efficiency of a telecommunications network.

For the given range of the interference temperature I_P the outage probability of the underlying system decreases as the interference temperature I_P increases. This is because as the interference temperature increases, the secondary users and relays can afford to transmit at higher transmit powers without causing interferences beyond I_P. The outage probability curves reach error floors when I_P grows towards infinity. This is because the transmit power of the secondary nodes is a function of the maximum user transmit power and the interference temperature. The minimum of the two is always selected, as illustrated in equations (4.3) and (4.4). The point on the graph when error floor starts is the instance when the interference temperature consistently remains higher than the maximum transmit power of the nodes. The transmit power of the SUs and relays are relaxed and are only dependent on the harvested energies. If all the other parameters are kept constant, the graph logically floors since the maximum transmit power of the nodes is also a constant. Figure 5.2 also shows us the difference in performance of the 2 simulation curves. This is due to the different number of base station antennas. The system with more antennas performs better, further supporting the notion that massive MIMO improves the performance of a network.

The outage probability investigations can also be extended to investigate how the outage performance of the proposed system varies with the threshold SNR γ_{th}.

The simulations in Figure 5.3 are plotted for different values of the average SNR and an I_P of 20dB. In each of the three plotted cases, it is evident that as the value of γ_{th} increases, the outage probability gradually increases as well. At low γ_{th}, outage events occur less frequently and occur more often at high rates. This is because, as γ_{th} increases, the probability that the end-to-end SINR of the system falls below the threshold SNR increases. The 15dB average SNR curve has the best performance compared to the 10dB and 5dB average SNR curves respectively. This is attributed to the fact that the SUs and relay transmit powers are a function of the average SNR. This, therefore, implies that sufficient transmit power impacts positively to the overall performance of a system as indicated in Figure 5.3.

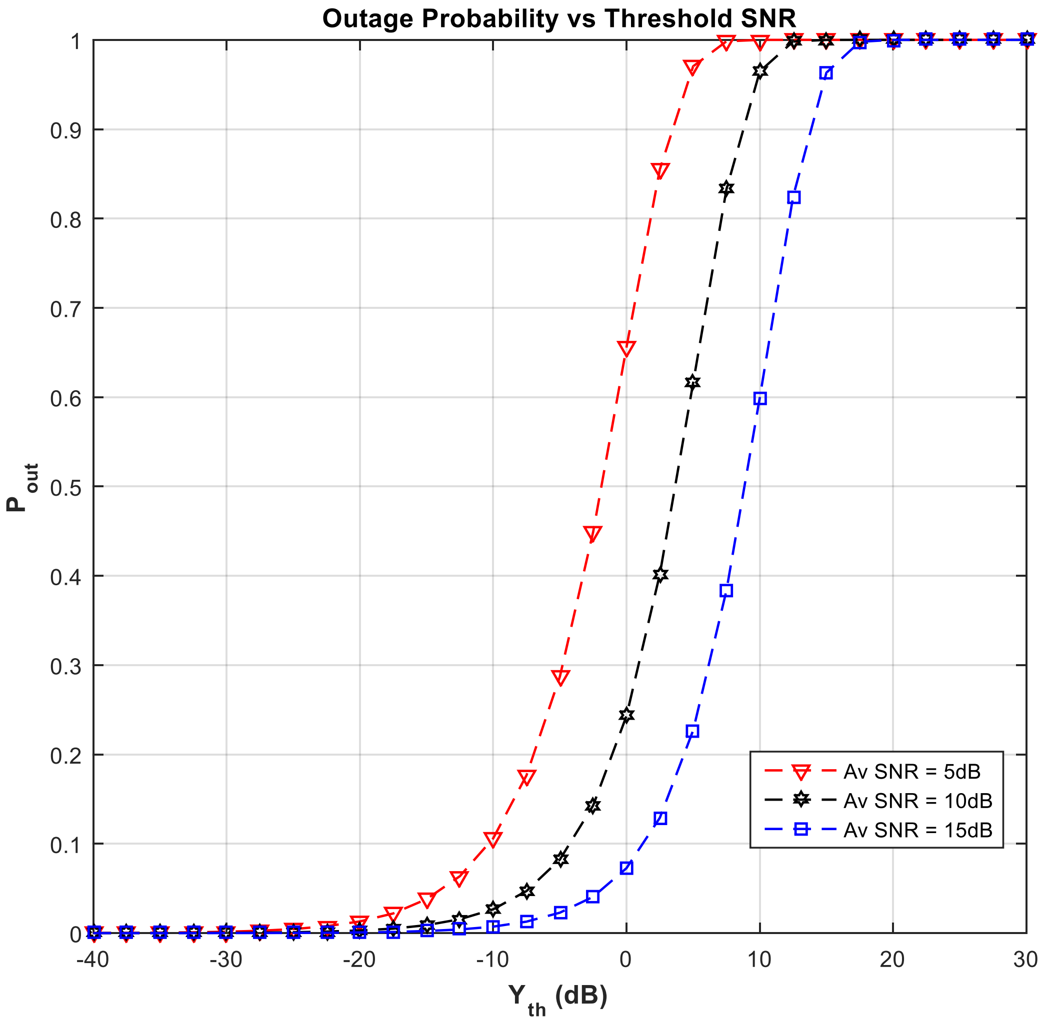

Figure 5.3: Outage probability as a function of γ_{th}.

The outage performance of the proposed system can also be presented as a function of the time-switching factor to assess the impact of wireless energy harvesting on the performance of the system. In Figure 5.4, a conversion efficiency η of 0.7, $P_{Ptx} = 10dB$, $\mathcal{R}_{th} = 1$ and $I_P = P_{Ptx}$ are assumed. The outage performance of the system is performed for three antenna configurations at the SBS. For each antenna configuration the outage probability decreases as α increases from 0 to a certain alpha value ($\alpha \cong 0.3$). After this point, the outage probability starts to increase.

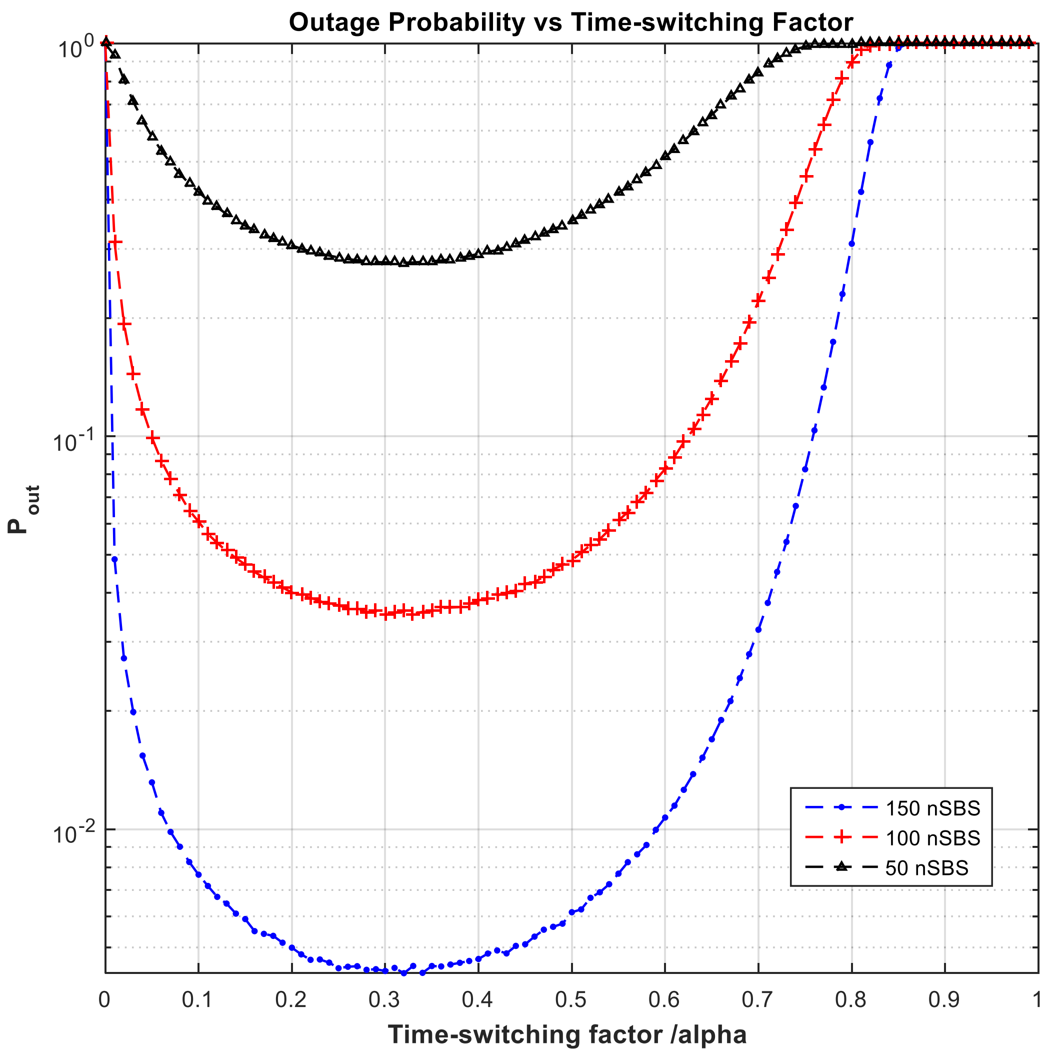

Figure 5.4: Outage probability against the time switching factor, α. The primary user transmit power, $P_{Ptx} = 10dB$, $\mathcal{R}_{th} = 1$, $I_P = P_{Ptx}$.

The results shown in Figure 5.4 are in agreement with the energy harvesting – information transfer trade-off narrative. A longer harvesting period will result in more accumulated energy but less time for information transmission and a smaller α will have less harvested energy but more time for information transmission.

5.5 Conclusion

This chapter looked at the performance of an energy harvesting massive MIMO underlay spectrum sharing network in terms of outage probability. The outage probability equations were formulated and subsequently plotted as a function of various metrics. The outage probability as a function of the average SNR showed that outage probability decreases as the average SNR increases. In a spectrum sharing network, it is of paramount importance to observe the interference temperature limit so as not to affect the primary network performance. To that effect, we analysed the outage probability performance against interference temperature. The graphical plots showed how outage probability decreases as the interference temperature increases until a point when the interference temperature is now larger than the maximum transmit powers of the nodes. A variation of the outage probability against the threshold SNR is also plotted and from this it can be deduced how an increase on the threshold SNR affects the outage probability of the proposed system. This comparison is performed for different average SNR values. To conclude the numerical results section for the chapter, a variation of outage probability against the time ratio for energy harvesting was performed. The outage probability is lowest at a time-switching factor of around, $\alpha \approx 0.3$. This corresponds to a sum-rate value in Figure 4.8 which reaches its maximum at around the same time-switching factor value.

The graphical representations in this chapter collectively prove how massive MIMO, transmit power constraint, energy harvesting and the average SNR all contribute to the performance of the proposed system. Guided by these, system parameters can be designed to achieve the optimum network performance.

Chapter 6 - Relay Selection for Massive MIMO Spectrum Sharing Networks

6.1 Introduction

This chapter focuses on the multi-relay component of the proposed system and subsequently performing relay selection with the main goal of choosing the best possible path to transmit our signals from the source to the destination. As previously highlighted in the literature review, cooperative relaying communication will play a pivotal role in addressing the ever-growing demand for wireless applications and services. The availability of a relay makes it easy to transmit information between nodes since the relay acts as an intermediate repeater. This will also improve the energy efficiency of the proposed system by reducing the transmission distances thereby lowering the users transmit powers. Cooperative communications also improve the reliability and overall quality of a network by increasing network coverage.

Wireless networks may have several nodes that can be used to relay signals from the source to the destination. Transmissions from the source to the destination can be necessitated through any of the available relays. Choosing the best relay to assist with transmissions is the relay selection problem. This selection process can be limited to selecting a single node to act as a relay or selecting several relays to assist with transmissions. Single relay selection schemes select only a single node to act as a relay while multiple relay selection schemes choose many nodes to act as relays. The following sections look at these relay selection schemes.

6.2 Relay Selection Model

Owing to the poor channel quality marred with deep fading and heavy shadowing, secondary users only communicate with the SBS through N relay candidates. The proposed model is based on the following assumptions:

- The primary base station, secondary relays and the secondary base station are massive MIMO enabled and the relays operate in half-duplex mode.
- Selection is performed by considering just the user-to-relay link.

- CSI-assisted AF relaying schemes are considered in this model.
- The source-to-relay and relay-to-base station channels are assumed to be mutually independent and identically distributed.

6.2.1 System and Signal Model

A complete system model has been discussed in Chapter 4, Figure 4.1. This section however only considers the component of the system that deals with multiple relays and subsequently relay selection.

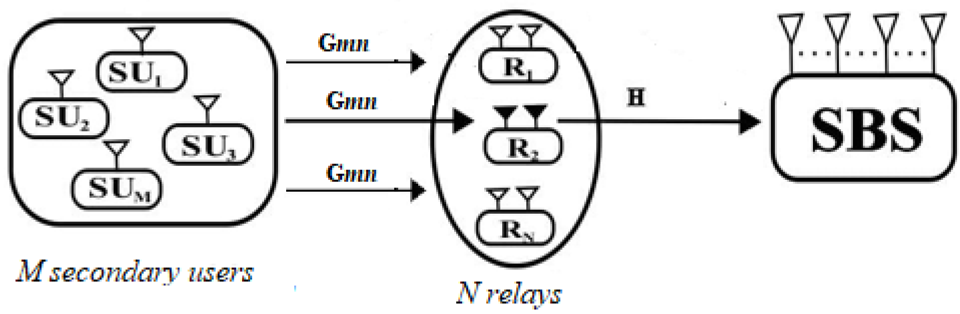

Figure 6.1: System model only showing the multiple relay cluster

As depicted in Figure 6.1, relay selection is going to be performed on the first hop of transmission. The best relay(s) is(are) going to be selected based on the instantaneous channel strength between the source-to relay link for all the *N* available relays.

$$l^* = \arg \underbrace{max}_{n \in \{1,..,N\}} \ min \left\{ \underbrace{\gamma_{SR_n}^{(k)}}_{k \in \{1,..,N_R\}} \right\}, \tag{6.1}$$

where l^* is the selected relay index for the cognitive relay network and $\underbrace{\gamma_{SR_n}^{(k)}}_{k \in \{1,..,N_R\}}$ is the instantaneous SINR at each relay antenna, $k \in \{1, .., N_R\}$, for all the available relays, $n \in \{1, .., N\}$. This selection scheme instantaneously selects the best relay that ultimately maximises the end-to-end SINR and the selected relay is used for both reception and transmission. The expression in (6.1) clearly shows that the selected relay, l^*, is the relay with the strongest bottleneck link.

6.2.2 Selection Schemes

The proposed system model comprises of multiple users and multiple relay nodes. The max-min selection criterion is implemented on the source-to-relay link. These are channels to every relay antenna since the relay nodes are massive MIMO enabled. This single-hop selection criterion is known as partial relay selection and it is implemented in the following two schemes:

(a) selecting a relay with the best source-to-relay average SINR

- all-users-one-relay

$$l^* = \arg \underbrace{max}_{n\in\{1,..,N\}} \left\{ \underbrace{min}_{m\in\{1,..,M\}} \bar{\gamma}_{SR_1}^{(m)}, \ldots, \underbrace{min}_{m\in\{1,..,M\}} \bar{\gamma}_{SR_N}^{(m)} \right\}, \tag{6.2}$$

where $\bar{\gamma}_{SR_1}^{(m)}$ is the average SNR at the relay for each secondary user.

- each-user-per-relay

$$l^* = \arg \underbrace{max}_{n\in\{1,..,N\}} \left\{ \bar{\gamma}_{SR_1}, \ldots, \bar{\gamma}_{SR_N} \right\} \tag{6.3}$$

(b) selecting a relay that maximises the worst data-stream SINR

- all-users-one-relay

$$l^* = \arg \underbrace{max}_{n\in\{1,..,N\}} \ min \left\{ \underbrace{min}_{k\in\{1,..,N_{R_1}\}} \gamma_{SR_1}^{(k)}, \ldots, \underbrace{min}_{k\in\{1,..,N_{R_N}\}} \gamma_{SR_N}^{(k)} \right\}, \tag{6.4}$$

where $\gamma_{SR_1}^{(k)}$ is the instantaneous channel SNR at each relay antenna for each secondary user.

- each-user-per-relay

$$l^* = \arg \underbrace{max}_{n\in\{1,..,N\}} \left\{ \underbrace{min}_{k\in\{1,..,N_{R_1}\}} \gamma_{SR_1}^{(k)}, \ldots, \underbrace{min}_{k\in\{1,..,N_{R_N}\}} \gamma_{SR_N}^{(k)} \right\}, \tag{6.5}$$

where $l^*$is the index of the selected relay in all of the above-mentioned strategies.

The relays are located at different positions with reference to the users and the secondary base station and this varies the path-loss component of the channel gains hence resulting in different system capacity parameters.

6.3 Numerical Results and Discussions

In this section, simulation results are presented to investigate the performance of the proposed selection strategies. To this end, the average sum-rate of the proposed system is plotted. The sum-rate is presented as a function of average first-hop SNR, the time-switching factor, and the interference temperature. The following system parameters are set and maintained for a fair comparison of the strategies: consider a fixed number of relay antennas and the same number of SBS antennas. A path-loss exponent of 2.0 is considered and the distances between the nodes are set as follows: secondary users-to-relay is set to vary in the 40m-to-100m region, relay-to-SBS is 100m, primary user-to-SBS is 1000m, secondary users-to-PBS, primary users-to-relay and the relay-to-PBS are all 500m. The interference temperature is set at 30dBm.

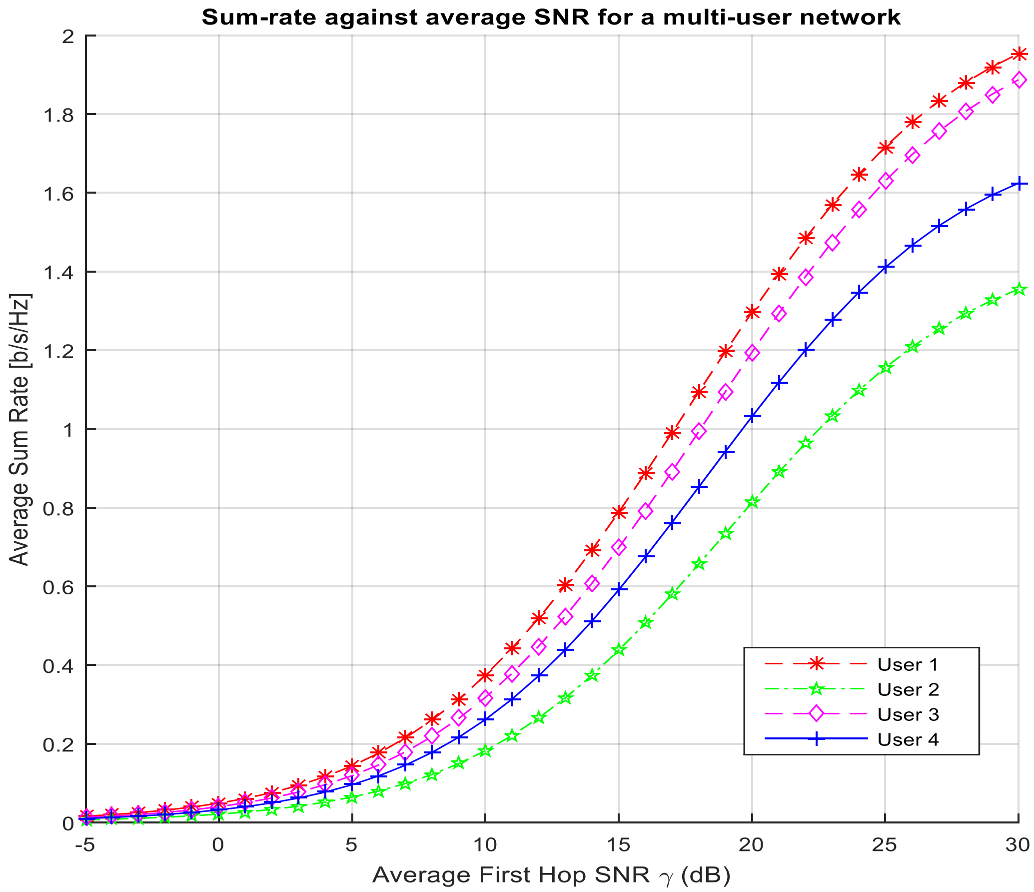

Figure 6.2: Average sum-rate against the average first-hop SNR for a 4-user 2-relay network.

Figure 6.2 demonstrates the selection criteria where each user selects its own relay for transmissions. This is the best relay selection per user. The difference in the performance of the 4 users is because of the different channel conditions and different path losses since these users are scattered around a radius of 40 - 100m with respect to the relays. Collectively at the base station, this kind of selection is supposed to yield better performance since each user would have transmitted through the best possible route. Selecting a single relay would only average the performance of the high performing users. Figure 6.3 compares the performances of each user selecting its relay against all the users transmitting through the same 'best' relay. The selection strategies are illustrated in equations (6.4) and (6.5) where a relay that maximises the worst data-stream SINR is selected.

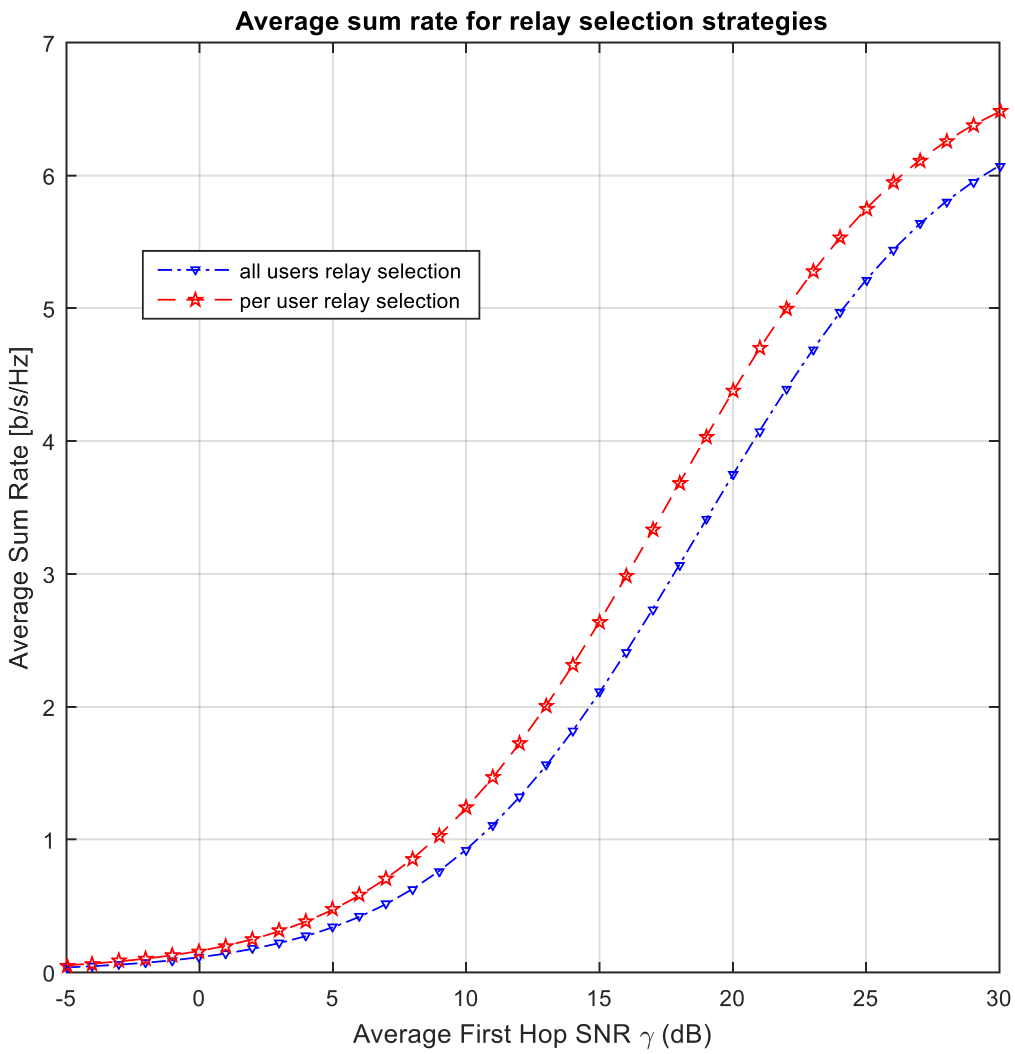

Figure 6.3: Average sum-rate against the average first-hop SNR for 2 different relay selection strategies that consider maximising the worst data-stream SINR

It is evident from Figure 6.3 that having each user select its own 'best' relay will slightly outperform a scenario where a single relay is selected to assist with transmissions for all users. The difference is not so huge though because of the close similarities in channel gains and also because the network just considered two relays. As the pool of available relays increases, the overall performance of the system is expected to increase and this will be quantified in Figure 6.5.

Selecting a relay with the best source-to-relay average SINR as illustrated in equations (6.2) and (6.3) can also be presented graphically to analyse how this selection strategy performs. This selection criterion is based purely on the average SINR for the first hop. Numerical results are going to be divided into the per-user scenario where each user selects its relay and an all-user scenario where all the users select the same 'best' relay for transmissions.

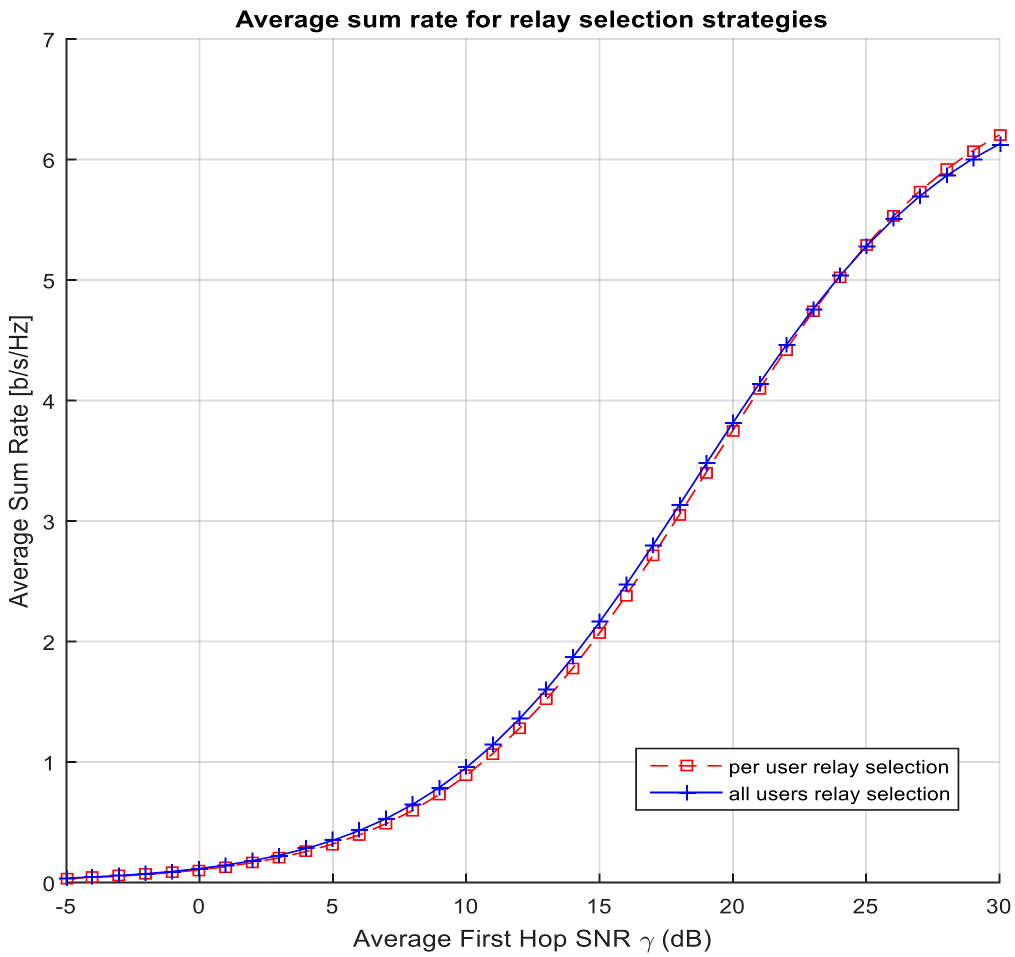

Figure 6.4: Average sum-rate against the average first-hop SNR for 2 different relay selection strategies that consider the best source-to-relay average SINR

The performance of the two scenarios follows the same profile. This is because calculating the average SINR for selection purposes gives a median value for both scenarios thereby making the performance the same.

The above scenarios were limited to selecting the best relay for transmissions by just considering two relays. To get more useful insights into how much the number of antennas affects the performance of the proposed system, the performance comparisons are extended to more relays. By considering an energy harvesting network, an analysis of how the system performs by varying the time-switching factor and increasing the number of available relays from one relay to four relays is performed.

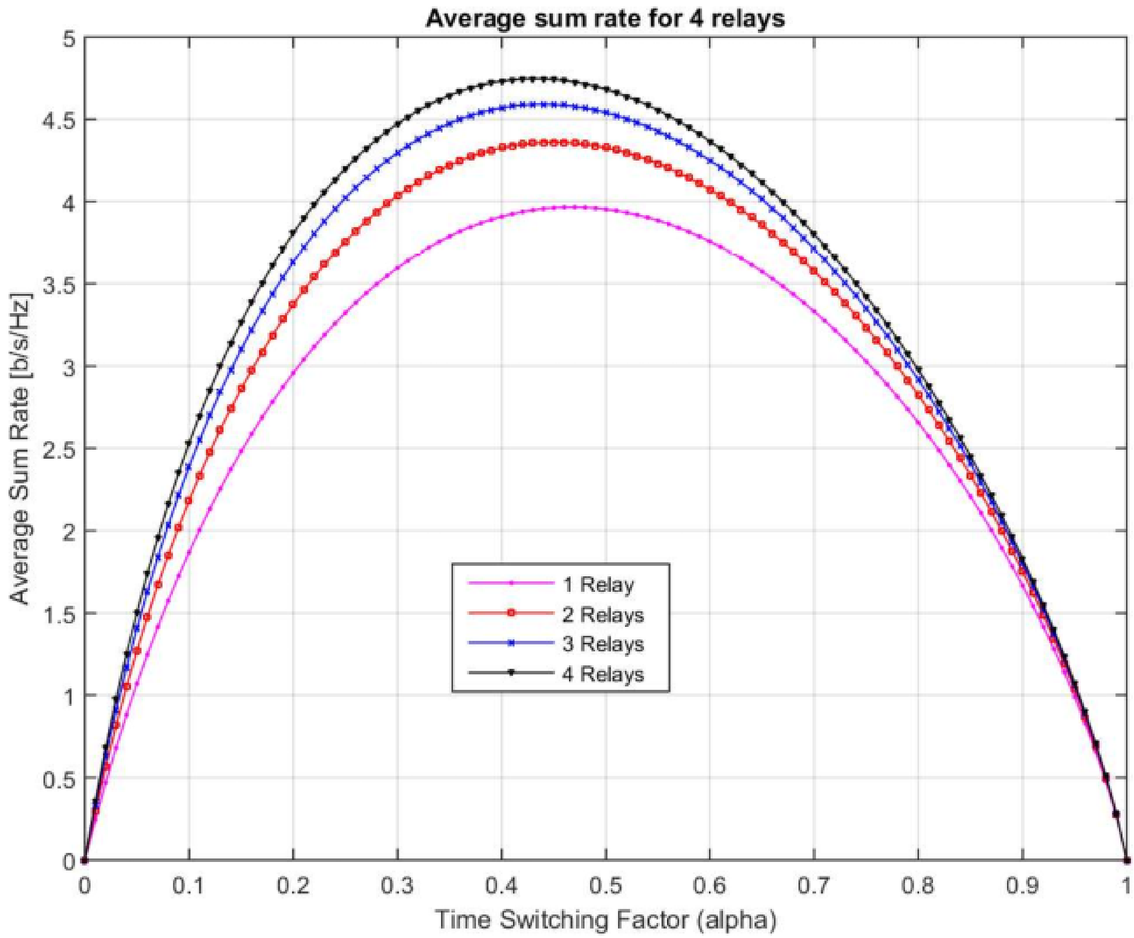

Figure 6.5: Average sum-rate against the time switching factor for different number of relays

Figure 6.5 portrays the different sum-rate curves against the time switching factor after performing relay selection for the different number of relay nodes in the network. Figure 6.5 shows that as the number of relays increases, the sum-rate also increases but with a decreasing gain. This, therefore, implies that an increase in the number of relays for selection can only increase the sum-rate of the system to a certain degree before such gain reduces as it is evident for the sum-rates when there are three and four relays in the network. A gain of approximately 0.4 bit/s/Hz is observed by moving from a single relay to two relays but only a gain of roughly 0.12 bit/s/Hz is observed between three and four relays. The number of relay antennas is maintained the same for a fair comparison.

The same analysis is extended to study the outage performance of the system as the number of relays to select from is increased. The number of relays is increased from one to four and it is subsequently observed how the outage probability of the system varies with the interference temperature constraint as previously illustrated in Figure 5.2. The number of relay antennas and base station antennas is kept constant throughout the simulation for a conclusive comparison.

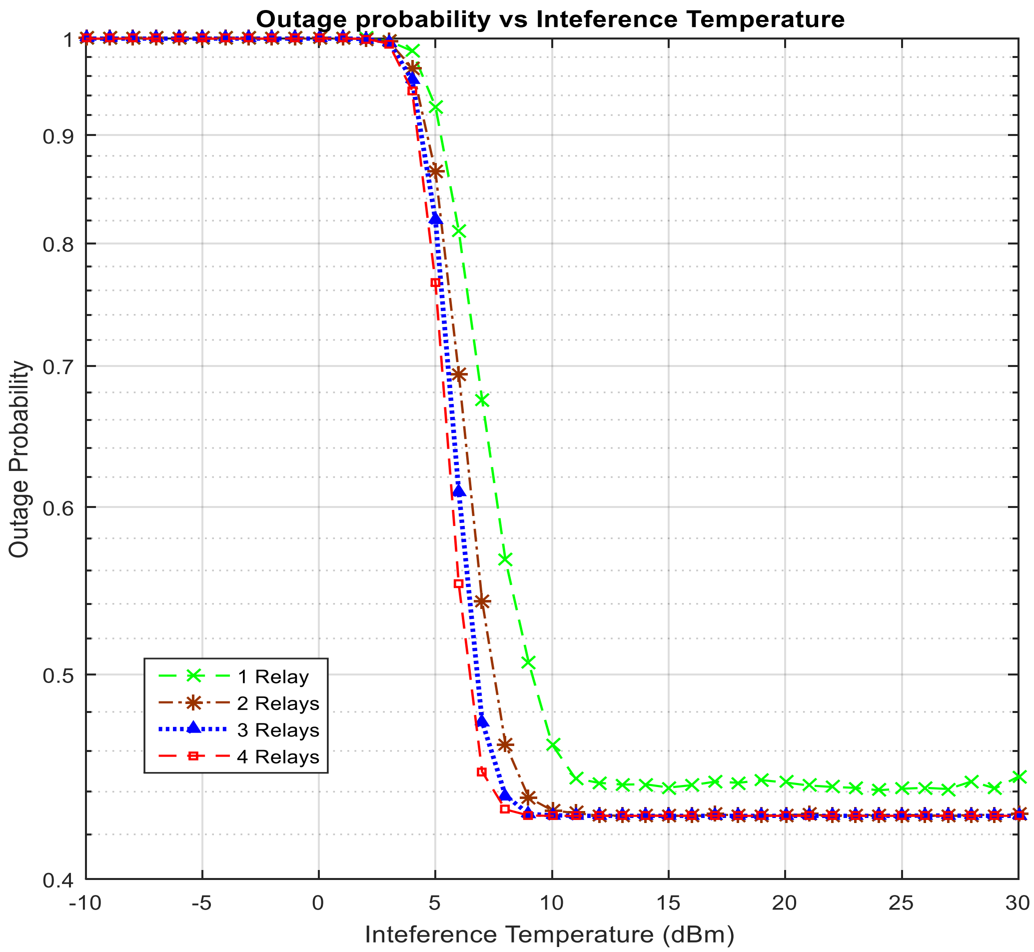

Figure 6.6: Outage probability of a multi-relay multi-user network.

The graphical results from Figure 6.6 indicate that the outage probability of the system decreases as the number of antennas increase. Increasing from one relay to two relays, a decrease in outage probability of about 0.15 is observed which is quite a significant decrease. From two relays to three relays, there is a slight drop in the decrease of outage probability from 0.15 to around 0.1. These results support the claim that cooperative communications improve the performance of a wireless network.

6.4 Conclusion

The work in this chapter presented relay selection strategies and how they perform against each other in improving the operations of a wireless network. Two selection criteria were presented and investigated how much in terms of gain they bring to the performance of the proposed system. Each user selecting its own best relay for transmissions proved to yield slightly better results as compared to a single relay being selected to assist with transmissions for all the users. This is because the selected relay might have very bad conditions for specific users and this will negate the performance of the other users. Selection of the best relay based on the average SINR at the relay has also been analysed and the performance is quantified. Both criterion proved to have the same values of performance. This is because calculating the average SINR would create an equilibrium of operation for all the users. Increasing the number of relays can create a slight shift to this equilibrium. Performance variation by increasing the number of relays was plotted in Figure 6.5 and Figure 6.6 to observe how this would improve the performance of a network. As the number of relays was increased, performance also increased although with a decreasing rate. This, therefore, implies that the performance of a network will increase as the number of relays increases but only to a certain point. Deploying cooperative relaying with other technologies like massive MIMO improves the system performance even better. Direct communications from the source to the destination have been studied in [81] and from the numerical results in Chapter 6, it is conclusive that the outage performance of a network is better with the aid of relays. Amplify-and-forward relays assist in boosting the signal strength and thereby improving the gains.

It is worth noting that the multiple relay selection schemes have some undesirable complexities that arise due to the phase adjustments needed at the transmitters to allow for the addition of multiple received signals coherently at the destination [44]. This complexity makes the single relay selection schemes more favourable and also the numerical results in this sub-section supported this notion.

Chapter 7 – Conclusion

This chapter concludes the dissertation by providing a summary of the contributions, the obtained results and creating a framework for future research into the studied concepts.

7.1 Concluding remarks

The main objective of this research, as outlined in Chapter 1, was to answer to what extent does relay selection and massive-MIMO affect the system performance of a multiuser multi-relay energy harvesting cooperative cognitive radio network in terms of sum-rate and outage probability. This question guided all the chapters that form this dissertation. This conclusion summarises each chapter as follows:

Chapter 1 discussed the research question and the sub-questions. The objectives were also introduced in this chapter as well as the contributions of this research. With the continuous growth of bandwidth-hungry devices and services, the strain on the available spectrum continues to increase and hence the need to continuously look for technologies that improve the spectral efficiency of the spectrum. A background of wireless communications that is provided in Chapter 1, provided a guideline to what the research focused on. This chapter was followed by the literature review in Chapters 2 and 3. Chapter 2 provided an intensive look into the cognitive radio technology and cooperative communications. Spectrum sharing networks are set to decongest the already congested spectrum by allowing unlicensed users to opportunistically access the licenced bandwidth. This allows more users to transmit although this comes with transmit power constraints. These transmit power constraints however limit the network coverage, a drawback which can be addressed by introducing relays to assist with transmissions. Cooperative communications improve system reliability by increasing network coverage and reducing the transmit powers.

Chapter 3 took an in-depth look into wireless energy harvesting and the concept of massive MIMO. Energy efficiency is of paramount importance in design and deployment of the next generation of wireless communications. An energy-efficient network will have a prolonged lifetime of operation and this becomes difficult to maintain in battery-operated nodes. This makes wireless energy harvesting a perfect fit in managing this setback. Due to the availability nature of ambient radio frequency signals, wireless energy harvesting is favourable to power the batteries of the nodes. Critical services that are strict on the Quality-of-Service need a continuous supply of power. The concept of massive MIMO which entails deploying antennas at a network node in very high orders has been studied in this chapter. This technique carries several advantages that include eliminating the effects of small scale fading and noise at the receivers, eliminating the inter-cell interference, brings on board a very high energy efficiency and scaling the transmit power inversely proportional to the number of transmit antennas at the base station. After an intensive study into the advantages of all the aforementioned techniques, this research integrated these techniques and subsequently analysed how they improve the overall performance of a network. As is illustrated in the chapters that followed, these techniques proved to be beneficial to the end-to-end operations of the proposed system.

Chapter 4 analysed the performance of the network in terms of sum-rate and presented the numerical results. The numerical results showed that as the number of antennas increases the performance of the network also increases. This proved correct the claim that massive MIMO improves the spectral efficiency of a network. The Monte-Carlo simulations matched the analytical analysis, and this was proof of the correctness of the simulation model. Graphical representations of the sum-rate against the time-switching factor showed the effects of energy harvesting on the performance of the network. The trade-off between energy harvesting and information transfer was also quantified and optimal values of network operation were deduced. Several numerical results have been presented and they validated the analysis that massive MIMO and energy harvesting provide substantial sum-rate improvements while allowing the transmit powers at the nodes to become exceedingly small. Chapter 5 looked at the performance of the network in terms of outage probability. Authors in ([10] and [18] and references therein) presented outage performance of their respective systems but did not consider massive MIMO enabled nodes. The implementation of wireless energy harvesting and massive MIMO made this work's outage probability results unique. The comparisons were investigated as functions of the average first hop SNR, interference temperature I_P, threshold SNR, γ_{th} and the time-switching factor, α. The obtained results all proved the benefits that come with massive MIMO and wireless energy harvesting.

Chapter 6 proposed and analysed two relay selection strategies for our network. The first strategy selects a relay that maximises the worst data-stream SINR. This is done for two selection schemes where either each user selects its own 'best' relay or all the users transmit through the single selected relay. The second strategy minimises the outage probability of the user nodes by selecting the relay with the best source-to-relay average SINR. It is easily noticeable by introducing massive MIMO enable relays that the overall multiplexing gain can be improved by equally distributing the antennas in the pool of available relays. Several numerical results were presented to compare the performance gains of the proposed relay selection strategies and to validate our analysis. The results in this chapter revealed that the proposed relay selection strategies provide substantial improvements in outage probability and the average sum-rate. This study, therefore, confirmed the potential use of relay selection for massive MIMO spectrum sharing networks in the context of emerging next-generation wireless networks.

7.2 Future Directions

This research studied only a bit in a large pool of research that focuses on the design and deployment of the next generation of wireless communications. This section presents several future research directions have been proposed for the continuation of this research.

• Analysing channel correlation among the sub-channels

This research assumed that all the channel amplitudes are independently and identically distributed. However, due to practical limitations such as the closeness of multiple antennas at the relay and the base stations, this assumption may not be strictly true since the channel amplitudes will be correlated. Thus, further research can investigate the impact of correlations.

• Analysing imperfect CSI at the user nodes

This research assumed that the channel state information (CSI) is freely available at the user nodes. However, this assumption is unrealistic in a practical scenario and methods to acquire channel state information should be used at the user nodes. This results in imperfect channel state information at the user nodes due to practical limitations of such methods. Thus, the impact of imperfect channel state information at the user nodes should be analysed for the proposed network. This is essential research for the practical implementation of this network to be able to correctly analyse the sum-rate performance, outage probability performance and the relay selection schemes.

• Using harvested energy for transmissions of information

This research used the assumption that the secondary users and the relays used all of the harvested energy to transfer information in the transmission time slot. This is not entirely true practically since some nodes can use only a fraction of the harvested energy and remain with some energy. This energy needs to be accounted for and subsequently perform correct performance formulations.

• Pilot contamination effects for the massive MIMO user nodes

Massive MIMO relay nodes and base stations are analysed in Chapters 4, 5 and 6 but the numerical results and discussions ignored the effect of pilot contamination. Pilot contamination is the residual interference caused by the reuse of non-orthogonal pilot sequences. The work of [8] and [79] – [80] have identified pilot contamination as the main performance-limiting factor in massive MIMO systems. The effect of pilot contamination cannot be mitigated by increasing the number of antennas. Thus, its impact must be assessed properly before implementing massive MIMO on the proposed system. As massive MIMO promises to be a key component for the next generation of wireless communications, this will be a great problem to study and solve in future research.

References

[1] International Telecommunications Union. (2016) ITU key 2005 - 2016 ICT data. [Online]. Available: http://www.itu.int/en/ITU-D/Statistics/Pages/stat/default.aspx.

[2] Q. Zhao and B. M. Sadler, "A Survey of Dynamic Spectrum Access," in *IEEE Signal Processing Magazine*, vol. 24, no. 3, pp. 79-89, May 2007.

[3] A. Goldsmith, S. A. Jafar, I. Maric and S. Srinivasa, "Breaking spectrum gridlock with cognitive radios: An information theoretic perspective," in *Proceedings of the IEEE*, vol. 97, no. 5, pp. 894-914, May 2009.

[4] L. Liu, R. Zhang and K. Chua, "Wireless information transfer with opportunistic energy harvesting," *IEEE Transactions on Wireless Communications*, vol. 12, no. 1, pp. 288-300, January 2013.

[5] M. Xia and S. Aissa, "Cooperative AF Relaying in Spectrum-Sharing Systems: Performance Analysis under Average Interference Power Constraints and Nakagami-m Fading," *IEEE Transactions on Communications*, vol. 60, no. 6, pp. 1523-1533, June 2012.

[6] P. Das, N. B. Mehta, and G. Singh, "Novel relay selection rules for average interference constrained cognitive AF relay networks," *IEEE Transactions on Wireless Communications*, vol. 14, no. 8, pp. 4304-4315, August 2015.

[7] J. Chen, J. Si, Z. Li, and H. Huang, "On the performance of spectrum sharing cognitive relay networks with imperfect CSI," *IEEE Communication Letters*., vol. 16, no. 7, pp. 1002-1005, July 2012.

[8] T. L. Marzetta, "Non-cooperative cellular wireless with unlimited numbers of base station antennas," *IEEE Transactions on Wireless Communications*, vol. 9, no. 11, pp. 3590 – 3600, November 2010.

[9] M. Xia and S. Aissa, "Cooperative AF Relaying in Spectrum-Sharing Systems: Outage Probability Analysis under Co-Channel Interferences and Relay Selection," *IEEE Transactions on Communications*, vol. 60, no. 11, pp. 3252-3262, November 2012.

[10] J. M. Moualeu, W. Hamouda and F. Takawira, "AF relaying in underlay spectrum-sharing systems with outdated CSI," *2016 IEEE International Conference on Communications (ICC)*, Kuala Lumpur, pp. 1-6, May 2016.

[11] L. R. Varshney, "Transporting information and energy simultaneously," *2008 IEEE International Symposium on Information Theory*, Toronto, Ontario, pp. 1612-1616, July 2008.

[12] R. Zhang and C. K. Ho, "MIMO Broadcasting for Simultaneous Wireless Information and Power Transfer," *IEEE Transactions on Wireless Communications*, vol. 12, no. 5, pp. 1989-2001, May 2013.

[13] A. Nasir, X. Zhou, S. Durrani, and R. Kennedy, "Relaying protocols for wireless energy harvesting and information processing," *IEEE Transactions on Wireless Communications*, vol. 12, no. 7, pp. 3622–3636, July 2013.

[14] G. Amarasuriya, S. Liu, H. V. Poor, "Wireless energy harvesting massive MIMO relays," *IEEE Transactions on Wireless Communications*, vol. 15, no. 6, pp. 3837–3855, February 2016.

[15] H. Al-Hraishawi, G. Amarasuriya and A. Baduge, "Wireless energy harvesting in cognitive massive MIMO systems with underlay spectrum sharing" *IEEE Transactions on Wireless Communications*, vol. 6, no. 1, February 2017.

[16] D. Gore, J. Heath. R.W., and A. Paulraj, "On the performance of the zero-forcing receiver in presence of transmit correlation," in *Proceedings IEEE International Symposium on Information Theory (ISIT)*, Lausanne, Switzerland, pp. 1-2, July 2002.

[17] X. Zhou, R. Zhang and C. K. Ho, "Wireless Information and Power Transfer: Architecture Design and Rate-Energy Trade-off," *IEEE Transactions on Communications*, vol. 61, no. 11, pp. 4754-4767, November 2013.

[18] S. A. Mousavifar, Y. Liu, C. Leung, M. Elkashlan and T. Q. Duong, "Wireless energy harvesting and spectrum sharing in cognitive radio," *2014 IEEE 80th Vehicular Technology Conference (VTC2014-Fall)*, Vancouver, BC, pp. 1-5, September 2014.

[19] P. A. Anghel and M. Kaveh, "Exact symbol error probability of a cooperative network in a Rayleigh-fading environment," *IEEE Transactions on Wireless Communications*, vol. 3, no. 5, pp. 1416– 1421, May 2004.

[20] T. L. Marzetta, "Non-cooperative cellular wireless with unlimited numbers of base station antennas," *IEEE Transactions on Wireless Communications*, vol. 9, no. 11, pp. 3590 – 3600, November 2010.

[21] H.Q. Ngo. E. G Larsson and T. L. Marzetta, "Energy and spectral efficiency of very large multiuser MIMO systems," *IEEE Transactions on Communications*, vol. 61, no. 4, pp. 1436 - 1449, April 2013.

[22] H. Yang and T. L, Marzetta, "Performance of conjugate and zero-forcing beamforming in large scale antenna systems," *IEEE Journal on Selected Areas in Communications*, vol. 13, no. 2, pp. 172-179, February 2013.

[23] L. Wang, H. Q. Ngo, M. Elkashlan, T. Q. Duong and K. Wong, "Massive MIMO in spectrum sharing networks: Achievable rate and power efficiency," *IEEE Systems Journal*, vol. 11, no. 1, pp. 20-31, March 2017.

[24] S. Timilsina, G. A. Aruma Baduge and R. F. Schaefer, "Secure communication in spectrum-sharing massive MIMO systems with active eavesdropping," *IEEE Transactions on Cognitive Communications and Networking*, vol. 4, no. 2, pp. 390-405, June 2018.

[25] Electronic Communications Act: Terrestrial broadcasting frequency plan: 6 July 2009 No. 32385 Notice 960 OF 2009.

[26] D. Treeumnuk and D. C. Popescu, "Enhanced spectrum utilisation in dynamic cognitive radios with adaptive sensing," *IET Signal Processing*, vol. 8, no. 4, pp. 339–346, June 2014.

[27] Independent Communications Authority of South Africa. (2017, Mar) 2nd report on the state of the ICT sector in South Africa. [Online]. Available: https://www.icasa.org.za/LegislationRegulations.

[28] A. Ahmad, S. Ahmad, M. H. Rehmani, and N. U. Hassan, “A survey on radio resource allocation in cognitive radio sensor networks,” *IEEE Communications Surveys Tutorials*, vol. 17, no. 2, pp. 888–917, February 2015.

[29] A. Plummer, “Distributed spectrum assignment for cognitive networks with heterogeneous spectrum opportunities,” *Wireless Communications and Mobile Computing*, vol. 11, no. 9, pp. 1239–1253, September 2011.

[30] M. A. Albreem, M. Juntti and S. Shahabuddin, "Massive MIMO Detection Techniques: A Survey," *IEEE Communications Surveys & Tutorials*, vol. 21, no. 4, pp. 3109-3132, Fourth-quarter 2019.

[31] J. N. Laneman and G. W. Wornell, "Distributed space-time coded protocols for exploiting cooperative diversity in wireless networks," *Global Telecommunications Conference, 2002. GLOBECOM '02. IEEE*, Taipei, Taiwan, November 2002.

[32] A. Sendonaris, E. Erkip, and B. Aazhang, “User cooperation diversity– part I: system description," *IEEE Transactions on Communications*, vol. 51, no. 11, pp. 1927-1938, November 2003.

[33] A. Sendonaris, E. Erkip and B. Aazhang, "User cooperation diversity. Part II. Implementation aspects and performance analysis," *IEEE Transactions on Communications*, vol. 51, no. 11, pp. 1939-1948, November 2003.

[34] M. Janani, A. Hedayat, T. E. Hunter, and A. Nosratinia, “Coded cooperation in wireless communications: space-time transmission and iterative decoding," *IEEE Transactions on Signal Processing*, vol. 52, no. 2, pp. 362-371, February 2004.

[35] R. U. Nabar, H. Bölcskei, and F. W. Kneubühler, “Fading relay channels: Performance limits and space-time signal design," *IEEE Journal on Selected Areas in Communications*, vol. 22, no. 6, pp. 1099-1109, August 2004.

[36] J. N. Laneman, D. N. C. Tse, and G. W. Wornell, “Cooperative diversity in wireless networks: efficient protocols and outage behaviour," *IEEE Transactions on Information Theory*, vol. 50, no. 12, pp. 3062-3080, December 2004.

[37] T. Cover and A. E. Gamal, "Capacity theorems for the relay channel," *IEEE Transactions on Information Theory*, vol. 25, no. 5, pp. 572-584, September 1979.

[38] A. Raja and P. Viswanath, “Compress-and-Forward scheme for relay networks: backwards decoding and connection to bi-submodular flows,” *IEEE Transactions on Information Theory*, vol. 60, pp.5627-5638, September 2014.

[39] U. Khair, Suwadi and Wirawan, "Performance of hybrid relay selection in cooperative communications system," *2017 2nd International conferences on Information Technology, Information Systems and Electrical Engineering (ICITISEE)*, Yogyakarta, pp. 402-405, November 2017.

[40] T. Liu, L. Song, Y. Li, Q. Huo and B. Jiao, "Performance Analysis of Hybrid Relay Selection in Cooperative Wireless Systems," *IEEE Transactions on Communications*, vol. 60, no. 3, pp. 779-788, March 2012.

[41] X. Song, M. Zhang, W. Liu and F. Liu, "Threshold-based hybrid relay selection scheme," *2016 12th World Congress on Intelligent Control and Automation (WCICA)*, Guilin, pp. 222-227, June 2016.

[42] S. Atapattu, Y. Jing, H. Jiang, and C. Tellambura, “Relay selection schemes and performance analysis approximations for two-way networks,” *IEEE Transactions on Communications*, vol. 61, no. 3, pp. 987–998, March 2013.

[43] Y. Tang and M. C. Valenti, "Coded transmit macrodiversity: block space-time codes over distributed antennas," *IEEE VTS 53rd Vehicular Technology Conference, Spring 2001. Proceedings (Cat. No.01CH37202)*, vol.2, Rhodes, Greece, pp. 1435-1438, May 2001.

[44] Y. Jing and H. Jafarkhani, "Single and multiple relay selection schemes and their achievable diversity orders," *IEEE Transactions on Wireless Communications*, vol. 8, no. 3, pp. 1414–1423, March 2009.

[45] V. Sreng, H. Yanikomeroglu, and D. D. Falconer, "Relayer selection strategies in cellular networks with peer-to-peer relaying," *2003 IEEE 58th Vehicular Technology Conference,* vol. 3, Orlando, pp. 1949-1953, October 2003.

[46] A. Muller and J. Speidel, "Relay selection in dual-hop transmission systems: selection strategies and performance results," *2008 IEEE International Conference on Communications*, Beijing, pp. 4998-5003, May 2008.

[47] A. Bletsas, A. Khisti, D. P. Reed, and A. Lippman, "A simple cooperative diversity method based on network path selection," *IEEE Journal on Selected Areas in Communications*, vol. 24, no. 3, pp. 659-672, March 2006.

[48] Y. Liu, S. A. Mousavifar, Y. Deng, C. Leung and M. Elkashlan, "Wireless Energy Harvesting in a Cognitive Relay Network," *IEEE Transactions on Wireless Communications*, vol. 15, no. 4, pp. 2498-2508, April 2016.

[49] D. Pamela, M. Osorio and E. E. B. Olivo, "Underlay cognitive networks with partial relay selection and primary-user interference", XXXV *Simposio Brasileiro De Telecomunicacoes*, Sao Pedro, 3-6 September 2017.

[50] A. Bletsas, H. Shin, M. Z. Win, "Cooperative communications with outage-optimal opportunistic relaying," *IEEE Transactions on Wireless Communications*, vol. 6, no. 9, September 2007.

[51] R. Ghallab, M. Shokair "Cognitive radio networks with best relay selection method", *International Journal in Information and Communication Technology Research*, November 2012.

[52] M. Ju, K. Hwang, and H. Song, "Relay selection of cooperative diversity networks with interference-limited destination" *IEEE Transactions on Vehicular Technology,* vol. 62, no. 9, November 2013.

[53] M. Seyfi, S. Muhaidat, J. Liang, "Relay selection in cognitive radio networks with interference constraints", *IET Communications,* vol. 7, issue. 10, pp. 922-930, February 2013.

[54] J. Mitola, "Cognitive radio: An integrated agent architecture for software-defined radio", (Doctor of Technology, Royal Inst. Technol (KTH), Stockholm, Sweden, 2000).

[55] S, Haykin, 'Cognitive radio: brain-empowered wireless communications', *IEEE Journal on Selected Areas in Communications,* vol 23, Issue 2, pp. 201–220, February 2005.

[56] A. Goldsmith, S.A. Jafar, I. Maric, S. Srinivasa, 'Breaking spectrum gridlock with cognitive radios: an information-theoretic perspective', in *Proceedings of the IEEE*, vol 97, Issue 5, pp. 894–914, April 2009.

[57] H.A. Suraweera, P.J Smith, M. Shafi, 'Capacity limits and performance analysis of cognitive radio with imperfect channel knowledge', *IEEE Transactions on Vehicular Technology,* Vol 59, Issue 4, pp. 1811–1822, February 2010.

[58] F. Zhao, L. Wei and H. Chen, "Optimal time allocation for wireless information and power transfer in wireless powered communication systems," *IEEE Transactions on Vehicular Technology*, vol. 65, no. 3, pp. 1830-1835, March 2016.

[59] L. R. Varshney, "Transporting information and energy simultaneously," *2008 IEEE International Symposium on Information Theory,* Toronto, Ontario, pp. 1612-1616, July 2008.

[60] Z Ding *et al*. "Application of smart antenna technologies in simultaneous wireless information and power transfer*,"* *IEEE Communications Magazine*, vol. 53, no 4, pp 86 – 93, April 2015.

[61] L. Liu et al, “Wireless information transfer with opportunistic energy harvesting,” *IEEE Transactions on Wireless Communications*, vol. 12, no. 1, January 2013.

[62] X. Shang et al, “A new outer bound and the noisy-interference sum-rate capacity for Gaussian interference channels,” *IEEE Transactions on Information Theory,* vol. 55, no.2, pp.689-699, February 2009.

[63] V. R. Cadambe and S.A. Jafar, “Interference alignment and degrees of freedom of the K-User interference channel,” *IEEE Transactions on Information Theory,* vol.54, no.8, pp.3425-3441, August 2008.

[64] L. Liu, R. Zhang and K. Chua, "Wireless information and power transfer: A dynamic power splitting approach," *IEEE Transactions on Communications,* vol. 61, no. 9, pp. 3990-4001, September 2013.

[65] I. Krikidis, S. Sasaki, S. Timotheou and Z. Ding, "A low complexity antenna switching for joint wireless information and energy transfer in MIMO relay channels," *IEEE Transactions on Communications*, vol. 62, no. 5, pp. 1577-1587, May 2014.

[66] X. Lu, P. Wang, D. Niyato, D. I. Kim and Z. Han, “Wireless networks with RF energy harvesting: A contemporary survey”, *IEEE Communication Surveys & Tutorials,* vol. 17, no. 2, second quarter 2015.

[67] X. Chen, C. Yuen and Z. Zhang, "Wireless energy and information transfer trade-off for limited-feedback multiantenna systems with energy beamforming," *IEEE Transactions on Vehicular Technology*, vol. 63, no. 1, pp. 407-412, January 2014.

[68] Z. Ding *et al*., "Application of smart antenna technologies in simultaneous wireless information and power transfer," *IEEE Communications Magazine*, vol. 53, no. 4, pp. 86-93, April 2015.

[69] A. A. Nasir, X. Zhou, S. Durrani and R. A. Kennedy, "Relaying protocols for wireless energy harvesting and information processing," *IEEE Transactions on Wireless Communications*, vol. 12, no. 7, pp. 3622-3636, July 2013.

[70] Z. Ding, S. M. Perlaza, I. Esnaola and H. V. Poor, "Power allocation strategies in energy harvesting wireless cooperative networks," *IEEE Transactions on Wireless Communications*, vol. 13, no. 2, pp. 846-860, February 2014.

[71] A. Nasir, X. Zhou, S. Durrani, R. A. Kennedy, “Throughput and ergodic capacity of wireless energy harvesting based DF relaying network,” *2014 IEEE International Conference on Communications (ICC)*, Sydney, Australia, pp. 4066-4071, August 2014.

[72] Z Ding, I. Krikidis, B. Sharif, H.V. Poor, “Wireless information and power transfer in cooperative networks with spatially random relays.” *IEEE Transactions on Wireless Communications*, vol. 13, no. 8, pp. 4440-4453, March 2014.

[73] Z. Chen, Z. Chi, Y. Li, and B. Vucetic, “Error performance of maximal-ratio combining with transmit antenna selection in flat Nakagami-m fading channels,” *IEEE Transactions on Wireless Communications*, vol. 8, no. 1, pp.407-412, January 2014.

[74] M. Costa, "Writing on dirty paper (Corresp.)," *IEEE Transactions on Information Theory*, vol. 29, no. 3, pp. 439-441, May 1983.

[75] T. L. Marzetta, “Non-cooperative cellular wireless with unlimited numbers of base station antennas,” *IEEE Transactions on Wireless Communications*, vol. 9, no. 11, pp. 3590 – 3600, November 2010.

[76] G. Amarasuriya, "Sum Rate Analysis for Multi-User Massive MIMO Relay Networks," *2015 IEEE Global Communications Conference (GLOBECOM)*, San Diego, CA, pp. 1-7, December 2015.

[77] D. Kudathanthirige and G. A. Aruma Baduge, "Massive MIMO configurations for multi-cell multi-user relay networks," *IEEE Transactions on Wireless Communications*, vol. 17, no. 3, pp. 1849-1868, March 2018.

[78] D. Kudathanthirige and G. Amarasuriya, "Multi-Hop massive MIMO relay networks," *2018 IEEE International Conference on Communications (ICC)*, Kansas City, Missouri, pp. 1-7, May 2018.

[79] H. Yang and T. L. Marzetta, "Performance of Conjugate and Zero-Forcing Beamforming in Large-Scale Antenna Systems," *IEEE Journal on Selected Areas in Communications*, vol. 31, no. 2, pp. 172-179, February 2013.

[80] J. Jose, A. Ashikhmin, T. Marzetta, and S. Vishwanath, “Pilot contamination and precoding in multi-cell TDD systems,” *IEEE Transactions on Wireless Communications*, vol. 10, no. 8, pp. 2640–2651, August 2011.

[81] M. V. Banđur, Đ. V. Banđur and B. M. Popović, "Outage probability analysis in shadowed fading channel with multiple cochannel interferences," *2013 21st Telecommunications Forum Telfor (TELFOR)*, Belgrade, pp. 299-302, November 2013.

Appendix A – Achievable Sum-Rate

A.1 Received signal at the SBS

The transmitted signal by the relay towards the secondary base station is given in (4.8) as shown below:

$$\mathbf{x}_R = \Phi_R, \tag{A1.1}$$

where $\mathbf{y}_R$ is the received signal at the relay as shown in (4.6). Substituting (4.6) in (4.10) gives the following:

$$\mathbf{x}_R = \Phi_R\left(\sqrt{P_S}\mathbf{G}\mathbf{x}_S + \sqrt{P_P}\mathbf{U}\mathbf{x}_P + \mathbf{n}_R\right), \tag{A1.2}$$

$$\mathbf{x}_R = \Phi_R\sqrt{P_S}\mathbf{G}\mathbf{x}_S + \Phi_R\sqrt{P_P}\mathbf{U}\mathbf{x}_P + \Phi_R\mathbf{n}_R. \tag{A1.3}$$

The received signal at the secondary base station is given as follows:

$$\mathbf{y}_S = \mathbf{W}_S\left(\mathbf{H}\mathbf{x}_R + \sqrt{P_P}\mathbf{V}\mathbf{x}_P + \mathbf{n}_S\right). \tag{A1.4}$$

$\mathbf{x}_R$ has been defined in (A1.3) and by substituting (A1.3) into (A1.4) gives the following:

$$\mathbf{y}_S = \mathbf{W}_S\left(\mathbf{H}(\Phi_R\sqrt{P_S}\mathbf{G}\mathbf{x}_S + \Phi_R\sqrt{P_P}\mathbf{U}\mathbf{x}_P + \Phi_R\mathbf{n}_R) + \sqrt{P_P}\mathbf{V}\mathbf{x}_P + \mathbf{n}_S\right), \tag{A1.5}$$

$$\mathbf{y}_S = \sqrt{P_S}\Phi_R\mathbf{x}_S + \sqrt{P_P}\Phi_R\mathbf{W}_S\mathbf{H}\mathbf{U}\mathbf{x}_P + \Phi_R\mathbf{W}_S\mathbf{H}\mathbf{n}_R + \sqrt{P_P}\mathbf{W}_S\mathbf{V}\mathbf{x}_P + \mathbf{W}_S\mathbf{n}_S. \tag{A1.6}$$

But $\mathbf{W}_s = \left((\mathbf{HG})^H(\mathbf{HG})\right)^{-1}(\mathbf{HG})^H$, therefore (A1.6) can now be restructured as equation (A1.7) below:

$$\mathbf{y}_S = \left(\left((\mathbf{HG})^H(\mathbf{HG})\right)^{-1}(\mathbf{HG})^H\mathbf{HG}\Phi_R\sqrt{P_S}\mathbf{x}_S + \mathbf{W}_S\mathbf{H}\Phi_R\sqrt{P_P}\mathbf{U}\mathbf{x}_P + \mathbf{W}_S\mathbf{H}\Phi_R\mathbf{n}_R + \mathbf{W}_S\sqrt{P_P}\mathbf{V}\mathbf{x}_P + \mathbf{W}_S\mathbf{n}_S\right), \tag{A1.7}$$

$$= \sqrt{P_S}\Phi_R\mathbf{x}_S + \sqrt{P_P}\Phi_R\mathbf{W}_S\mathbf{H}\mathbf{U}\mathbf{x}_P + \Phi_R\mathbf{W}_S\mathbf{H}\mathbf{n}_R + \sqrt{P_P}\mathbf{W}_S\mathbf{V}\mathbf{x}_P + \mathbf{W}_S\mathbf{n}_S. \tag{A1.8}$$

It is worth noticing how the zero-forcing decoder, $\mathbf{W}_S$, cancelled out with the channel matrices $\mathbf{H}$ and $\mathbf{G}$ to leave (A1.8) the same as (4.10)

A.2 Derivation of the asymptotic SINR

In this appendix, the asymptotic SINRs are derived. Firstly, by substituting (4.5) into (4.3) and (4.4), the denominators of the second terms of the transmit power constraints of the secondary networks in (4.3) and (4.4) become:

$$\mathcal{D}_S = \mathcal{E}\left\{Tr\left(\left(\frac{\mathbf{F}^{\mathbf{H}}\mathbf{F}}{N_P}\right)^{-1}\left(\frac{\mathbf{F}^{\mathbf{H}}\mathbf{Q}}{N_P}\right)\left(\frac{\mathbf{Q}^{\mathbf{H}}\mathbf{F}}{N_P}\right)\left(\frac{\mathbf{F}^{\mathbf{H}}\mathbf{F}}{N_P}\right)^{-1}\right)\right\}, \tag{A2.1}$$

$$\mathcal{D}_R = \mathcal{E}\left\{Tr\left(\left(\frac{\mathbf{F}^{\mathbf{H}}\mathbf{F}}{N_P}\right)^{-1}\left(\frac{\mathbf{F}^{\mathbf{H}}\mathbf{T}}{N_P}\right)\left(\frac{\mathbf{T}^{\mathbf{H}}\mathbf{F}}{N_P}\right)\left(\frac{\mathbf{F}^{\mathbf{H}}\mathbf{F}}{N_P}\right)^{-1}\right)\right\}. \tag{A2.2}$$

The column vectors of an MxN random matrix $\mathbf{A}$, which is distributed as $\mathbf{A}\sim\mathcal{CN}_{M\,X\,N}(\mathbf{0}_{M\,X\,N}, \mathbf{I}_M \otimes \mathbf{I}_N)$ become orthogonal as $M \to \infty$. Therefore, it can be shown that

$$\lim_{M\to\infty} \frac{[\mathbf{A}]_i^H[\mathbf{A}]_j}{M} = \begin{cases} 1, & i = j \\ 0, & i \neq j \end{cases} \text{ and } \lim_{M\to\infty} \frac{\mathbf{A}^H\mathbf{A}}{M} = \mathbf{I}_N. \tag{A2.3}$$

Hence, by using (A2.3), as $N_P \to \infty$, it becomes clear that $\mathcal{D}_S$ and $\mathcal{D}_R$ asymptotically disappear as:

$$\lim_{N_P\to\infty} \mathcal{D}_S \to 0 \text{ and } \lim_{N_P\to\infty} \mathcal{D}_R \to 0 \tag{A2.4}$$

Now substituting (A2.4) into the transmit power constraints (4.3) and (4.4), the transmit powers asymptotically approach:

$$\lim_{N_P\to\infty} P_S = \lim_{N_P\to\infty} \min\left(P_{S_{max}}, \frac{I_P}{\mathcal{D}_S}\right) = P_{S_{max}}, \tag{A2.5}$$

$$\lim_{N_P\to\infty} P_R = \lim_{N_P\to\infty} \min\left(P_{R_{max}}, \frac{I_P}{\mathcal{D}_R}\right) = P_{R_{max}}. \tag{A2.6}$$

The above two equations (A2.5) and (A2.6) stand as proof to how massive MIMO allows secondary nodes to operate at their maximum average transmit power without “worrying” about the interference temperature set on the primary base station.

Now by extending the above to the derivation of the asymptotic sum-rate when the PBS, SBS and relay antennas all approach infinite.

Firstly, by substituting $P_P = E_P/N_P$ and $P_S = E_S/N_R$ into (4.7) and it can now be rewritten as

$$\Phi_R^2 = \frac{P_R}{P_S Tr(\mathbf{G}^{\mathbf{H}}\mathbf{G}) + P_P Tr(\mathbf{U}^{\mathbf{H}}\mathbf{U}) + \sigma_R^2 N_R}, \tag{A2.7}$$

but $P_P = E_P/N_P$ and $P_S = E_S/N_R$ therefore (A2.7) becomes

$$\Phi_R^2 = \frac{P_R}{E_S Tr\left(\frac{\mathbf{G}^{\mathbf{H}}\mathbf{G}}{N_R}\right) + \frac{E_P}{\beta\lambda} Tr\left(\frac{\mathbf{U}^{\mathbf{H}}\mathbf{U}}{N_R}\right) + \sigma_R^2 N_R}, \tag{A2.8}$$

since $N_P = \beta\lambda N_R$

Therefore, by letting $N_R \to \infty$, equations (A2.7) and (A2.8) become:

$$\Phi_R^2 = \frac{P_R}{\sigma_R^2 N_R}, \tag{A2.9}$$

This is after recalling equation (A2.3). Therefore, this summarises to:

$$\lim_{N_R\to\infty} \Phi_R^2 N_R = \frac{P_R}{\sigma_R^2}\,. \tag{A2.10}$$

By applying the same procedure to equations (4.15) – (4.18) it becomes easy to calculate the asymptotic formula for the SINR.

$$P_{I_1} N_R^2 = \frac{(\Phi_R^2 N_R) E_P}{\beta\lambda}\left[\left(\frac{\mathbf{G}^{\mathbf{H}}\mathbf{H}^{\mathbf{H}}\mathbf{H}\mathbf{G}}{N_S N_R}\right)^{-1}\left(\frac{\mathbf{G}^{\mathbf{H}}\mathbf{H}^{\mathbf{H}}\mathbf{H}\mathbf{U}}{N_S N_R}\right)\left(\frac{\mathbf{U}^{\mathbf{H}}\mathbf{H}^{\mathbf{H}}\mathbf{H}\mathbf{G}}{N_S N_R}\right)\left(\frac{\mathbf{G}^{\mathbf{H}}\mathbf{H}^{\mathbf{H}}\mathbf{H}\mathbf{G}}{N_S N_R}\right)^{-1}\right]_{m,m}, \tag{A2.11}$$

$$P_{I_2} N_R^2 = (\Phi_R^2 N_R)\sigma_R^2\left[\left(\frac{\mathbf{G}^{\mathbf{H}}\mathbf{H}^{\mathbf{H}}\mathbf{H}\mathbf{G}}{N_S N_R}\right)^{-1}\left(\frac{\mathbf{G}^{\mathbf{H}}\left(\mathbf{H}^{\mathbf{H}}\mathbf{H}\right)^{\mathbf{2}}\mathbf{G}}{{N_S}^2 N_R}\right)\left(\frac{\mathbf{G}^{\mathbf{H}}\mathbf{H}^{\mathbf{H}}\mathbf{H}\mathbf{G}}{N_S N_R}\right)^{-1}\right]_{m,m}, \tag{A2.12}$$

$$P_{I_3} N_R^2 = \frac{E_P}{\beta\lambda}\left[\left(\frac{\mathbf{G}^{\mathbf{H}}\mathbf{H}^{\mathbf{H}}\mathbf{H}\mathbf{G}}{N_S N_R}\right)^{-1}\left(\frac{\mathbf{G}^{\mathbf{H}}(\mathbf{H}^{\mathbf{H}}\mathbf{V})(\mathbf{V}^{\mathbf{H}}\mathbf{H})\mathbf{G}}{N_S^2 N_R}\right)\left(\frac{\mathbf{G}^{\mathbf{H}}\mathbf{H}^{\mathbf{H}}\mathbf{H}\mathbf{G}}{N_S N_R}\right)^{-1}\right]_{m,m}, \tag{A2.13}$$

$$P_{I_4} N_R^2 = \frac{\sigma_S^2}{\lambda}\left[\left(\frac{\mathbf{G}^{\mathbf{H}}\mathbf{H}^{\mathbf{H}}\mathbf{H}\mathbf{G}}{N_S N_R}\right)^{-1}\right]_{m,m}. \tag{A2.14}$$

By applying random matrix identity in (A2.3), it is quite clear that the contributions of equations (A2.11) and (A2.13) will reduce to zero in the limit of infinitely many relays and secondary base station antennas. This leaves equations (A2.12) and (A2.14).

$$\lim_{N_S, N_{R\to\infty}} P_{I_2} N_R^2 = (\Phi_R^2 N_R)\sigma_R^2 \left[\left(\frac{\mathbf{G^H G}}{N_R}\right)^{-1}\right]. \tag{A2.15}$$

But in (A2.10) $\lim_{N_R\to\infty} \Phi_R^2 N_R\, \sigma_R^2 = P_R$, therefore:

$$\lim_{N_S, N_{R\to\infty}} P_{I_2} N_R^2 = P_R \zeta_{G_m}^{-1}. \tag{A2.16}$$

Applying the same to (A2.14) gives:

$$\lim_{N_S, N_{R\to\infty}} P_{I_4} N_R^2 = \sigma_S^2 \zeta_H^{-1} \zeta_{G_m}^{-1}/\lambda. \tag{A2.17}$$

With the above asymptotic equations having been derived, substituting them into (4.14) and performing mathematical manipulations gives the asymptotic end-to-end SINR:

$$\gamma_m^\infty = \lim_{N_S, N_{R\to\infty}} \left(\frac{P_S N_R^2}{\sum_{n=1}^4 P_{I_n} N_R^2}\right) = \frac{E_S P_R}{\sigma_R^2\left(P_R \zeta_{G_m}^{-1} + \sigma_S^2 \zeta_H^{-1} \zeta_{G_m}^{-1}/\lambda\right)}. \tag{A2.18}$$